



**UIT**

THE ARCTIC  
UNIVERSITY  
OF NORWAY

FACULTY OF SCIENCE AND TECHNOLOGY

Department of Geosciences

# The regional upper Paleozoic development of the SE part of the Norwegian Barents Sea - from seismic interpretation

**Hanne-Lise Slettehaug**

*Master's thesis in Geology, GEO-3900*

*May 2018*





## **Abstract**

This thesis focuses on the Barents Sea South East (BSSE), and the overall goal has been to investigate the regional upper Paleozoic development in the SE part of the Barents Sea. After more than four decades of negotiation between Norway and Russia, a delineation agreement came in effect in 2011. Today, the area known as BSSE is opened up for petroleum operations. As part of the opening of the BSSE, high quality 2D seismic data of the area were acquired by NPD. These 2D seismic data have been used in this thesis together with seismic stratigraphic analysis and correlation to wells in order to describe and discuss the late Carboniferous and Permian sequence. Three seismic units equivalent to the Gipsdalen, Bjarmeland and Tempelfjorden groups have been described with focus on internal horizon configuration and geometry, which forms the basis for interpreting the dominating depositional system for the different seismic units.

This study finds that an overall marine setting has dominated during the upper Paleozoic interval in the BSSE. Carbonate deposition prevailed during major periods of the time interval. Thick sequences of Gipsdalen Group evaporites are found to be present in Nordkapp and Tiddlybanken basins. Salt diapirs within the basins are observed to be up to 4000 ms (twt) thick, in some places almost reaching the sea floor. Evaporites are also present in small and more locally developed basins and on nearby areas on the Finnmark and Bjarmeland platforms. The depositional environment graded from a configuration of platforms and basins that were progressively infilled by the Gipsdalen Group to a regional carbonate platform covering the entire BSSE during the deposition of the Bjarmeland Group. The youngest studied sequence is characterized by a regional open ocean environment where the sediments of the Tempelfjorden Group were mainly deposited from suspension.



## Acknowledgements

Først vil jeg takke min hovedveileder Stig-Morten Knutsen og mine biveiledere Iver Martens og Rune Mattingsdal. Jeg setter pris på all hjelp jeg har fått – takk for all gjennomgang, alle forklaringer og innspill underveis. Oppgaven hadde ikke blitt den samme uten dere.

5 år gikk jo raskt. Takk til mamma, som uavhengig av motivasjonsnivået mitt har holdt fast med at det aldri er for sent å gi opp og flytte hjem. Jeg setter pris på at du alltid er der og at du motiverer meg. Takk til pappa og Elisabeth for pauser i mastergradseventyret, dere er gode å ha. Thomas, takk for Johan – han er det beste du har fått til (så langt). Pluss at du er ganske god du også.

Takk til Alex, som leste gjennom oppgaven og rettet alle skrivefeilene han kom over. Jeg setter også pris på at du prøvde å hjelpe ellers, selv om du hovedsakelig var ubrukelig (og spiste alle knekkebrødene mine). I tillegg så har jeg jo ikke vært den eneste med oppgaveskriving på programmet sitt. Tusen takk folkens, jeg har satt stor pris på alle lunsjpausene og samtalene.

Og selvsagt, en stor takk til Johanne. Blandingen din av høy arbeidsinnsats (herlighet) og hjemmelagde boller har til tider vært hele min motivasjon. Jeg kunne ikke bedd om noen bedre å dele kontor med enn deg.

Hanne-Lise Slettehaug

Tromsø, Mai 2018



# Table of Contents

1. Introduction and objective .....	1
1.1 Objective .....	1
1.2 Study area .....	1
2. Geological background.....	5
2.1 Tectonic development .....	5
2.1.1 Paleozoic .....	6
2.1.2 Post-Paleozoic development of the greater Barents Sea.....	7
2.2 Paleozoic stratigraphy and depositional environment .....	9
2.2.1 Billefjorden Group.....	9
2.2.2 Gipsdalen Group.....	10
2.2.3 Bjarmeland Group .....	10
2.2.4 Tempelfjorden Group .....	11
2.3 Structural setting.....	13
2.3.1 Bjarmeland Platform .....	14
2.3.2 Finnmark Platform.....	14
2.3.3 Nordkapp Basin.....	14
2.3.4 Tiddlybanken Basin.....	15
2.3.5 Fedynsky High .....	15
2.3.6 Domes in the BSSE .....	15
3. Data and methods .....	17
3.1 Dataset .....	18
3.1.1 Wells and well correlation.....	19
3.2 Seismic reflection theory .....	21
3.2.1 Reflection coefficient .....	22
3.2.2 Seismic resolution .....	22
3.3 Seismic interpretation .....	28
3.3.1 Seismic attributes .....	28
3.3.2 Seismic stratigraphy .....	29
4. Results .....	33
4.1 Seismic Areas .....	36
4.2 Paleozoic horizons.....	39
4.2.1 Top Billefjorden .....	39
4.2.2 Base Intra Gipsdalen.....	39
4.2.3 Top Gipsdalen .....	40
4.2.4 Top Bjarmeland.....	40
4.2.5 Top Tempelfjorden.....	40

4.3 Seismic units.....	45
4.3.1 Gipsdalen Group.....	46
4.3.2 Bjarmeland Group .....	54
4.3.3 Tempelfjorden Group .....	58
5. Discussion .....	71
5.1 General notes .....	71
5.2 Gipsdalen Group.....	72
5.3 Bjarmeland Group .....	80
5.4 Tempelfjorden Group .....	83
6. Summary and conclusion .....	87
7. References .....	89

# **1. Introduction and objective**

In the following subchapters the objective of this thesis is presented, as well as placing the study area into a geographical and recent historical context. The second chapter of this thesis presents the geological background for the study area in terms of tectonic development and stratigraphic evolution of the greater Barents Sea. Additionally, the second chapter ends with an introduction to the main structural setting within the study area. The third chapter introduces the data and the methods used to achieve the objective by presenting the applied data and giving an introduction to seismic reflection and seismic interpretation theory. Subsequently, the fourth chapter will present the results of the seismic investigation by describing the observations of mapped horizons and units. The fifth chapter considers these observations and interprets and discusses the results in an effort to accomplish the objective of the thesis. Finally, a summary and conclusion of the findings are presented together with recommendations for future work.

## **1.1 Objective**

The main goal of this thesis is to investigate the Paleozoic geological history of the southeastern part of the Norwegian Barents Sea (BSSE). The focus is on the different depositional systems during the late Carboniferous and Permian.

The main data applied is 2D seismic data from two recent surveys acquired by the Norwegian Petroleum Directorate (NPD), and information from released exploration wells.

## **1.2 Study area**

The Barents Sea (Figure 1.1) is a shallow sea with an average water depth of 230 m. It has a border to the west along the shelf edge towards the Norwegian-Greenland Sea and to the north with the Svalbard archipelagos (Havforskningsinstituttet, 2005). Further delineating the borders are the Norwegian and Russian coasts to the south and Novaya Zemlya to the east. Finally, the northeastern borders are with Franz Josef Land and the shelf edge towards the Arctic Ocean. With an area of approximately 1,4 million km<sup>2</sup> the Barents Sea is almost four times the size of mainland Norway (Smelror et al., 2009).

Geophysical investigations of the Barents Sea were started by the Norwegian authorities in 1969, and the subsequent collection efforts through the 1970s confirmed the existence of promising sedimentary successions and basins (Doré, 1995). Activities related to petroleum operations in the Barents Sea started in 1980, the first exploration well was drilled the same year and the first discoveries were made the following year. Throughout the 1980s several exploration wells were drilled and there were an activity level that was severely lowered during the next decade, before rising again (Faleide et al., 2010, Quarles et al., 2016). Recent estimates (NPD, 2016) state that 48% of total recoverable undiscovered resources on the Norwegian Continental Shelf (NCS) are to be found in the Barents Sea.

Disagreement concerning the demarcation between the Norwegian and Russian parts of the Barents Sea has hampered geological investigation of the BSSE (Meld. St. 36 (2012-2013)). However, after almost 40 years of negotiations a delimitation agreement was signed in 2010 and became effective in 2011. In 2013 the area known as Barents Sea South East (BSSE) opened for petroleum operations. This was the first opening of new areas on the Norwegian continental shelf since 1994. The study area in this thesis spans an area of approximately 44 000 km<sup>2</sup> previously (pre-2013) unopened parts of the Norwegian continental shelf in the Barents Sea (Figure 1.1). The area lies between the previously opened parts of the southwest Barents Sea and the Russian continental shelf, while the northern boundary is 74°30'N (Meld. St. 36 (2012-2013)).



*Figure 1.1* Map of the Barents Sea and its bordering elements (Esri, 2011). The study area is outlined in purple.



## 2. Geological background

This chapter presents the geological background of the study area in terms of tectonic development and stratigraphic evolution. As the objective of this thesis is to investigate the upper Paleozoic development of the BSSE the main focus is put on the Paleozoic development of the Barents Sea. Additionally, a summary of the post-Paleozoic development of the Barents Sea and an introduction to the main structural elements dominating in the BSSE are given.

### 2.1 Tectonic development

A monoclinical structural divide between the eastern Barents shelf and the western region named the “Central Barents Monocline” (Smelror et al., 2009) roughly separates the Barents Sea into two provinces. The eastern part is represented by deeper sediment basins while the western part has a more complex mosaic of basins, platforms and structural highs present (Figure 2.1). The divide is oriented from north to south and has approximately the same position as the offshore boundary between Norway and Russia (Worsley, 2008). Different tectonic events shaped the current appearance of the eastern and western provinces. The Uralian Orogeny was the main influence on the appearance of the eastern part while the western part was mainly influenced by the Caledonian Orogeny and several phases of rifting (Worsley, 2008).

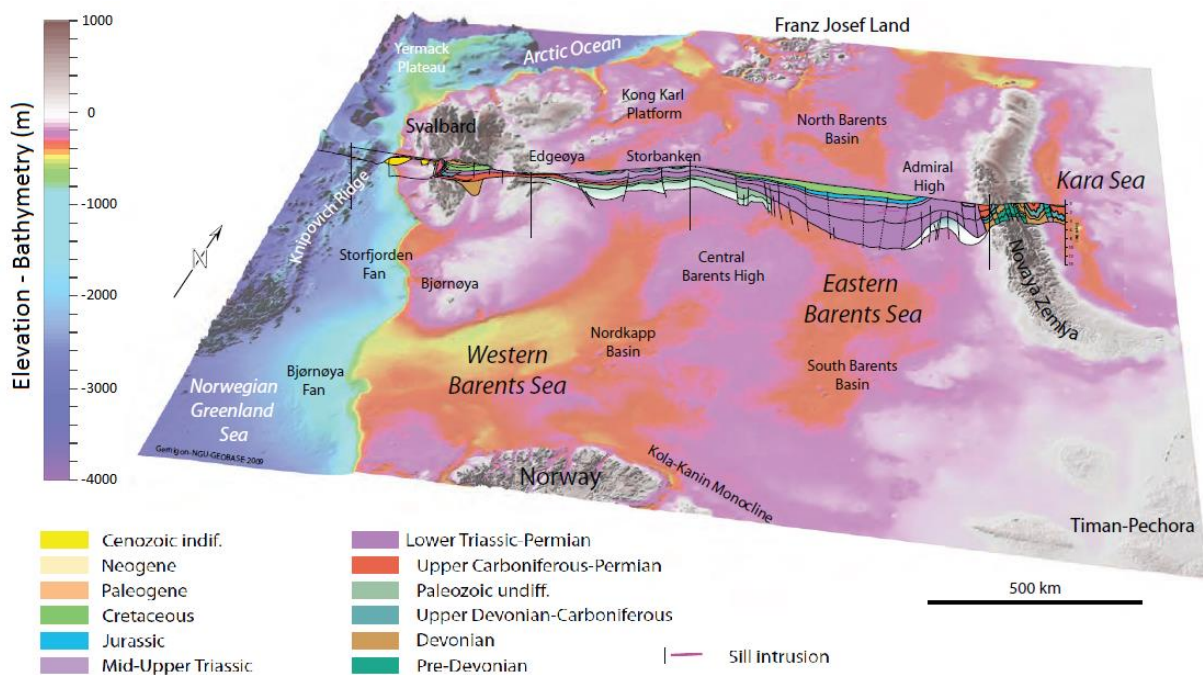


Figure 2.1 Bathymetry map of the Barents Sea continental shelf. A regional geological profile shows the difference between deep basins of the Eastern Barents Sea and the assortment of structures found in the Western Barents Sea. From Smelror et al. (2009).

## **2.1.1 Paleozoic**

### ***2.1.1.1 Western Barents Sea***

The Iapetus Ocean formed in Cambrian, where it gradually spread and overflowed large parts of the peneplane Baltic continent (Nakreim and Worsley, 2013). Its position was reminiscent of, though oblique to, the current northeast Atlantic Ocean. The plate movement behind the spreading was reversed at some point in the transition from Cambrian to Ordovician. This started the closure of the Iapetus Ocean and the subsequent subduction of the Baltic continent beneath the Laurentian continent (Worsley, 2008).

The Caledonian Orogeny as it were, ended around 400 Ma. As the mountain-building ceased the elements started working on the hinterlands. Exhumation and erosion of the Barents Sea region gradually tore it down again, and it became peneplaned in Frasnian times (Smelror et al., 2009). Most of the erosional products from the Caledonian mountains ended up away from the mountain range. From the northernmost extension of the mountain range the most effective transport mechanisms were the river system that led the sediments westward. This made the western parts of the Barents Sea the recipient of erosional products, as the so called “Old Red Sandstones” accumulated (Fossen et al., 2013).

Large parts of the crystalline bedrock in the western part were metamorphosed during the Caledonian Orogeny, creating NE-SW trending grains (Faleide et al., 2010). While the depth to top basement in the entire Barents Sea varies it is generally found at depths of more than 10 km (Smelror et al., 2009).

Crustal movements throughout most of Devonian and Carboniferous led to widespread rifting. Formation of rift basins, half-grabens and tilted fault blocks on the Barents shelf occurred, and these were filled with syn-rift sediments (Worsley, 2008). The rift basins were confined by fractures which followed the older fracture zones of the Caledonian Orogeny. Movements ceased during Permian and for large parts of the Barents Sea the structural relief was gradually infilled and eventually covered by one stable platform (Gudlaugsson et al., 1998). This wide post-rift platform had only thin layers of sedimentation (Nøttvedt and Worsley, 2013).

### ***2.1.1.2 Eastern Barents Sea***

The basement east and west of the larger Barents Sea shelf reflects the differences in geological evolution. While the Caledonian Orogeny is assumed to have metamorphosed the bedrock in the western region, folded Timanian basement is important in the eastern region (Johansen et al., 1992). The compressional Timanian event took place during Ediacaran. The NW lineaments the event created were important for deposition and deformation of subsequent sediment packages (Gernigon et al., 2014).

The tectonic setting until late Middle to early Late Devonian was that of a stable passive continental margin (Smelror et al., 2009). As it did in the western Barents Sea, rifting also took place in the eastern Barents Sea during Devonian, though it started earlier than in its western counterpart (Stoupakova et al., 2011).

Further collision of the continent consolidated by the Caledonian Orogeny, Laurasia, with Western Siberia resulted in another important mountain-building event: the Uralian Orogeny. This event is the main influence of structural trends in the eastern margin of the Barents Sea, and marked the conclusion of the merging of most existing landmasses into the supercontinent Pangea (Doré, 1995). The orogeny continued beyond the Paleozoic era (Smelror et al., 2009).

### **2.1.2 Post-Paleozoic development of the greater Barents Sea**

The Uralian Orogeny terminated during Triassic, after which the eastern part of the Barents Sea became dominated by epicontinental basins (Smelror et al., 2009). During Mesozoic the Barents Sea generally experienced a quiet tectonic regime. However, rifting did occur along the western margin, and local movements also occurred closer to the study area. Both the Bjarmeland and Finnmark platforms experienced some rifting (Smelror et al., 2009). In addition, triggering of salt diapirism took place in the Nordkapp and Tiddlybanken basins during Triassic (Lundschien et al., 2014).

Several pulses of regional extension in Middle Jurassic to Early Cretaceous marked an end to the overall quiet tectonic regime and led to the creation of more rift-basins in the western

Barents Sea. At the culmination of this tectonic activity the current structural arrangement of basins and highs in the Barents Sea was established (Henriksen et al., 2011).

Another major tectonic event important to the evolution of the western Barents Sea took place at the onset of Cenozoic times, as the Norwegian-Greenland Sea started to open. Later, the Cenozoic evolution gave way to extensive uplift and erosion which mostly removed the Cenozoic sediment package, especially in the western Barents Sea. Both SW Barents Sea and eastern Barents Sea erosion estimates have been calculated to be great, in the range of 1000-1500 m and 250-1000 m respectively (Faleide et al., 2010).

While the western part of the Barents Sea went through its bouts of rifting, stable tectonic conditions have more or less prevailed in the eastern part of the regional basin aside from epeirogenic movements (Faleide et al., 2010).

## **2.2 Paleozoic stratigraphy and depositional environment**

Most of the Barents Sea shelf contains upper Paleozoic rocks, which in turn can be divided into four major sequences from different regimes: Billefjorden, Gipsdalen, Bjarmeland and Tempelfjorden (Figure 2.2). Climate, sea level and tectonic regime changed throughout the era. Crustal movements made long term impact on the sea level while short-time geological processes were related to glaciations at the southern parts of Pangea (Smelror et al., 2009). New circulation patterns resulting from the consolidation of Pangea combined with drifting of the northern continental margin changed the climate conditions in the Barents Sea. The paleo-latitude changed from approximately 20°N to 45°N through Carboniferous and Permian. Consequently, the climate changed from warm and humid to cooler conditions (Stemmerik and Worsley, 2005, Smelror et al., 2009)

In the western part of the Barents Sea there are limited instances of Early Devonian deposits, and they are only encountered in some grabens and sub-basins created by Caledonian tectonic movements. Most of the region was highland subjected to erosion (Smelror et al., 2009). Unlike the terrestrial environment of the west most of the eastern region was covered by shallow-water basins where carbonate sedimentation dominated, which changed into a depression of black shale sedimentation later on (Smelror et al., 2009).

### **2.2.1 Billefjorden Group**

Strata that exist of Late Devonian to Early Carboniferous age in the western region of the Barents Sea, the Billefjorden Group, largely consist of continental siliciclastics with the presence of coal beds. The environment was humid, warm, and terrestrial, with large amounts of lacustrine and fluvial sediments being deposited in developing half-grabens (Larsen et al., 2002). Southeastern parts of the Finnmark Platform include the only known marine influence, where the platform exhibit a transition between a continental to a marine environment from west to east. Worsley (2008) suggest that a seaway through the Nordkapp Basin connected the Finnmark Platform with the marine eastern parts of the Barents Sea at this time. Correlative marine sequences are assumed to exist in the Tiddlybanken and Nordkapp basins (Larsen et al., 2005).

In the eastern Barents Sea there existed a marine environment during Late Devonian, with a shallow marine carbonate platform covering areas south, west and north of Novaya Zemlya and the Timan-Pechora area. To the east there were deeper marine conditions, and the overall extent of the marine basins was increased by a marked marine flooding that graded into continental environments towards the west and northwest (Smelror et al., 2009).

### **2.2.2 Gipsdalen Group**

The Middle Carboniferous to Early Permian is stratigraphically represented by the Gipsdalen Group (Larssen et al., 2002). The extent of the eastern carbonate shelf conditions continued to expand with a regional transgression during Late Carboniferous, and as such reached the western Barents shelf as well. While the environment was still warm, the area additionally drifted northward into semi-arid and arid conditions (Smelror et al., 2009). The deposition of the Gipsdalen Group was influenced by frequent glacially induced sea level fluctuations. Sea level lows episodically left most of the highs subaerially exposed and led to widespread dolomitization and karstification. In addition, rhythmic parasequences are a characteristic of the group. The main regional depositional environment throughout the Barents Sea was that of a warm-water carbonate platform with shallow marine carbonate, sabkha evaporites and local siliciclastics being the dominant deposition. Western basins were semi-enclosed and filled with evaporites because of their isolated nature, while the deep basins in the eastern Barents and Kara seas were filled with shales and carbonate mudstones (Henriksen et al., 2011). Studies on the Finnmark Platform have indicated that the area experienced a larger degree of lateral variability in depositional environments of the Gipsdalen Group than equivalent deposits found on Svalbard (Samuelsberg et al., 2003).

### **2.2.3 Bjarmeland Group**

While the area containing the present-day Barents Sea was still moving further north towards its current location, several factors contributed to an abrupt change in depositional regime. As the ice cap at the southern parts of Pangea waned and disappeared so did the rhythmic high-frequency depositions of the Gipsdalen Group (Worsley, 2008). The western Barents Sea was mostly made up of a distal marine low-energy shelf, whereas the eastern region was made up of a shallow-marine to slope and deep basin facies (Henriksen et al., 2011). A major flooding event marked the shift to a temperate environment, where cool-carbonates dominated in the

Early to Middle Permian Bjarmeland Group. While large build-ups developed in the major basinal margins the group is much thinner or absent over inner platforms and structural highs, e.g. on the southern Finnmark Platform, which experienced uplift and karstification during this time interval (Worsley, 2008). Equivalent deposits are found to be missing or very thin in outcrops on Svalbard, and the group is mainly correlated with North Greenland and other offshore areas (Samuelsberg et al., 2003).

#### **2.2.4 Tempelfjorden Group**

A shift in depositional environment occurred during Middle to Late Permian as large-scale compression resulted in the development of the Uralides. This was associated with a shift in seaway connections and concurrent major plate reorganization (Worsley, 2008). The carbonate platform deposition in the Barents Sea area came to an end as a regional sag basin became the depocenter for the Tempelfjorden Group, the last of the four main upper Paleozoic sequences. A consequence of the Uralian Orogeny was that the connection between the Barents Sea shelf and one of the existing seas, warm-water bringing Tethys, was severed. Additionally, the orogeny brought a flux of clastic sediment supply (Smelror et al., 2009, Lundschieen et al., 2014). With the plate reorganization an intracratonic seaway was established in the west and as the region experienced increased subsidence rates cold- and deep-water fine clastics and silica-rich spiculites were deposited (Worsley, 2008). Along the northern Pangean shelf margins spiculite build-ups related to transgressive events are found (Larssen et al., 2002), though these are not found in outcrop areas or most offshore areas other than on the Finnmark Platform (Samuelsberg et al., 2003).

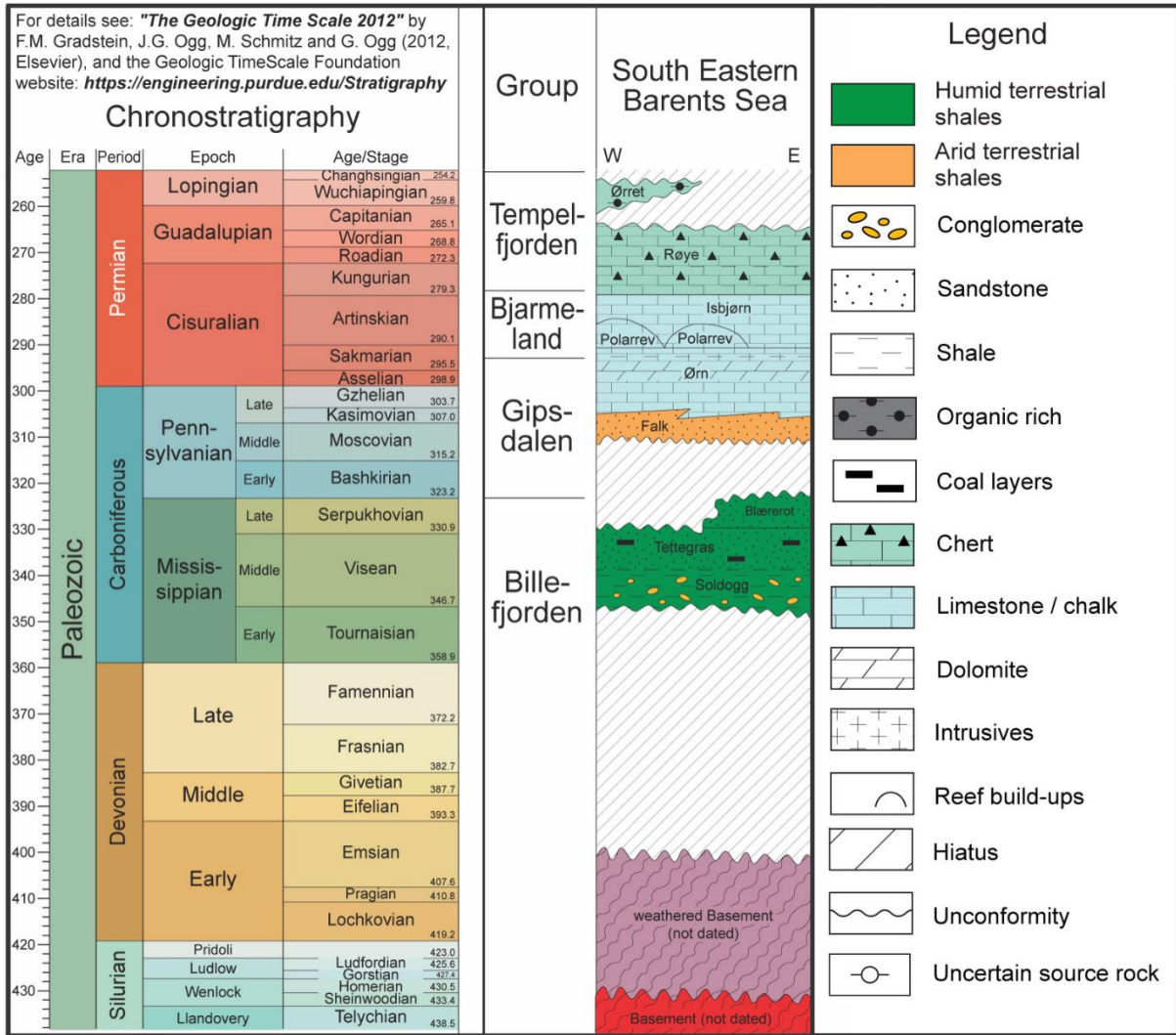


Figure 2.2 Chronostratigraphy and facies summary of Paleozoic strata in the southeastern Barents Sea. Chart modified from Ogg (2013).

## 2.3 Structural setting

There are five large structures within the study area: the Bjarmeland and Finnmark platforms, the Nordkapp and Tiddlybanken basins and the Fedynsky High (Figure 2.3). Additionally, the opening of the BSSE led to new structural elements being defined: the Veslekari, Haapet and Signalhorn domes (Mattingsdal et al., 2015). As previously mentioned, throughout the Barents Sea there are two main structural trends that dominate the orientation of the structures as a function of two major collision events, i.e. the Caledonian and Uralian orogens. These trends are present in the following structural elements as the overall SW-NE orientation of the Nordkapp Basin and the NW-SE orientation of the Tiddlybanken Basin (Dodson, 2014).



Figure 2.3 The main structural elements present in the Barents Sea South East. Modified from NPD (2018).

### **2.3.1 Bjarmeland Platform**

The Bjarmeland Platform is a stable area located north of the Nordkapp Basin and it is the main structural element in the northern part of the study area (Figure 2.3). Formed during Late Carboniferous and Permian, the platform has been mostly stable since upper Paleozoic. Uplift during Tertiary times has made it dip slightly to the south. There are relatively few structures within the platform and most of the structuring is related to salt tectonics and weak extension (Gabrielsen et al., 1990, NPD, 2013b).

### **2.3.2 Finnmark Platform**

The Finnmark Platform is located south in the study area (Figure 2.3). It is located north of the Norwegian coast and west of the Russian sector of the Barents Sea, and it has southern termination outside the coast of Tromsø. As with the Bjarmeland Platform, the tectonic regime of the Finnmark Platform has been stable since Late Paleozoic, though a Tertiary effect is assumed to be behind the gentle northerly tilt of the platform (Gabrielsen et al., 1990). Most of the basement configuration of the eastern Finnmark Platform was hardly affected by the Caledonian Orogeny and was instead mainly influenced by the Timanian Orogeny. While the SW Finnmark Platform had extensive rift-structures developing during Carboniferous rifting there is no evidence of this taking place on the eastern part of the platform (Stemmerik and Worsley, 2005, Colpaert et al., 2007).

### **2.3.3 Nordkapp Basin**

The Nordkapp Basin is located in the western part of the study area, between the Bjarmeland and Finnmark platforms (Figure 2.3). It is a several kilometers deep basin thought to have been one of several major rift-basins formed during the Carboniferous rift-phase which followed the SW-NE orientation trend. Its extensional structures were stabilized prior to Permian, and throughout Carboniferous and Permian the Nordkapp Basin was a shallow basin with thick evaporite deposits. As the depositional environment changed and terrestrial deposition took place the evaporites was overlain by thick successions of shale and sand whose added load acted as a driving force for movement. Several bouts of salt movement took place in the basin during Triassic and Paleogene, leaving large salt diapirs which at some instances reach the sea floor (Gudlaugsson et al., 1998, NPD, 2013b).

#### **2.3.4 Tiddlybanken Basin**

Also located on the Finnmark Platform is the Tiddlybanken Basin, whose axis is oriented almost perpendicular to the Nordkapp Basin (Figure 2.3). Like the Nordkapp Basin, large amounts of salt were deposited through Carboniferous and Permian. The salt started to move during Middle Triassic, leading to large diapiric structures within the basin (NPD, 2013b, Lundschieen et al., 2014). Overall, the development of the Tiddlybanken Basin is not well-known, though Gabrielsen et al. (1990) state that it is reasonable to assume that its development was similar to the Nordkapp Basin.

#### **2.3.5 Fedynsky High**

The Fedynsky High is located east in the study area, across from the Nordkapp basin (Figure 2.3). It is a large area that was thoroughly eroded when fault movements elevated it and left it above sea level. This erosion, which was quite deep, resulted in an absence of layers centrally on the high (NPD, 2013a). The Carboniferous and Permian layers of the area are cut by a deep graben which is oriented in the same direction as the Tiddlybanken Basin. Later inversion of the deep graben has formed the current highest point of the Fedynsky High in the Norwegian sector. The Fedynsky High lies mostly on the Russian side of the border, which is why the Russian name of the structure is currently used; Hjalmar Johansen High is another name used for the structure, e.g. in the article by Henriksen et al (2011) (NPD, 2013a, Mattingsdal et al., 2015).

#### **2.3.6 Domes in the BSSE**

The Veslekari Dome appears on the Bjarmeland Platform NE of the Nordkapp Basin, the Haapet Dome appears furthest NE in the BSSE on the Bjarmeland Platform and the Signalhorn Dome appears SW of the Tiddlybanken Basin on the Finnmark Platform (Figure 2.3). Carboniferous to Early Permian evaporites whose withdrawal triggered doming are assumed to be behind the dome structures (Mattingsdal et al., 2015). The genesis of the structures presumably started at different times; with the Signalhorn Dome starting to develop during Triassic to Early Cretaceous, the Haapet Dome during Early Cretaceous and the Veslekari Dome during Paleogene (Mattingsdal et al., 2015).



### 3. Data and methods

The main data applied are 2D seismic lines acquired by NPD: NPD-BA-11 and NPD1201 (Figure 3.1). In addition to the seismic data two key exploration wells, 7229/11-1 and 7128/4-1, have been used to correlate the seismic units to chrono- and lithostratigraphy and to estimate the resolution of the data sets. The following subchapters present the dataset, elaborate on seismic reflection theory and introduce the seismic interpretation methods that will be used for describing the data in the next chapter.

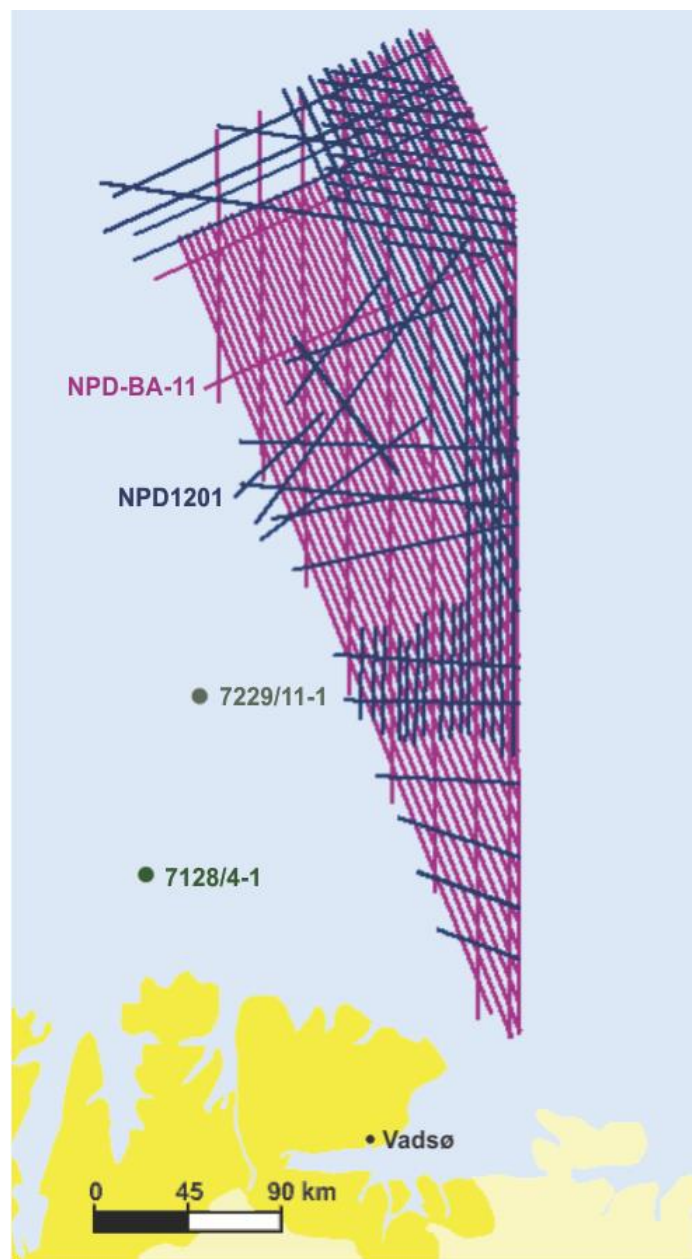


Figure 3.1 Location of the datasets and wells used in this thesis.

### 3.1 Dataset

NPD-BA-11 was acquired by PGS for the Norwegian Petroleum Directorate (NPD) during the summer of 2011 using GeoStreamer-technology. It consists of 42 lines that comprise approximately 11500 km. NPD1201 consist of 55 lines which comprise approximately 6800 km and was acquired by Dolphin Geophysical using conventional methods. NPD1201 was collected to fill in and supplement the previous survey and covers areas that are deemed especially interesting (NPD, 2013b).

The data in this thesis have been processed by NPD. The z-axis is displayed in two-way travel time (twt) as the seismic data is not depth-converted. The seafloor in seismic sections is represented by a positive reflection coefficient (see Chapter 3.2) which takes the form of either a trough or a peak depending on the processing. In using the seafloor and the SEG polarity from Sheriff (2002) as a reference, the polarity and phase of the datasets can be shown to exhibit a zero-phase signal with reverse polarity, shown by Figure 3.2, where an increase in acoustic impedance is displayed as a trough (blue).

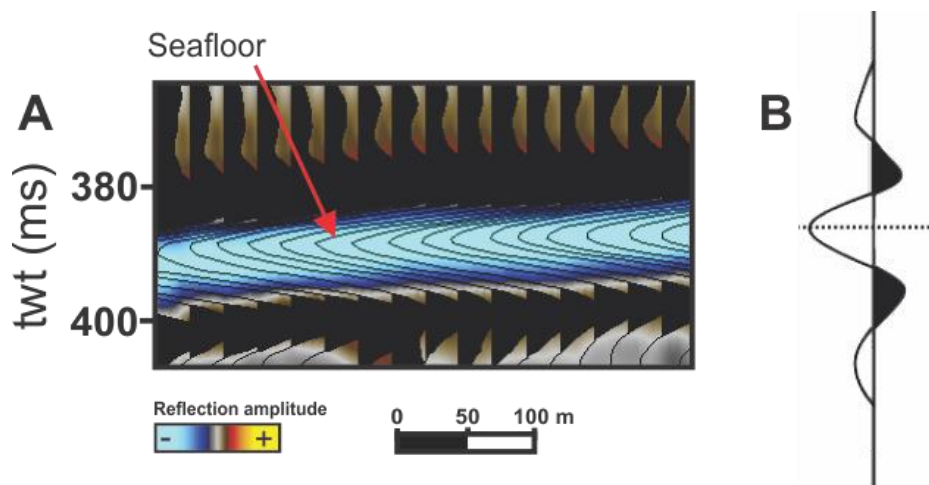


Figure 3.2 A) Seismic section showing the wiggle trace and reflection amplitude of the sea floor horizon using a representative 2D seismic line from dataset NPD-BA-11. B) Model of a zero-phase, reverse polarity wavelet adapted from the SEG polarity standard as explained in Sheriff (2002).

### 3.1.1 Wells and well correlation

To correlate the seismic interpretation to lithostratigraphy use was made of well tops at stratigraphic boundaries provided by NPD in well 7229/11-1 (Figure 3.3). Emphasis was put on mapping three seismic units of the late Carboniferous and Permian sequence, which are equivalent to the Gipsdalen, Bjarmeland and Tempelfjorden groups. Additionally, information about acoustic velocities was collected from wells 7229/11-1 and 7128/4-1.

7229/11-1 was a dry wildcat exploration well drilled by A/S Norske Shell in 1993. Den norske stats oljeselskap a.s. (Statoil) was the drilling operator on 7128/4-1, a wildcat exploration well which was permanently abandoned in 1994 as an oil and gas discovery (NPD, 2018). Both wells are located on the Eastern Finnmark Platform west of the study area (Figure 3.1).

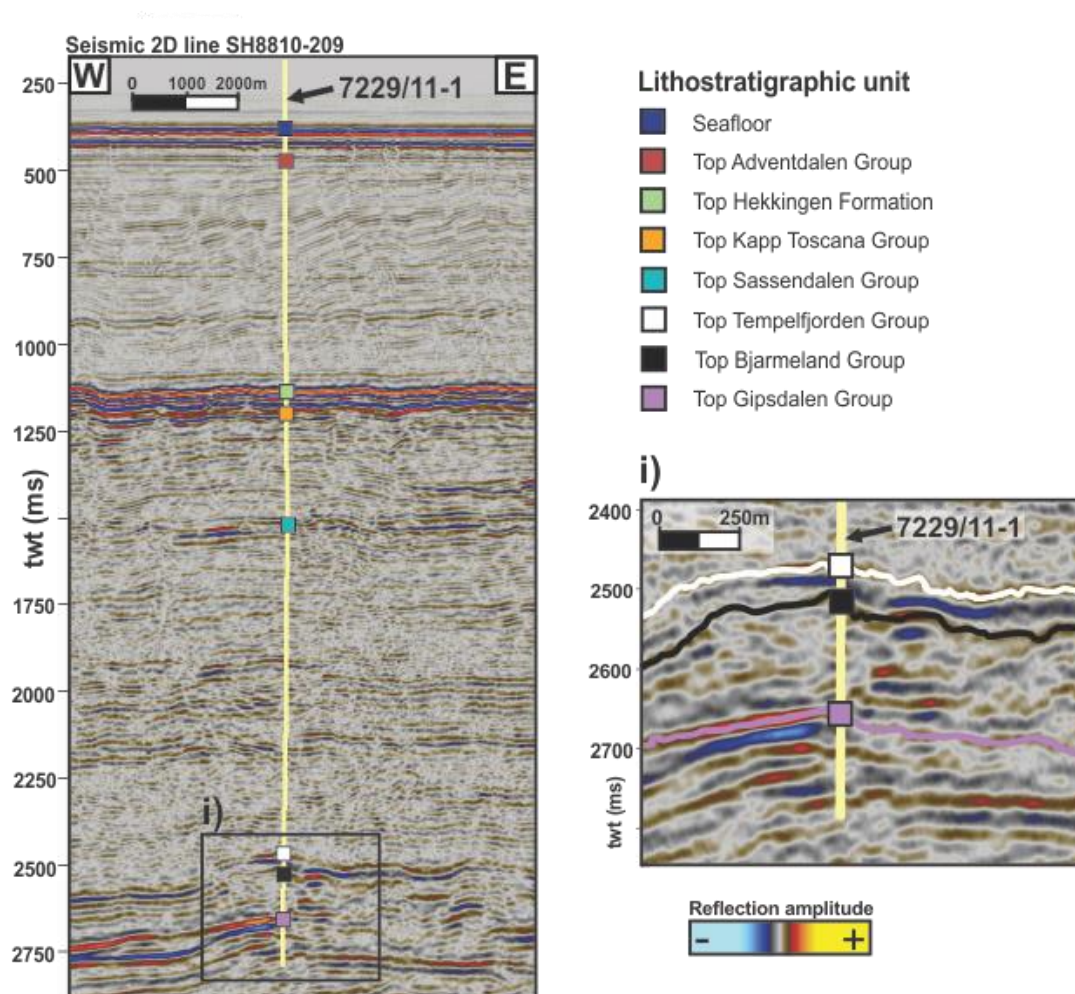


Figure 3.3 Illustration of well tops of lithostratigraphic units in well 7229/11-1 and their correlation to interpreted horizons in the datasets, as shown in i).

### 3.1.1.1 Units not tied to exploration wells

The top of the Billefjorden Group was mapped to provide a lower limit to the Gipsdalen Group (Figure 3.4B). The interpretation of the Top Billefjorden horizon is not tied to a well, as the oldest penetrated formation of well 7229/11-1 is the Ørn Formation of the Gipsdalen Group. Instead the horizon follows a conceptual model (Figure 3.4). In some areas the Top Billefjorden horizon is picked as the first discernable horizon with a negative reflection coefficient that appear underneath the interpreted Top Gipsdalen horizon (Figure 3.4B1). In other areas it is picked as the horizon appearing at the bottom of accumulations of recognizable semi-continuous horizons (Figure 3.4B2).

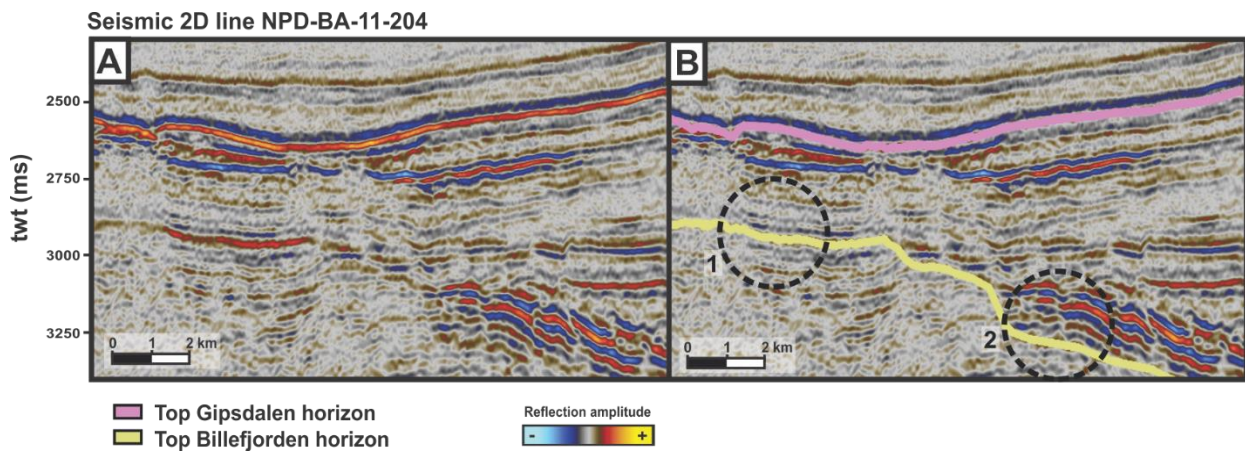


Figure 3.4 The conceptual model for the interpretation of the Top Billefjorden horizon is shown in the figure. A) Uninterpreted seismic section. B) Seismic section with the interpreted Top Billefjorden horizon: 1) area where the horizon has interpreted as the first discernable continuous negative reflection coefficient horizon below the interpreted Top Gipsdalen horizon, and 2) area where the horizon has been picked at the bottom of accumulations of semi-recognizable horizons.

## 3.2 Seismic reflection theory

The seismic reflection technique utilizes the different arrival times that seismic waves use when hitting interfaces to map the subsurface and its variations. A source sends out a pulse, the waves propagate, and the arrival times and amplitude of their reflections are recorded by seismic receivers and used to create seismic lines representing the travel times (Selley and Sonnenberg, 2014). One can convert these travel times into depth values, though this is not the case of the seismic data used for this thesis.

Seismic waves move through the earth as body and surface waves with speeds determined by the physical properties of the medium it moves through. Of these properties the porosity, mineral composition and the degree of cementation are the most important ones (Bjørlykke, 2015c). Seismic exploration methods are almost exclusively concentrated on the fastest of the elastic body waves, pressure waves. Pressure waves are easier to detect at short distances from the source than the other form of body waves, shear waves. Additionally, shear waves do not have the ability to travel through water. If the rock in question is homogenous the wave will travel at the same velocity through it away from the source (Kearey et al., 2002). Because of different properties of the subsurface rocks there are geological boundaries between them and these interfaces are what are recorded when using the seismic reflection technique. Seismic waves can be sent into the ground by using a controlled source (Kearey et al., 2002). The waves propagate through the subsurface until some of the energy of the seismic waves are reflected from the interfaces, given that there is a large enough contrast of the density and velocity of an interface between the two layers (i.e. acoustic impedance, Equation 3.1). These interfaces are known as seismic reflectors. Generally speaking the acoustic impedance increase with the hardness of the rock (Kearey et al., 2002).

$$Z = \rho V$$

*Equation 3.1:* For seismic layers the acoustic impedance,  $Z$ , equals the density  $\rho$  ( $\text{kg/m}^3$ ) multiplied by the layers' acoustic velocity  $V$  ( $\text{m/s}$ ).

### 3.2.1 Reflection coefficient

A measure for the amount of energy that is reflected at an interface is the reflection coefficient,  $R$  (Bjørlykke, 2015c). A calculation of  $R$  that is valid for a normally incident ray is shown in Equation 3.2. The values of  $R$  lie between  $-1 \leq R \leq +1$ , where a value of  $\pm 1$  means that 100% of the energy is reflected (Selley and Sonnenberg, 2014). As for the reason behind strong reflections there are several possibilities, such as lithology changes and pore contents. In most cases the reflection coefficients have a value between  $\pm 0,1$  and a reflector is considered strong if it has a reflection strength of  $\pm 0,2$  (Selley and Sonnenberg, 2014).

$$R = \frac{Z_2 - Z_1}{Z_2 + Z_1}$$

*Equation 3.2:* The reflection coefficient is calculated by using the acoustic impedance of the layer above an interface,  $Z_1$  and the layer below,  $Z_2$ . When  $Z_1$  is higher than  $Z_2$  the coefficient will be negative.

### 3.2.2 Seismic resolution

Seismic resolution is a description of how large a stratigraphic feature must be to be able to discern it in a seismic section, and has both a vertical and a horizontal aspect. If the feature is less than the seismic resolution it is not possible to determine where the effect of one feature ends and another one begins to contribute to the observed data (Sheriff, 1985). The wavelength, which can be described as a function of the quotient of formation velocity and the predominant frequency (Equation 3.3), is used. As the depth increases so will the velocity increase and the frequency decrease, leading to a change in the resolution. Rocks get more compacted and attenuation of higher frequencies occur, which together result in an increase in wavelength/decrease in resolution (Brown, 2011).

$$\lambda = \frac{V}{f}$$

*Equation 3.3:* The wavelength in meters,  $\lambda$ , can be found as a function of velocity,  $V$  (m/s), and the frequency,  $f$  (Hz).

### 3.2.2.1 Vertical resolution

When it comes to separating two reflectors the vertical resolution of the dataset is needed to determine the minimum distance between them. As reflections are generated at geological boundaries, a too thin layer (Figure 3.5) will create signals at its top and bottom which appear as a single response, interfering with the true picture (Mondol, 2015). There are two limits to the vertical resolution: the limit of separability (Equation 3.4) and the limit of visibility. Basically, the limit of separability is the wavelength needed to be able to separate two wavelets, while the limit of visibility is a variable fraction of the wavelength below which the signal becomes obscured by background noise (Brown, 2011). Badley (1985) mentions three critical parameters for vertical resolution: half-wavelength for no interference, quarter-wavelength for maximum interference, and one-thirtieth-wavelength for minimum thickness.

$$\text{Vertical resolution} = \frac{\lambda}{4}$$

*Equation 3.4:* The vertical resolution is a function of the acoustic wave's wavelength ( $\lambda$ ). A layer needs to be thicker than a quarter of the wavelength to be distinguished in a seismic section.

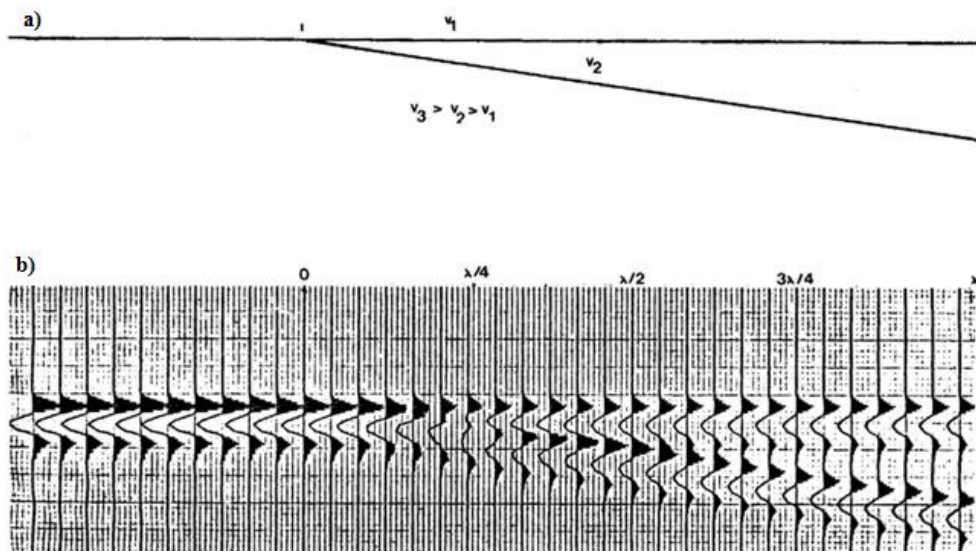


*Figure 3.5* Reflection of a wedge between two layers where the velocity increases with depth of the layers, illustrating vertical resolution. a) Shows a model and b) shows a seismic section in which the thickness of the wedge is described by a fraction of the wavelength. From Badley (1985).

### 3.2.2.2 Horizontal resolution

The horizontal resolution is the minimum lateral distance at which two reflection points can be separated (Kearey et al., 2002). Energy reflected from seismic reflectors stems from a larger area than a single point. When the reflected energy from the area is recorded within a half-wavelength from the first arrival they will interfere with each other and constructively build up the reflected signal (Kearey et al., 2002). With the vertical limit of separability being one-quarter of the wavelength, one can envision one wavefront appearing tangent to the seismic reflector and another appearing one-quarter wavelength ahead. Points within this diameter cannot be discerned from each other, and their intersection with the reflector is the Fresnel zone (Figure 3.6) (Bulat, 2005).

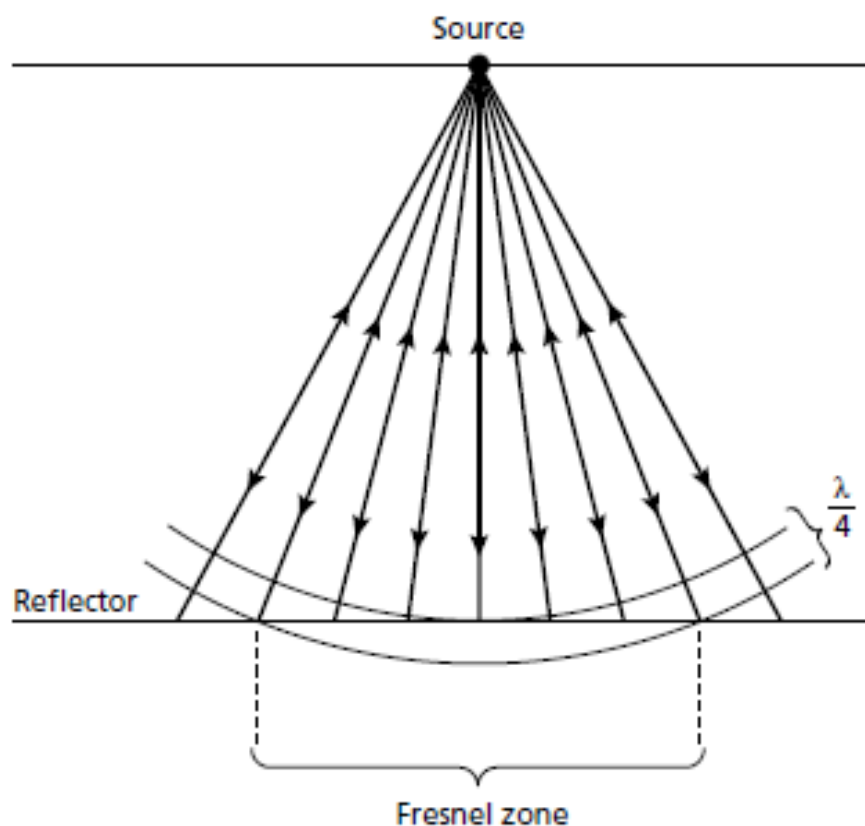


Figure 3.6 Illustration of the Fresnel zone on a reflector. From Kearey et al. (2002).

For unmigrated data the radius of the Fresnel zone is given by Equation 3.5.

$$\text{Fresnel zone} = \frac{V}{2} \sqrt{\frac{twt}{f}}$$

*Equation 3.5:* The horizontal resolution in meters as the radius of the Fresnel zone. V is average velocity in m/s, f is the dominant frequency in hertz and twt is the two-way time in seconds. From Badley (1985).

In 2D data acquisition a line of receivers is used to record the seismic signals, which does not always produce a clear image of the subsurface. The seismic signals can often be distorted by diffractions and geological features outside of the line (Brown, 2011). The horizontal resolution can be improved by migration, by which reflections that are out-of-place because of dip are repositioned, energy spread over a Fresnel zone is focused, and diffraction patterns from points and edges are collapsed. These issues are three-dimensional issues, since a seismic wavefront travels in three dimensions, and can only be partly improved when working with 2D lines. The post-migration Fresnel zone for 2D data can be collapsed in the inline direction (Figure 3.7) with a diameter of  $\lambda/4$  being the result of an optimal migration (Brown, 2011).

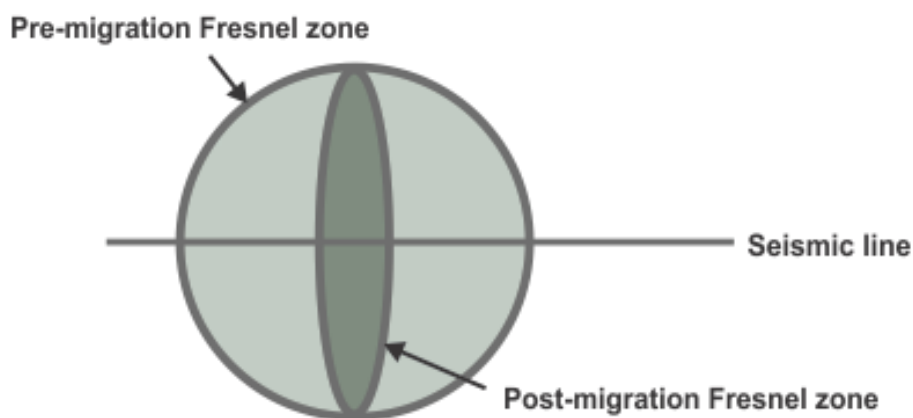


*Figure 3.7* An illustration of how the Fresnel zone differs between unmigrated and migrated 2D-data. The Fresnel zone can be shrunk in the inline direction, leaving an ellipsoid instead of a circle. Modified from Brown (2011).

### 3.2.2.3 Seismic resolution in NPD-BA-11 and NPD1201

For the approximate vertical resolution of the specific seismic data sets NPD-BA-11 and NPD1201 the sonic logs from wells and the inspector tool in Petrel were utilized. The velocities were picked at well tops in wells 7229/11-1 and 7128/4-1 (Figure 3.1) and converted from  $\mu\text{s}/\text{ft}$  to  $\text{m}/\text{s}$ . For the two-way travel time used in the calculations the average depths of the relevant reflectors were approximated from the depth distribution of the interpreted surfaces. The inspector tool allowed a spectral analysis to be performed on the seismic data, from which a frequency was picked. Using this tool, the peak value from the frequency spectrum of a chosen trace was picked from a line that had been cropped to represent the average upper Paleozoic depth interval. Table 3.1 shows a summary of the data used in calculating the vertical and horizontal resolutions, along with the measured depth at which the group well tops lie in the wells.

*Table 3.1* Summary of data used for calculating the vertical and horizontal resolution of the seismic data. Velocities are collected from sonic logs at well top depths in wells 7128/4-1 and 7229/11-1. Frequency and two-way travel time are approximated from seismic data.

Lithostratigraphic unit	7128/4-1		7229/11-1		From data sets	
	Velocity (m/s)	Depth (m)	Velocity (m/s)	Depth (m)	Frequency (Hz)	Two-way travel time (s)
Top Tempelfjorden Group	3425	1569	4386	3879	15	2,7
Top Bjarmeland Group	5255	1704	6084	3970	15	2,75
Top Gipsdalen Group	5644	1820	6252	4282	15	2,85

Using the values from Table 3.1 and Equations 3.3, 3.4 and 3.5 the resolutions for the lithostratigraphic units mapped in this thesis have been calculated, as summarized in Table 3.2. As seen in the Table 3.2, the calculated smallest vertical feature discernable of Tempelfjorden Group range between the sizes of 57 m and 73 m dependent on the values used in the calculation. Assuming a velocity of 3425  $\text{m}/\text{s}$  gives a value of 57 m as Example 3.1 shows:

$$\frac{\lambda}{4} = \frac{V}{4f} = \frac{3425\text{m/s}}{4 \cdot 15\text{Hz}} = 57\text{m}$$

*Example 3.1* The calculation of vertical resolution of the Tempelfjorden Group when using the velocity from well 7128/4-1, shown as an example of vertical resolution calculations. The rest of the calculations are summarized in Table 3.2.

NPD-BA-11 and NPD1201 have both been processed and gone through a migration process which has increased the horizontal resolution. For the horizontal resolution of the data sets one can assume that it equals the vertical resolution in the inline direction after migration, while the calculated numbers (Table 3.2) show the horizontal resolution as encountered in the transversal direction.

*Table 3.2* Estimates of the values of the vertical and horizontal resolution. All values are in reference to the size needed to separate two features.

	<b>7128/4-1</b>		<b>7229/11-1</b>	
<b>Lithostratigraphic unit</b>	Vertical resolution (m)	Horizontal resolution (m)	Vertical resolution (m)	Horizontal resolution (m)
Top Tempelfjorden Group	57	727	73	930
Top Bjarmeland Group	88	1130	101	1308
Top Gipsdalen Group	94	1230	104	1363

### 3.3 Seismic interpretation

Interpretations in this thesis have been done by using the Petrel E&P software from Schlumberger Limited. This software includes several tools and features used for analysis of seismic data, interpreting horizons, generating seismic attribute maps and for retrieving further geological information from datasets.

Most of the horizons are interpreted throughout all the seismic lines by using the seeded 2D auto tracker, for which the interpretation is performed automatically until irregularities not fitting defined parameters occur. For areas where the horizons were too discontinuous to use the 2D auto tracker use was made of the manual interpretation function, where the software interpolates a linear line between two picks. Generation of seismic attributes were also done to aid the interpretation path.

#### 3.3.1 Seismic attributes

Seismic attributes are measurements from seismic data which are used in order to better discern features and infer properties that are hard to define without them (Chopra and Marfurt, 2007). There are several attributes based on the same properties, and because of that there are a lot of duplicate attributes showing more or less the same image. Attributes are usually based on time, amplitude, frequency and/or attenuation measurements (Chopra and Marfurt, 2007).

The *Cosine of the phase*-attribute removes all amplitude contrasts. The purpose of the attribute is to enhance the continuity of events, as the events appear amplitude independent (Bitrus et al., 2016).

The *Time-thickness map*-attribute uses two seismic surfaces and calculates the thickness between them in two-way travel time.

The *Root Mean Square (RMS) amplitude* is defined by Sheriff (2002) as the “*average of the squares of a series of measurements*”. It is used as measure of how acoustic impedance varies over given areas (Bitrus et al., 2016).

### **3.3.2 Seismic stratigraphy**

Seismic stratigraphy is a way of identifying and mapping depositional systems by using seismic data. It is a branch of the wider sequence stratigraphy. Steps in seismic stratigraphy include identifying seismic sequences and seismic facies analysis. Essentially, seismic stratigraphy involves splitting a seismic section into units based on the appearance and relations of seismic reflectors. While the age and lithology of a unit cannot be directly identified in seismic data without well-data control the units are still mappable and can provide a basin-wide and regional image of the subsurface (Brown, 2011, Selley and Sonnenberg, 2014).

For any seismic section there are four main groups of reflections to be seen in the data: sedimentary reflections, unconformities, artefacts and non-sedimentary reflections. Each individual sedimentary reflection may be considered a timeline, representing a bedding plane and a fairly short time interval where continuous sedimentation conditions prevailed (Veeken and van Moerkerken, 2013). An implication of the seismic reflection being seen as a timeline is that a continuous reflector may laterally be part of changing environmental conditions. Sedimentary reflections are used in seismic facies analysis. As for the other main groups of reflections, artefacts include random and systematic noise from the acquisition of the data and unconformities represent time gaps in the geological record as surfaces of erosion and/or non-deposition. Additionally, non-sedimentary reflections includes several types of coherent reflections like fault planes, fluid contacts and mineral phase changes (Veeken and van Moerkerken, 2013, Mondol, 2015).

#### ***3.3.2.1 Seismic sequences***

Chronology can in favorable circumstances be deduced by identifying seismic sequences. Bound at their top and base by unconformities and/or their correlative conformities, a depositional sequence is a division of the rock record into a collection of individual beds with genetically related strata. These sequences are thought to represent instances of basically constant depositional environments and processes (Badley, 1985). A seismic sequence has all the properties of a depositional sequence, given that the properties in question are identifiable in a seismic section, and the top and base are marked by reflection terminations (Figure 3.8). Upper boundary terminations include erosional truncation, toplap and concordance, while lower boundary terminations include onlap, downlap and concordance (Mitchum Jr. et al.,

1977). Erosional truncation marks an unconformity and implies later removal of strata, while toplap implies non-deposition and limited erosion. Both upper and lower concordance indicate a common deformation of interface and substratum, which may or may not include a time gap between the layers. As for onlap termination, it is found where aggradation of deposits induced by relative increase in accommodation space takes place. Lastly, downlap terminations occur where inclined strata are deposited against an inclined or horizontal surface (Mitchum Jr. et al., 1977, Veeken and van Moerkerken, 2013).

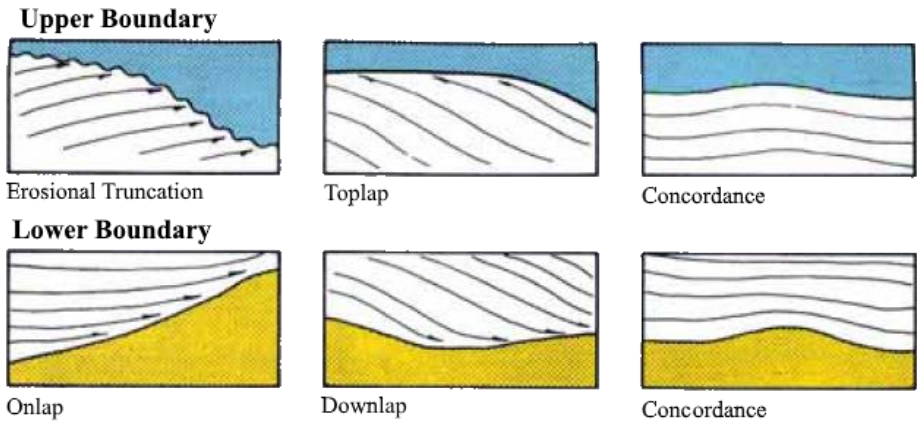


Figure 3.8 Strata relations to upper and lower boundaries of a seismic sequence. From Veeken (2007).

**3.3.2.2 Seismic facies**

Sedimentary facies is a term which encompasses all the characteristics of a sedimentary unit; its dimensions, grain size, biogenic content, etc. Together these characteristics form a basis for interpreting the paleoenvironment, as different environments with their different processes result in distinctive facies assemblages. Seismic facies and seismic facies analysis then, group seismic reflections together based on their similarities, assuming them to be a function of the paleoenvironment of the unit (Nichols, 2009). Several parameters make up the basis on which seismic facies are separated: the configuration, amplitude, continuity, frequency and interval velocity of the reflections (Mitchum Jr. et al., 1977).

### *3.3.2.3 Carbonates in seismic data*

Generally, the upper boundaries of carbonates show up as a horizon with a positive reflection coefficient. However, where the carbonates are very porous or fractured the boundary may have a negative reflection coefficient (Badley, 1985). Velocities of carbonates are generally much faster than those of siliciclastics found at the same depth. From Equations 3.3, 3.4 and 3.5 it can therefore be inferred that carbonates will have a lower seismic resolution given a constant frequency. Carbonates are additionally, in large parts, denser than siliciclastics. The higher density combined with the higher velocity result in a higher acoustic impedance and therefore strong reflection coefficients at the boundaries to its surroundings, as explained by Equations 3.1 and 3.2.

Furthermore, the appearance of carbonates in seismic sections have additional challenges compared to their siliciclastic counterparts (Palaz and Marfurt, 1997). For one, carbonates are sensitive to diagenetic alterations which may cause lateral velocity variations, seen as amplitude variations in continuous reflectors. Karstified rock, when the result of diagenetic processes, contribute to back-scattering and conversion of seismic waves making recognition of the reflections below the layer and the boundary difficult (Palaz and Marfurt, 1997). Also, diagenesis may change or destroy original depositional geometries by dissolution and karstification, leaving blank zones in carbonate reefs and platforms (Chopra and Marfurt, 2007).

A problem with recognizing carbonate build-ups lies with their often small size, as the resolution of the seismic may be too low to image them. Interference between individual sub-seismic mounds may result in large mound-like structures being observed in the seismic (Nielsen et al., 2004). There are four main major types of carbonate build-ups: barrier, pinnacle, shelf-margin and patch build-ups (Badley, 1985). With carbonate build-ups, though they are relatively porous, there might be a high degree of cementation which binds the grains together in a way that increases the velocity (Bjørlykke, 2015c).

### 3.3.2.4 Evaporites in seismic data

Salt is markedly less dense than other sediments. Furthermore, after the effective porosity of salt is lost by initial burial its density remains nearly unchanged, as salt largely does not compact with depth. Thus, with increasing depth there is an increased density difference between salt and its surroundings, as clays and sand do compact (Warren, 2006). Movement of halite due to density differences can create salt structures, where the lighter halite moves and either actively pierces overlying sediment layers or remains more-or-less at the same depth while its surrounding sediments subside (Sheriff, 2002). Salt dome formation requires a salt layer thickness of at least 100-200 m and is recognized in seismic data as a mushroom-shaped or columnar structure. Anhydrite, which is a mineral found in evaporite deposits (Allaby, 2013), is too dense to form salt domes (Bjørlykke, 2015a).

In addition to the external shape, internally salt is characterized in seismic data by an absence of parallel reflectors in the form of either a chaotic pattern with random reflectors or by a reflection-free appearance (Nichols, 2009). Additionally, the compressional wave velocities of evaporites are in large parts faster than other sediments, with halite having a velocity of 4500 m/s and anhydrite a velocity of 6000 m/s. With the faster travel times comes an added velocity pull-up pitfall where pre-salt reflectors may appear as anticlines in seismic data (Figure 3.9) (Selley and Sonnenberg, 2014).

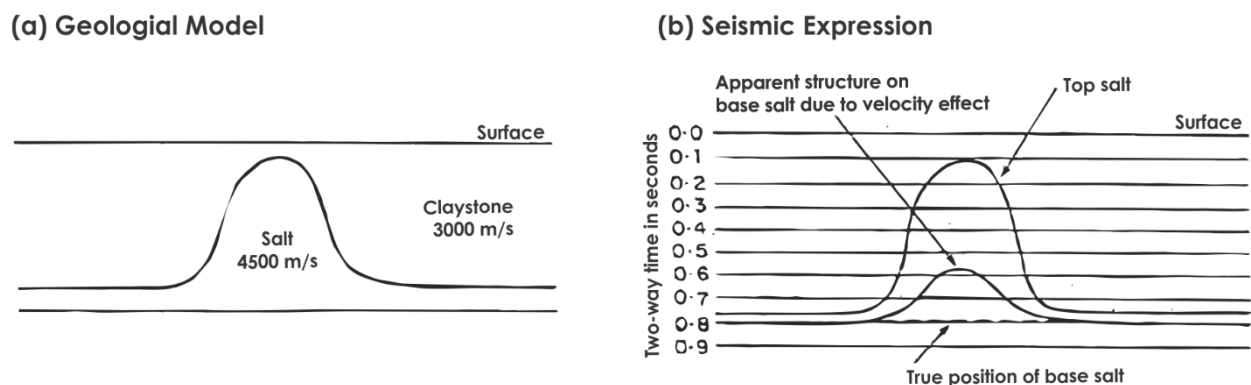


Figure 3.9 a) Geological model of a salt diapir. Compressional wave velocities between the salt and surrounding claystone differ by 1500 m/s. b) Seismic expression of salt diapir, showing how the true position of base salt is distorted by velocity effect. From Badley (1985).

## 4. Results

The main focus of this thesis is the different depositional systems of the late Carboniferous and Permian in the BSSE. Horizons corresponding to well tops from well 7229/11-1 provided by NPD were mapped (Figure 4.1). The horizons divide the discussed stratigraphy into three seismic units. Starting with a division of the BSSE into six main seismic areas, the following subchapters will present and describe the mapped horizons and seismic units. Furthermore, the general appearance of the mapped horizons, the general appearance of the seismic units, and the appearance of horizons and units as observed in specified seismic areas of the BSSE will be described.

The top of the Paleozoic sequence, the Top Tempelfjorden horizon, forms a consistent recognizable boundary to its overlying seismic horizons, as it is characterized by high amplitude and continuity (Figure 4.1). The base of the Paleozoic sequence, the Top Billefjorden horizon, has a less clear divide and is characterized by an overall low amplitude and semi-continuity. Figure 4.2 illustrates the regional time-thickness variations of the interpreted Paleozoic sequence, generated between the Top Tempelfjorden and the Top Billefjorden horizons. Generally, the interval vary between 200 and 1200 ms (twt), though areas within the Veslekari and Signalhorn domes are the thickest in the study area and exceed these values, reaching a time-thickness maximum of 2100 ms (twt). Within the Nordkapp and Tiddlybanken Basin there are zones of poor data quality and as such areas within the basins have been cropped out of the time structure and time-thickness maps presented in this chapter.

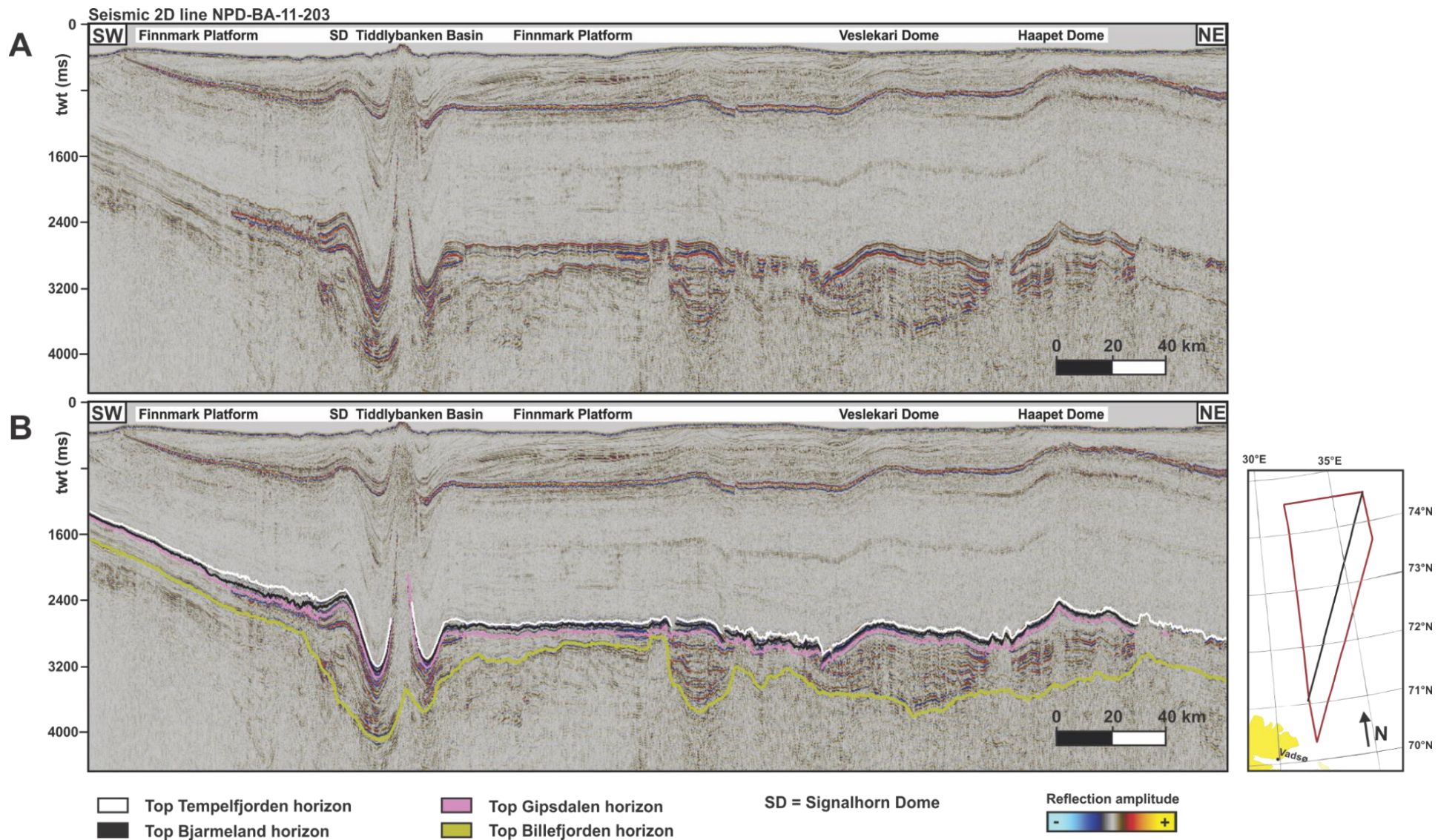
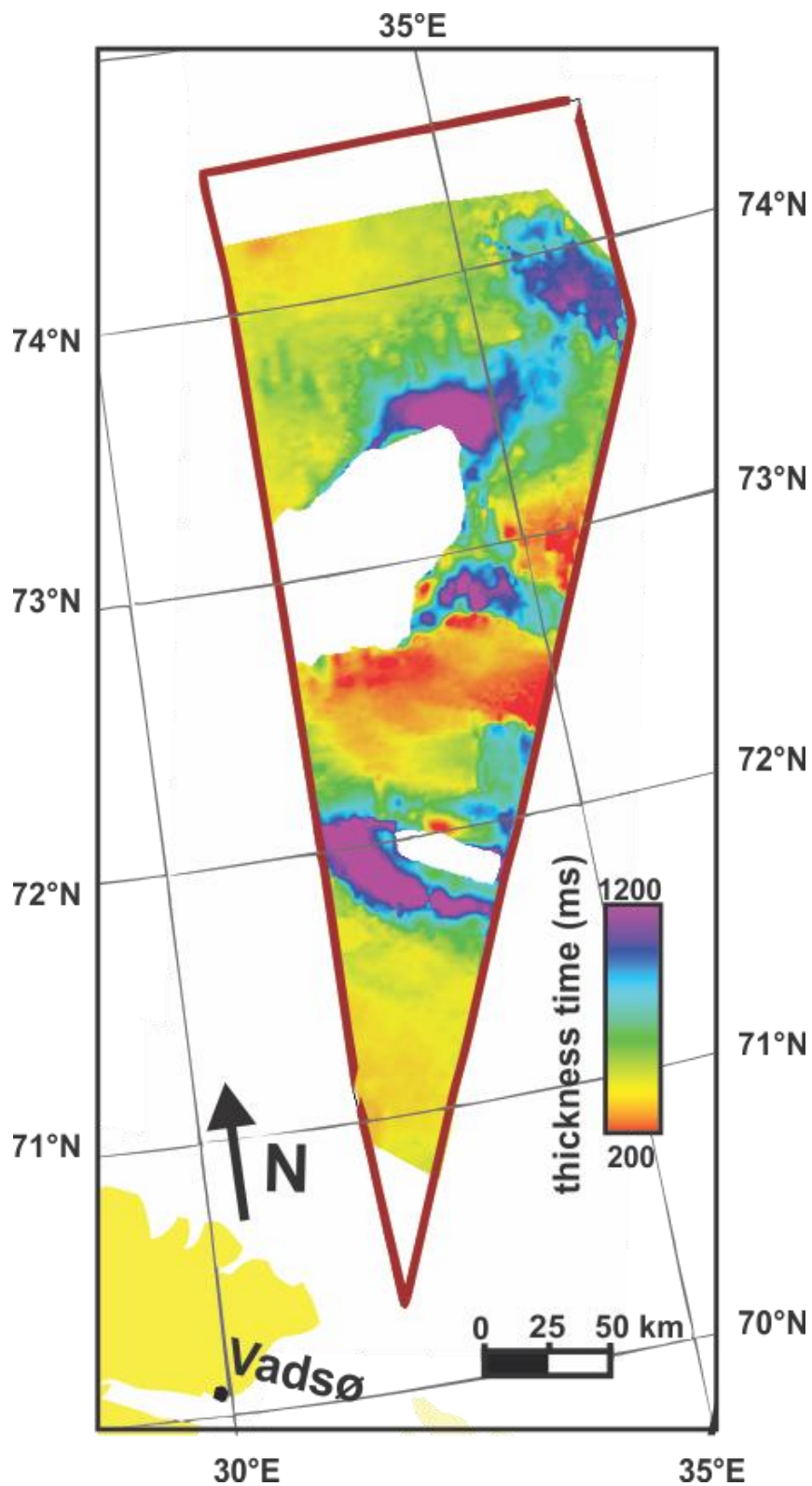


Figure 4.1 Regional profile of the Barents Sea South East from SW to NE. The location of the seismic line is shown on the index map to the lower right. A) Uninterpreted seismic section. B) Interpreted seismic section displaying the four main mapped horizons. With the exception of the Top Billefjorden Horizon, parts of the Tiddlybanken Basin are left uninterpreted because of poor resolution due to halokinesis.



*Figure 4.2* Time-thickness map of the interpreted upper Paleozoic sequence, as restricted by the interpreted Top Billefjorden and Top Tempelfjorden horizons. The thickest areas exceed the 1200 ms (tw) indicated by the map and in places reach a maximum time-thickness of 2100 ms (tw).

## 4.1 Seismic Areas

The BSSE spans an area of 44 000 km<sup>2</sup> with several features present, and is for the descriptions in this chapter geographically divided into six seismic areas based on changes in time-thickness and internal appearance of horizons (Figure 4.3).

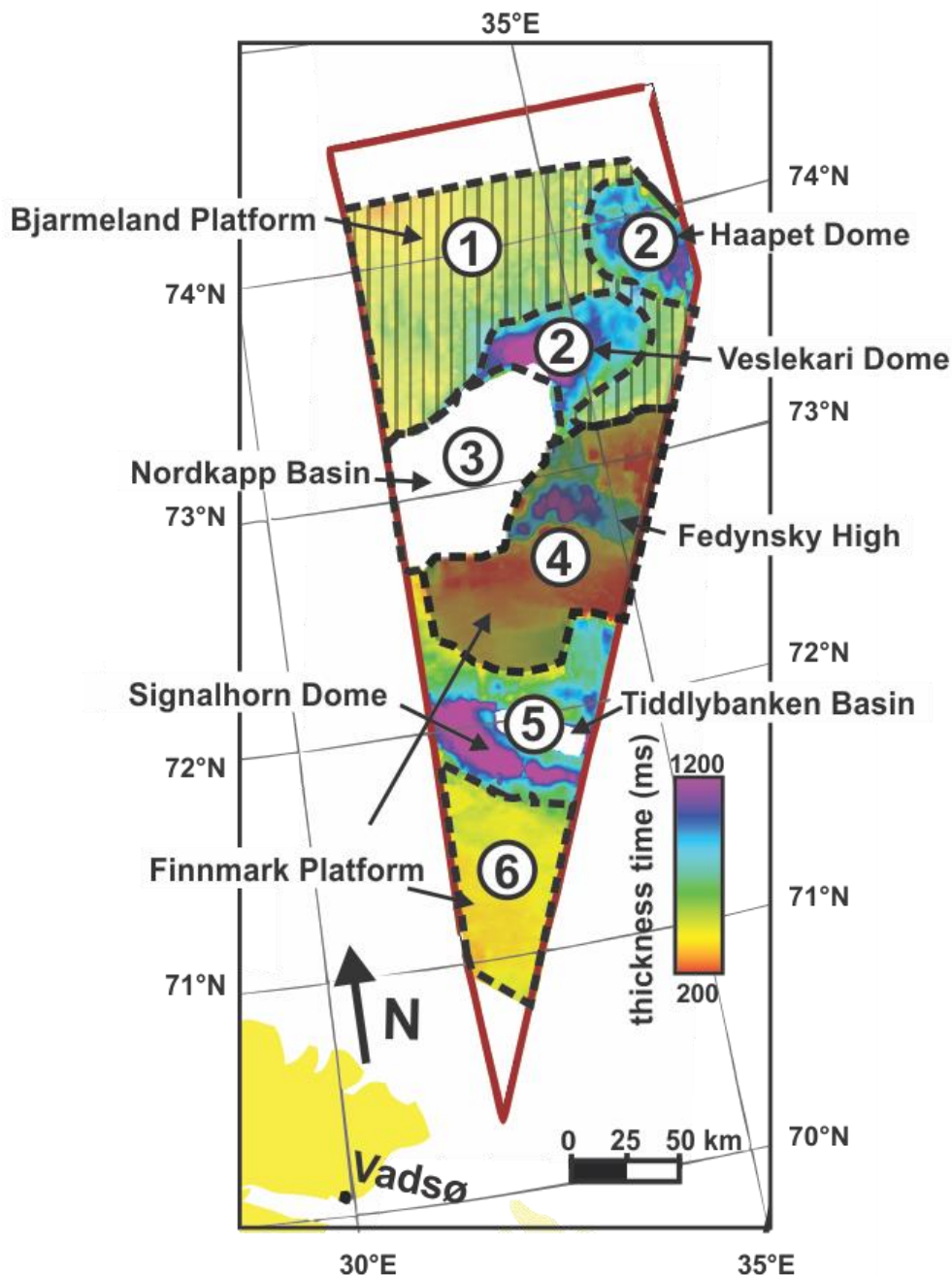


*Figure 4.3* Time-thickness map of interpreted upper Paleozoic sequence outlining seismic areas (1-6) described in chapter 4.3. 1) The Bjarmeland Platform, 2) Veslekari and Haapet domes, 3) Nordkapp Basin, 4) Fedynsky High and NE Finnmark Platform, 5) Tiddlybanken Basin and Signalhorn Dome, 6) Finnmark Platform.

Seismic Area 1 is defined as the Bjarmeland Platform. The platform is located in the northern part of the BSSE, bordering the Nordkapp Basin, Veslekari Dome and the Haapet Dome (Figures 2.3 and 4.3). Overall the area shows uniform time-thickness and internal configuration within the collective mapped groups.

Seismic Area 2 includes two large dome structures appearing in the study area: the Haapet and Veslekari domes (Figures 2.3 and 4.3). The Haapet Dome appears northeast in the BSSE and has a maximum time-thickness of 1400 ms (twt) mid-dome for the Paleozoic interval (Figure 4.2). The Veslekari Dome is situated north of the Nordkapp Basin and is the site of the thickest package of the mapped Late Paleozoic sequence, reaching a time-thickness of 2100 ms (twt) (Figure 4.2). Southwest of the Veslekari dome the group top horizons all follow a synclinal path moving into chaotic zones of the Nordkapp Basin (Figure 4.19).

The NE part of the Nordkapp Basin is within the study area and makes up Seismic Area 3 (Figures 2.3 and 4.3). The NE margin of the basin borders the Veslekari Dome, while the Bjarmeland Platform and Finnmark Platform border the basin to the north and south, respectively. Large parts of the basin have been cropped out in the time-structure and time-thickness maps due to disrupted seismic signals within the structure, defined in other studies as salt diapirs (Figure 4.19, NPD (2013b)). Common for all the salt diapirs are the upward bending of the horizons around them (Figure 4.19). While large parts of the Nordkapp Basin consist of largely chaotic signals the basin does in some instances contain separable disrupted zones with recognizable horizons between them. These horizons appear at a larger depth than elsewhere in the study area.

Seismic Area 4 includes the Fedynsky High and parts of the surrounding Finnmark Platform (Figures 2.3 and 4.3). The Fedynsky High as recognized in Figure 2.3 is defined at the Cretaceous level, contrasting the morphology made by the Top Billefjorden horizon. The Top Billefjorden horizon forms a depression under the Fedynsky High (Figure 4.20). On the flanks of this approximately 22 km wide NE-SW Top Billefjorden horizon depression the mapped Paleozoic interval has an average time-thickness of 250 ms (twt), making it the thinnest segment of the mapped Paleozoic interval in the BSSE.

The Tiddybanken Basin, the proximally appearing part of the Finnmark Platform and the Signalhorn Dome represent the structural elements found in Seismic Area 5 (Figures 2.3 and

4.3). The area appears within the Finnmark Platform. Parts within the Tiddlybanken Basin have been cropped out in the time-structure and time-thickness maps due to disrupted seismic signals within the structure, identified as a salt diapir (NPD, 2013b). As can be observed in Seismic Area 3, the upward bending of the horizons around the salt diapir is apparent (Figure 4.21).

Seismic Area 6 encompasses the Finnmark Platform appearing south in the BSSE (Figure 2.3 and 4.3). There is a change in the internal configuration of all the defined groups as one moves further south on the Finnmark Platform: the Intra Gipsdalen Group sub-unit disappears, the amplitude strength of the horizons lowers and distinct changes in the time-thickness of the groups occur. The area is divided into a northern and southern part for the purpose of the description (Figure 4.4). The extent of the divide can be found as the southern end of the highest amplitudes of the Gipsdalen Group, as where the time-thickness of the Bjarmeland and Tempelfjorden groups changes from approximately 70 ms (twf) to 40 ms (twf) and approximately 120 ms (twf) to 50 ms (twf), respectively.

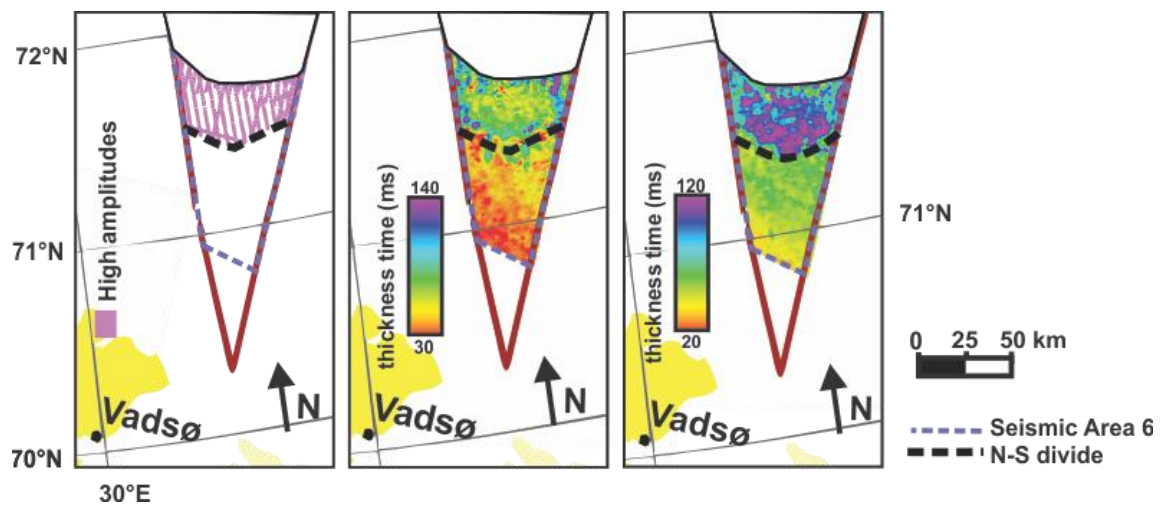


Figure 4.4 Basis for division of Seismic Area 6 (Finnmark Platform) into northern and southern part. A) Gipsdalen Group change in amplitude strength. B) Bjarmeland Group time-thickness change. C) Tempelfjorden Group time-thickness change.

## **4.2 Paleozoic horizons**

The Paleozoic interval of the BSSE has been divided into four main horizons traced throughout the study area (Figure 4.1). They represent the tops of the Billefjorden, Gipsdalen, Bjarmeland and Tempelfjorden groups and are based on well ties and a conceptual model for the Top Billefjorden horizon (Figures 3.3 and 3.4). The horizons define the three main units investigated. One additional horizon, the Base Intra Gipsdalen horizon, has also been mapped.

Regarding the overall time-structure trends of the Top Gipsdalen, Bjarmeland and Tempelfjorden horizons, they can be observed to show the same outline (Figures 4.6, 4.7 and 4.8). The deepest parts of the horizons are located at the edges of both of the large basins, i.e. the Nordkapp and Tiddybanken basins. Outside of the basin areas, the deepest parts are found surrounding the Nordkapp Basin from mid-west to mid-northeast. The horizons appear at shallower depths at the Veslekari and Haapet domes northeast of the outcropped parts of the Nordkapp Basin. The horizons become progressively shallower towards the southwest, east and northeast of the deeper areas.

### **4.2.1 Top Billefjorden**

Characterized by a decrease in acoustic impedance, the Top Billefjorden horizon is semi-continuous with a low to medium amplitude strength (Figure 4.1 and 4.9). It represents the boundary between the Billefjorden Group and the overlying Gipsdalen Group and forms the base of the seismic sequences interpreted and mapped in the study area. A trend of overall deepening from the southwest on the Finnmark Platform towards northeast of the Nordkapp Basin is apparent on a regional scale, whereas the horizon has an intermediate depth northwest of the Nordkapp Basin (Figure 4.5). On a regional basis the twt-values of the Top Billefjorden horizon ranges between 1500 and 4300 ms (twt), with the majority of the surface situated between 3500 and 3900 ms (twt).

### **4.2.2 Base Intra Gipsdalen**

The horizon is referred to as the Base Intra Gipsdalen horizon and is mapped between the Top Billefjorden Group and the Top Gipsdalen horizons. It is identified by an increase in acoustic impedance, shows medium to high continuity and has a high amplitude strength (Figure 4.9). It

occurs locally surrounding the larger basins in association with the highest amplitude areas of the Top Gipsdalen Group (Figure 4.10B). The twt-values for the horizon ranges from 2400 to 3300 ms (twt).

### **4.2.3 Top Gipsdalen**

In the seismic sections, the top of the Gipsdalen Group is identified by a decrease in acoustic impedance (Figure 4.1 and 4.9). The horizon is laterally continuous and differs largely in amplitude strength. The highest amplitudes of the mapped upper Paleozoic sequence appear along the Top Gipsdalen horizon, observed predominantly around the Nordkapp and Tiddlybanken basins. Elsewhere the horizon has an overall medium amplitude and the twt-values range between 1175 and 4700 ms (twt), with the majority of them being between 2300 and 3400 ms (twt) (Figure 4.6).

### **4.2.4 Top Bjarmeland**

The boundary between the overlying Tempelfjorden Group and the underlying Bjarmeland Group is represented by a decrease in acoustic impedance (Figure 4.1 and 4.9). On a regional scale the Top Bjarmeland horizon can be described as semi-continuous, with areas where the horizon either disappears entirely or is seemingly present as intermittent low amplitude negative horizons. The interpretation confidence is considered low due to data quality. Overall, the amplitude strength is low with local instances of medium strength. The twt-values range between 1150 and 4650 ms (twt) with main parts of the group located between 2200 and 3200 ms (twt) (Figure 4.7).

### **4.2.5 Top Tempelfjorden**

Representing the top of the Tempelfjorden Group and as such the top of the upper Paleozoic succession, the Top Tempelfjorden horizon is represented by a decrease in acoustic impedance (Figure 4.1 and 4.9) The horizon has a relatively high continuity and a medium amplitude. Though the horizon varies somewhat in amplitude on a local scale, it represents a continuous and well-defined boundary between the Tempelfjorden Group and the over-lying discontinuous horizons throughout the study area. Twt-values of the horizon ranges between 1100 and 4600 ms (twt), with main parts of the areas located between 2200 s and 3200 ms (twt) (Figure 4.8).

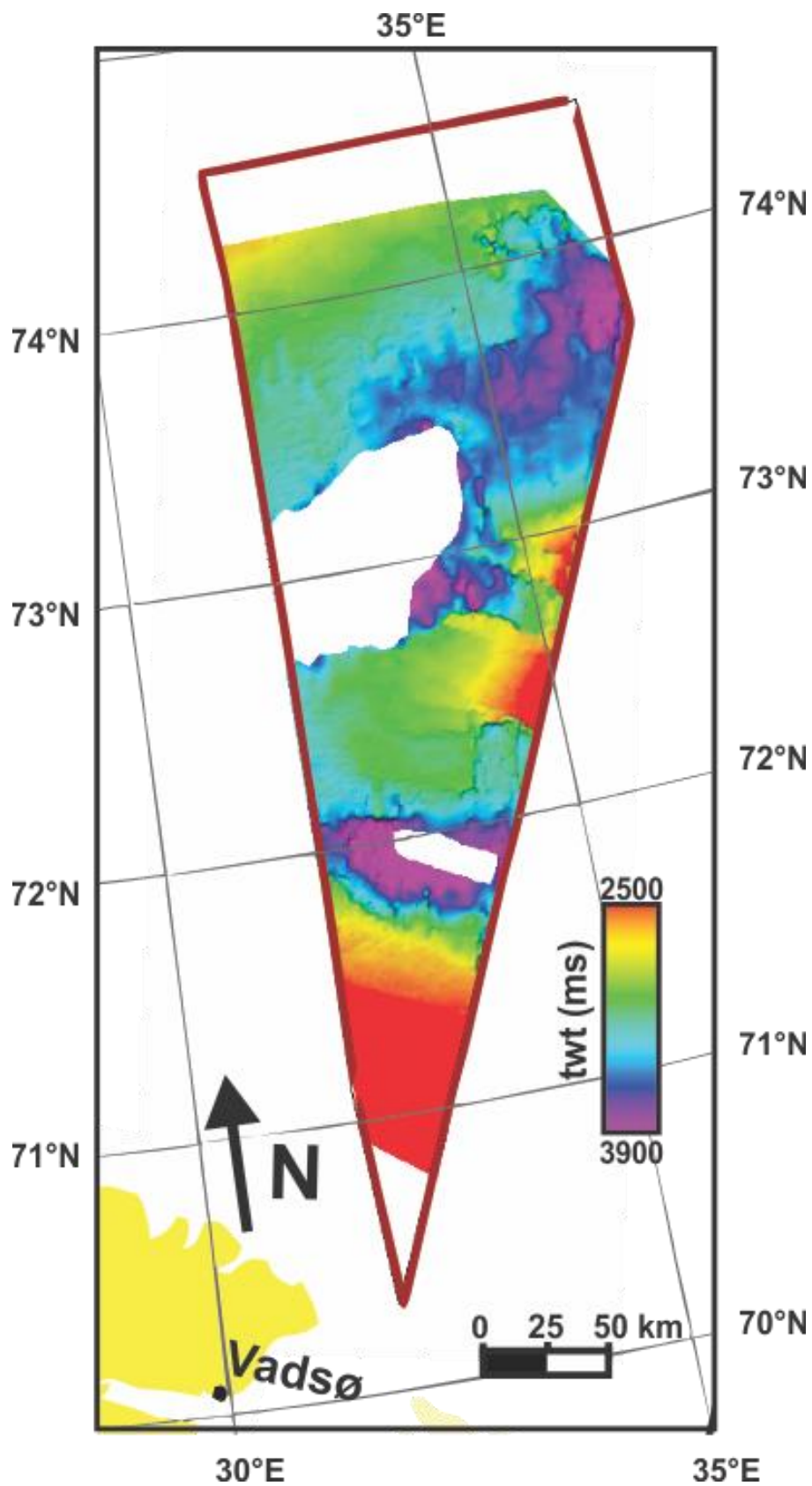


Figure 4.5 Time-thickness map of the Top Billefjorden horizon. Note that the twt-legend differs between the time-thickness maps and that the chaotic-reflection zones in the Nordkapp and Tiddlybanken Basins have been cropped out.

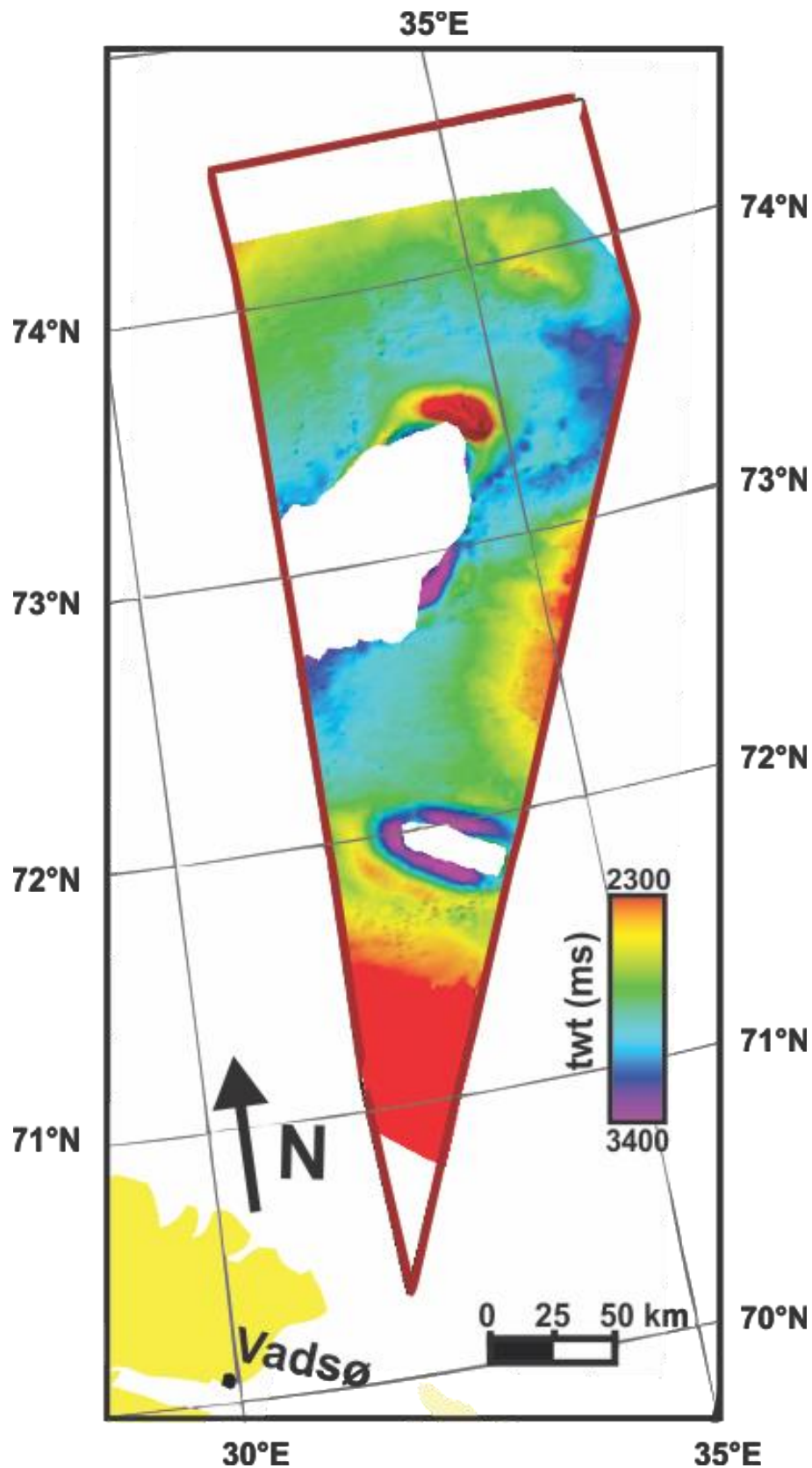


Figure 4.6 Time-thickness map of the Top Gipsdalen horizon. Note that the twt-legend differs between the time-thickness maps and that the chaotic-reflection zones in the Nordkapp and Tiddlybanken Basins have been cropped out.

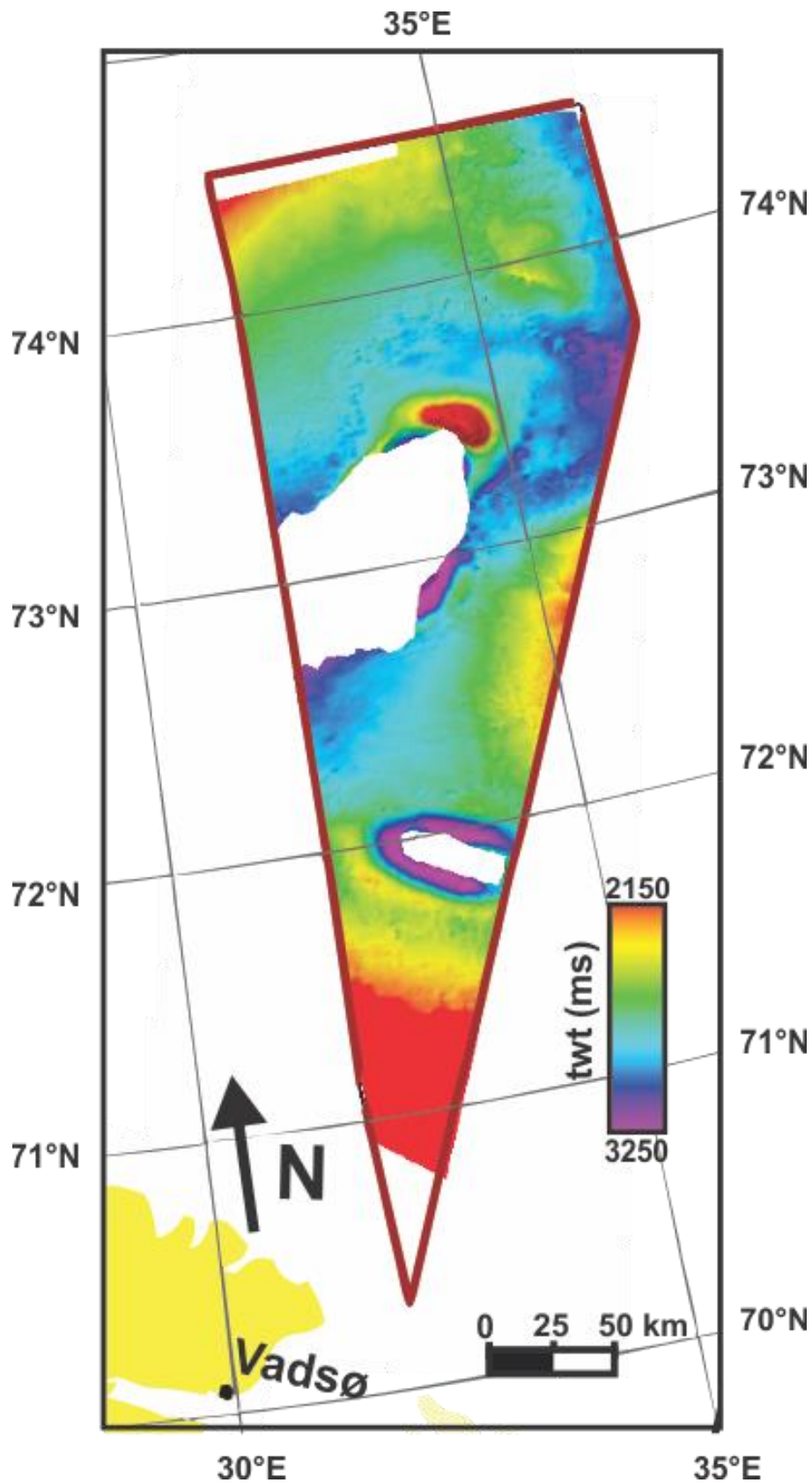
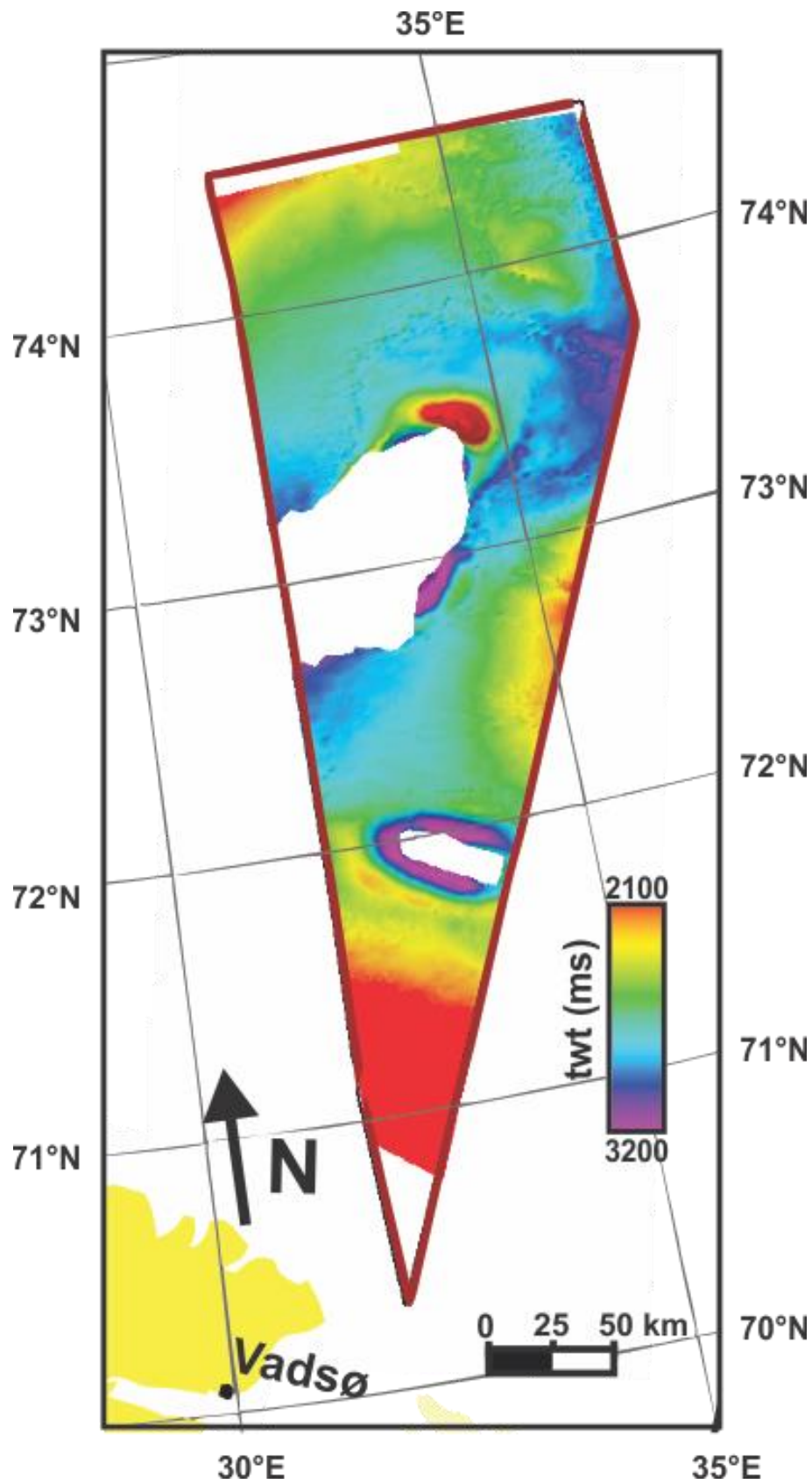


Figure 4.7 Time-thickness map of the Top Bjarmeland horizon. Note that the twt-legend differs between the time-thickness maps and that the chaotic-reflection zones in the Nordkapp and Tiddlybanken Basins have been cropped out.



*Figure 4.8* Time-thickness map of the Top Tempelfjorden horizon. Note that the twt-legend differs between the time-thickness maps and that the chaotic-reflection zones in the Nordkapp and Tiddlybanken Basins have been cropped out.

### 4.3 Seismic units

The four regional horizons divide the Paleozoic interval in the study area into three main units: the Gipsdalen, Bjarmeland and Tempelfjorden groups. Figure 4.9 illustrates the appearance of the interpreted units in a seismic section located on the Finnmark Platform in the study area. This chapter presents a general description of the appearance of the groups in the seismic data, then continues with a closer look at their appearance in the defined seismic areas (Figure 4.3) and ends with a summary of the observations. The seismic expression of the Gipsdalen Group shows large variations in both time-thickness, internal horizon configuration and amplitude strength of the horizons. For the Bjarmeland and Tempelfjorden groups however, the seismic expression is less varied. The disparity between the groups has led to a more detailed go through of the Gipsdalen Group, where the description of the group in each of the defined seismic areas is more elaborated on than for the Bjarmeland and Tempelfjorden groups.

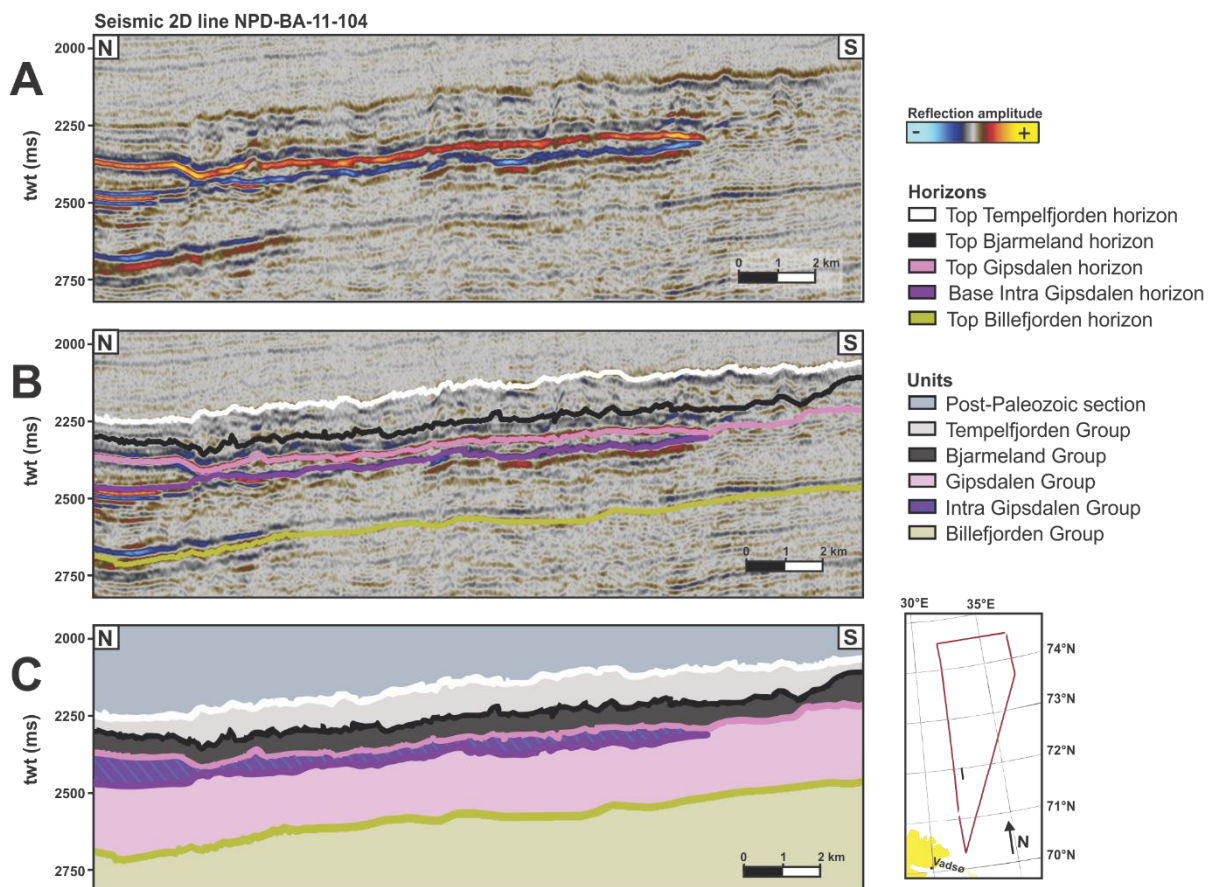


Figure 4.9 The Paleozoic interval on the Finnmark Platform in the BSSE, located as indicated on the index map. A) Uninterpreted seismic section. B) Seismic section showing the interpreted horizons. C) Geoseismic section with the interpreted horizons and units outlined. Also illustrated in the geoseismic section is an example of where the Intra Gipsdalen Group sub-unit appear, as limited by the Top Gipsdalen and Base Intra Gipsdalen horizons.

### 4.3.1 Gipsdalen Group

The Gipsdalen Group is bounded by the Top Billefjorden horizon at its base and the Top Gipsdalen horizon at its top (Figure 4.9). The average twt-thickness is approximately 400 ms (twt), and the group varies from approximately 100-1100 ms (twt) (Figure 4.10A). High values of 2100 ms (twt) appear within the Veslekari Dome and up to 1400 ms (twt) appear within the Signalhorn Dome. An additional interval of the Gipsdalen Group is defined by the highest amplitude horizons seen in the data set, and is referred to as the Intra Gipsdalen Group sub-unit (Figure 4.10B). The Intra Gipsdalen Group sub-unit is bounded by the Base Intra Gipsdalen horizon at its base and the Top Gipsdalen horizon at its top (Figure 4.9).

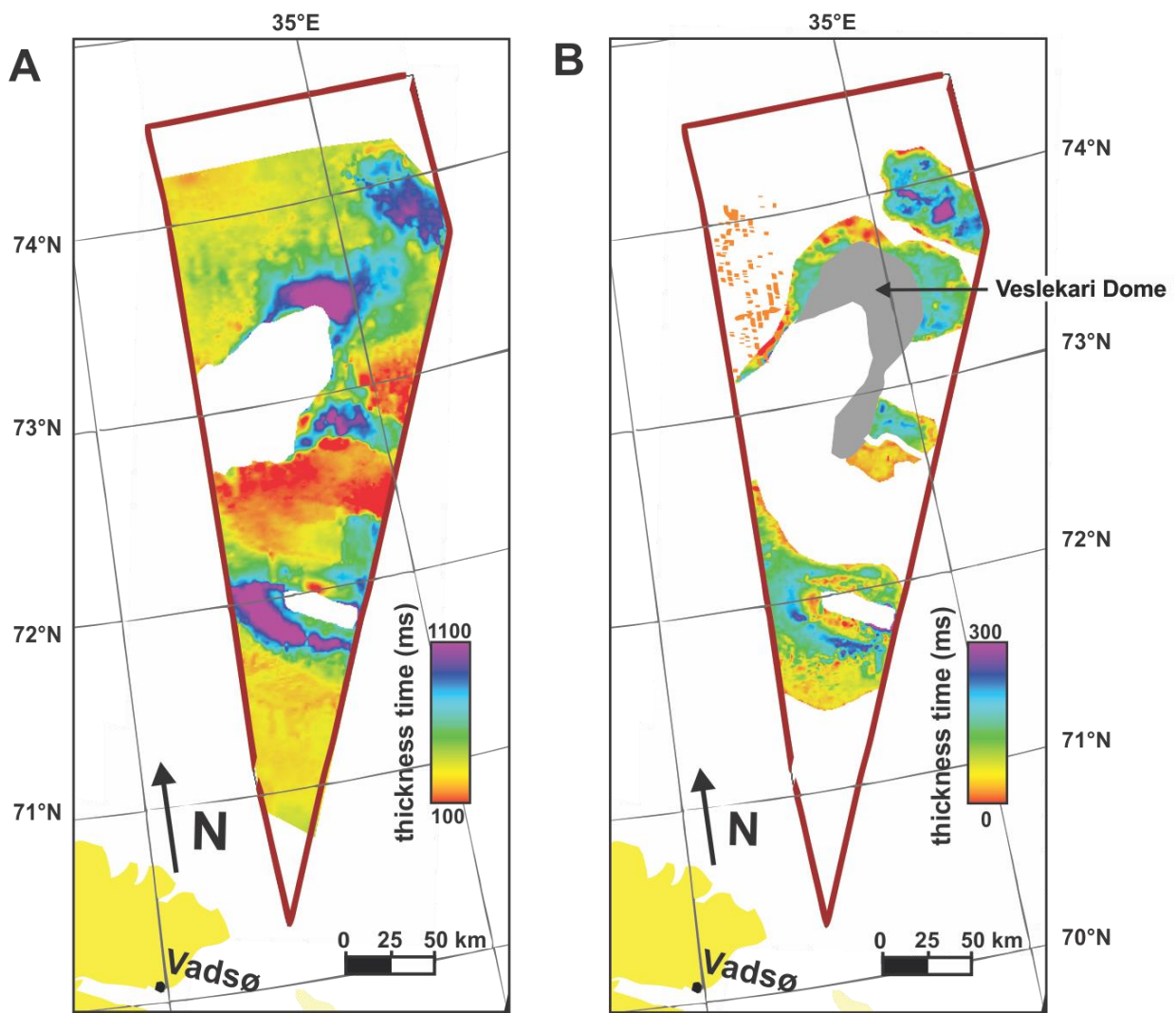


Figure 4.10 A) Time-thickness map of the Gipsdalen Group. Increased time-thickness in the Veslekari and Signalhorn Domes exceed the 1100 ms (twt) indicated in the map, reaching values of 2000 ms (twt). B) Time-thickness map of the Intra Gipsdalen Group sub-unit. Areas where the Intra Gipsdalen Group sub-unit is interpreted to appear but either the base or the top of the group is disrupted are shown in grey.

A general division of the Gipsdalen Group is made based on the time-thickness and the presence of the Intra Gipsdalen Group sub-unit (Figure 4.10). Low time-thickness value areas are here defined to be less than 400 ms (twt) and high time-thickness value areas more than 400 ms (twt). Lateral variation of the internal horizon configuration is mainly observed where there is a thickening of the group. Moreover, lateral variations are observed to a larger degree within the Gipsdalen Group than within the Bjarmeland and Tempelfjorden groups. Upward variation of the horizon configuration within the Gipsdalen Group is mainly restricted to the eventual appearance of the Intra Gipsdalen Group sub-unit (Figure 4.10B).

Where the Intra Gipsdalen Group sub-unit is absent (Figure 4.10B), the entire Gipsdalen Group is represented by an array of discontinuous, concordant, low amplitude and subparallel to chaotic horizons (Figure 4.11A). The base of the group, the Billefjorden horizon, forms the first discernable continuous horizon with a negative reflection coefficient. This configuration coincides to a large degree with a time-thickness of less than 400 ms (twt), though anomalies do occur.

Where the Intra Gipsdalen Group sub-unit appears (Figure 4.10B), the Base Intra Gipsdalen horizon generally forms a lens-shape with the highest amplitudes along the Top Gipsdalen horizon. The Base Intra Gipsdalen horizon in these occurrences appears as an undulating lower limit to an interval of discontinuous horizons of low to medium amplitude (Figures 4.9 and 4.11). This configuration is found both within low and high time-thickness value areas of the Gipsdalen Group (Figure 4.10A). The Intra Gipsdalen Group sub-unit goes through internal changes in its time-thickness, from a maximum of 400 ms (twt) to close to 0 at pinch-outs (Figure 4.10B). Additionally, some areas have the Base Intra Gipsdalen horizon appearing intermittently directly below high amplitudes along the Top Gipsdalen horizon, which is exclusively found within areas of low time-thickness value (Figure 4.10). As for the internal configuration of the lower segment of the Gipsdalen Group where the Intra Gipsdalen Group sub-unit is present, two general configurations appear. Low time-thickness areas are represented by the same horizon configuration as described for areas where the Intra Gipsdalen Group sub-unit is absent (Figure 4.11B), while high time-thickness areas consists of largely subparallel to slightly diverging horizons. The amplitude strength of the horizons in high time-thickness areas vary both laterally and vertically, from mostly high to medium with some low signals. The group termination is characterized by onlap (Figure 4.11C).

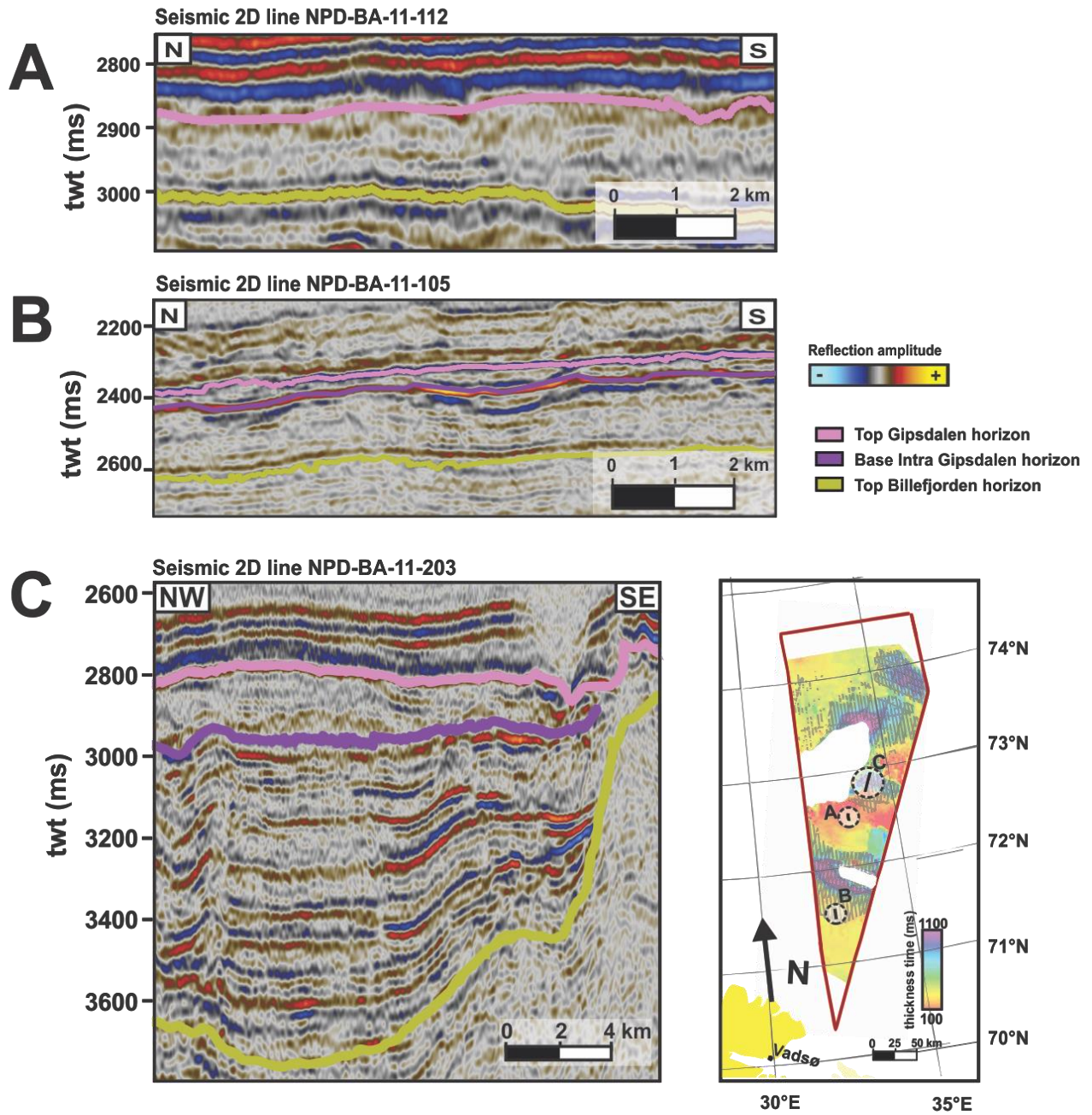


Figure 4.11 Seismic sections from arbitrary 2D lines showing the main outlines of the internal horizons observed in the Gipsdalen Group, located as shown on the time-thickness/Intra Gipsdalen sub-unit distribution map. A) Low time-thickness, discontinuous internal horizon configuration. B) Instances of the Intra Gipsdalen Group sub-unit in low time-thickness areas. C) High time-thickness areas.

#### ***4.3.1.1 Seismic area 1: Bjarmeland Platform***

The time-thickness of the Gipsdalen Group increases on the Bjarmeland Platform from the northwestern edge of the BSSE towards southwest and the neighboring structural elements. The unit is represented by discontinuous, concordant, low amplitude and subparallel to chaotic signals within the 200-400 ms (tw) time-thickness interval (i.e. Figure 4.11B, Figure 4.16). Exceptions to this largely monotonous arrangement of horizons are local thickness elevations over the platform (Figure 4.10A) and occurrences of the Intra Gipsdalen Group sub-unit (Figure 4.10B). The Intra Gipsdalen Group sub-unit is on the Bjarmeland Platform observed on the western platform area where the Base Intra Gipsdalen horizon appears intermittently directly beneath high amplitude occurrences of the Top Gipsdalen horizon. Additionally, the Intra Gipsdalen Group sub-unit appears in proximity to neighboring structural elements. As the Bjarmeland Platform grades into the Nordkapp Basin and the Veslekari and Haapet domes there is an abrupt change in reflection configuration and both the time-thickness increase of the Gipsdalen Group and the presence of the Intra Gipsdalen Group sub-unit becomes more prominent (Figures 4.16 and 4.17). The increase in reflection amplitude between the structural elements is further exemplified in Figure 4.16C.

#### ***4.3.1.2 Seismic Area 2: Veslekari and Haapet Domes***

The descriptions in this section concerns the internal configuration of the Gipsdalen Group as it appears within high time-thickness areas of the Veslekari and Haapet domes (Figure 4.10A). A recognizable thickening of the Gipsdalen Group unit takes place at the edges of the domes. The time-thickness of the Gipsdalen Group varies from approximately 300 ms (tw) at the edges of the Veslekari Dome to approximately 1950 ms (tw) mid-dome, and from approximately 300 ms (tw) to 1250 ms (tw) for the Haapet Dome (Figure 4.10A). The internal horizons can be subdivided into two: a lower collection of semi-continuous and subparallel to diverging horizons and an upper internally chaotic lens of the Intra Gipsdalen Group sub-unit (Figures 4.17, 4.18 and 4.19). The amplitude strength of the horizons within the dome varies, though is mostly medium to high. Moving closer to the center of the Veslekari dome the internal signals of the entire Gipsdalen Group are disrupted, leaving a chaotic configuration of the horizons mid-dome (Figure 4.17). The internal signals in the Haapet Dome are not disrupted to the same degree as the Veslekari Dome. The time-thickness of the Intra Gipsdalen Group sub-unit

appearing under the Haapet Dome changes from close to 0 ms (tw) at the pinch-outs to 400 ms (tw) maximum (Figures 4.10B and 4.18).

#### ***4.3.1.3 Seismic Area 3: Nordkapp Basin***

Where there are recognizable horizons within the Nordkapp Basin (e.g. Figure 4.19), the Gipsdalen Group has a time-thickness of approximately 350 ms (tw). Subparallel to slightly divergent low amplitude horizons are observed in the lower part of the group. The group contains 0-150 ms (tw) thick internally chaotic lens-shaped occurrences of the Intra Gipsdalen Group sub-unit (i.e. Figure 4.11C). The Gipsdalen Group shows an increase in thickness close to the basin, from its roughly uniform appearance on the Bjarmeland and Finnmark Platform to a thickening towards the basin (Figure 4.10A). Additional change in amplitude strength take place in the group surrounding the basin. The group is situated at its BSSE twt-value maximum within the basin, and the Top Gipsdalen horizon is observed at a maximum depth of 4725 ms (tw) (e.g. Figure 4.19). The Top Gipsdalen horizon has a depth of approximate 3075 ms (tw) surrounding the Nordkapp Basin (Figure 4.6), giving a difference of 1650 ms (tw) from basin edge to deep basin.

#### ***4.3.1.4 Seismic Area 4: Fedynsky High***

A distinct thickening of the Gipsdalen Group is apparent under the Fedynsky High in an approximately 22 km wide NE-SW section moving towards the Nordkapp Basin (Figure 4.10A). High time-thickness areas of Seismic Area 4 contain a stacked collection of discontinuous to semi-continuous and subparallel to diverging internal horizons in the lower segment of the Gipsdalen Group. The Intra Gipsdalen Group sub-unit, as defined by an internally chaotic lens-shape, appear in the upper segment. The internal horizons have a varying degree of mostly low to medium amplitude strength, excluding the high amplitude Base Intra Gipsdalen and Top Gipsdalen horizons. A change in thickness is observed perpendicular to the edges of the depression, and the time-thickness values of the eastern section average approximately 650 ms (tw) while closer to the Nordkapp Basin the time-thickness increases towards 1000 ms (tw) (Figure 4.10A). Like the overall thickening of the Gipsdalen Group towards NE, the Intra Gipsdalen Group sub-unit within this area also thickens from SW to NE.

The Gipsdalen Group has a time-thickness of 75 ms (tw) at its thinnest and 150 ms (tw) average surrounding the sub-Fedynsky High depression (Figures 4.3 and 4.10). In these areas the internal horizons are largely discontinuous and concordant with a low amplitude (i.e. Figure 4.11B) with the exception of a section with an Intra Gipsdalen Group sub-unit appearance south of the depression (i.e. Figure 4.11C).

#### ***4.3.1.5 Seismic Area 5: Tiddlybanken Basin/Finnmark Platform***

The appearance of the Gipsdalen Group within the Tiddlybanken Basin is partly distorted by a salt diapir, with the Top Billefjorden horizon interpreted to bulge under the diapir (Figure 4.21). The internal horizons mid-basin are distorted and chaotic, changing from the subparallel configuration with high amplitude observed from the basin edge towards the diapir. The Intra Gipsdalen Group sub-unit is observed within the basin (Figure 4.10B).

From SW of the Tiddlybanken Basin to the southern edge of the defined Seismic Area 5 (Figure 4.3) the Signalhorn Dome appears (Figures 2.3 and 4.21). The internal Gipsdalen Group horizons within the dome are discontinuous and sub-parallel with low to medium amplitude strengths. An internally chaotic 250 ms (tw) lens of the Intra Gipsdalen Group sub-unit appears within the dome (Figure 4.10B). The Gipsdalen Group reaches a time-thickness of 1400 ms (tw) mid-dome (Figure 4.10A).

An exception to the regional trend of the Intra Gipsdalen sub-unit coinciding with the thicker areas of the Gipsdalen Group take place between the Fedynsky High and the Tiddlybanken Basin SE in the BSSE (Figure 4.10). Here the Gipsdalen Group thickens as the Top Billefjorden horizon plunges approximate 600 ms (tw) SW (Figures 4.5, 4.10A and 4.21). The internal horizon configuration is also anomalous in this area compared to the rest of the BSSE, as an upward divide within the Gipsdalen Group can be observed (Figure 4.21). The divide is a locally appearing continuous horizon that is characterized by a decrease in acoustic impedance. Below the divide the horizons are semi-continuous and have a medium amplitude strength, while above the divide the horizons are discontinuous with a low amplitude. Common both below and above the divide is a sub-parallel configuration within the thicker time-thickness interval, with the lower termination being characterized by onlap and the upper by concordance.

#### ***4.3.1.6 Seismic Area 6: Finnmark Platform***

The lower part of the Gipsdalen Group in the northern part of Seismic Area 6 is characterized by discontinuous and diverging to chaotic horizons with low to medium amplitude strength (Figures 4.4 and 4.22). The Base Intra Gipsdalen horizon appears in the upper part of the Gipsdalen Group and has an undulating trend over large parts of this area, seemingly coinciding with an opposite undulating trend of the Top Gipsdalen horizon (Figures 4.10 and 4.22D). Depressions of the Base Intra Gipsdalen horizon coincide with mounds of the Top Gipsdalen horizon, with a time-thickness of 150 ms (tw) for the Intra Gipsdalen Group sub-unit under the mounds and close to 0 ms (tw) time-thickness between them. The trend straightens for the Top Gipsdalen horizon and the time-thickness of the Intra Gipsdalen Group sub-unit becomes more uniform, approximately 70 ms (tw), closer towards the southern part of the area. The undulating path continues for the Base Intra Gipsdalen horizon, though with a lesser relief and greater width, until it toplaps the Top Gipsdalen horizon and disappears at the defined divide between the northern and southern part of Seismic Area 6 (Figures 4.9 and 4.4).

For the southern part of the defined area (Figure 4.4), the internal horizons of the Gipsdalen Group become discontinuous to semi-continuous, concordant and subparallel with low amplitude strength (i.e. Figures 4.11B and Figure 4.23).

#### **Summary of Gipsdalen Group**

The Gipsdalen Group as it appears in Seismic Area 1 is largely uniform in time-thickness and horizon configuration, with low time-thickness, low reflection coefficient and discontinuous subparallel horizons. Intermittent instances of the Intra Gipsdalen Group sub-unit appear directly beneath high amplitude occurrences of the Top Gipsdalen horizon.

Seismic Area 2 has the time-thickness of the Gipsdalen Group vary largely, with a generally uniform lateral internal configuration of the group. The internal horizon configuration appears as described for high time-thickness value areas. Disruption of the horizons take place mid-Veslekari Dome.

Salt diapirs have disrupted the Gipsdalen Group within the Nordkapp Basin, Seismic Area 3. Where there are recognizable horizons they appear at their BSSE twt-value maximum and are

uniform in time-thickness and lateral internal horizon configuration. The internal horizon configuration appears as described for high time-thickness value areas.

Seismic Area 4 has a two-part division of horizon appearance. Underneath the Fedynsky High and NE-SW towards the Nordkapp Basin a depression of the Top Billefjorden Group appears, where the internal horizon configuration appears as described for high time-thickness value areas. The time-thickness of both the Gipsdalen Group and the Intra Gipsdalen Group sub-unit change perpendicular to the depression. Surrounding the sub-Fedynsky High depression on the Finnmark Area the Gipsdalen Group mainly appears as described for low time-thickness areas without the Intra Gipsdalen Group sub-unit and has a uniform time-thickness containing the lowest time-thickness values found of the Gipsdalen Group in the BSSE.

The NE Finnmark Platform within Seismic Area 5 has a uniform time-thickness and internal configuration of horizons with appearance of the Intra Gipsdalen Group sub-unit. The Tiddlybanken Basin and the Signalhorn Dome both appear as described for high time-thickness areas. An exception to the regional trend in the BSSE with high time-thickness areas coinciding with the Intra Gipsdalen sub-unit appears NE of the Tiddlybanken Basin.

Seismic Area 6 has two main configurations. In the north the Intra Gipsdalen Group sub-unit appears and the time-thickness of the group differ. The Gipsdalen Group time-thickness is low and ununiform. The lower internal horizons are without any organization. In the south the time-thickness is uniform, the internal horizons are uneventful, and the Intra Gipsdalen Group sub-unit does not appear.

### 4.3.2 Bjarmeland Group

The Bjarmeland Group is bounded by the Top Gipsdalen horizon at its base and the Top Bjarmeland horizon at its top (4.9C). Time-thickness values of the group range from 30 to 140 ms (twt) with 1% of the distribution reaching higher values (Figure 4.12A). Internally the unit is mainly represented by one horizon. This horizon is characterized by an increase in acoustic impedance with varying amplitude strength and contains some internal scatterings of discontinuous negative coefficient reflections (Figure 4.13A). The sections of the group with this configuration generally has a uniform time-thickness of 75 ms (twt). Anomalies to this trend occur in instances where the Bjarmeland Group unit has an upper concave mounded shape (Figure 4.13B). Mounds often occurs in association with thicker areas (Figure 4.12). Within these mounds the Bjarmeland unit has an internal chaotic assortment of horizons, and seismic units beneath these mounds appear to be affected and distorted (Figure 4.13B).

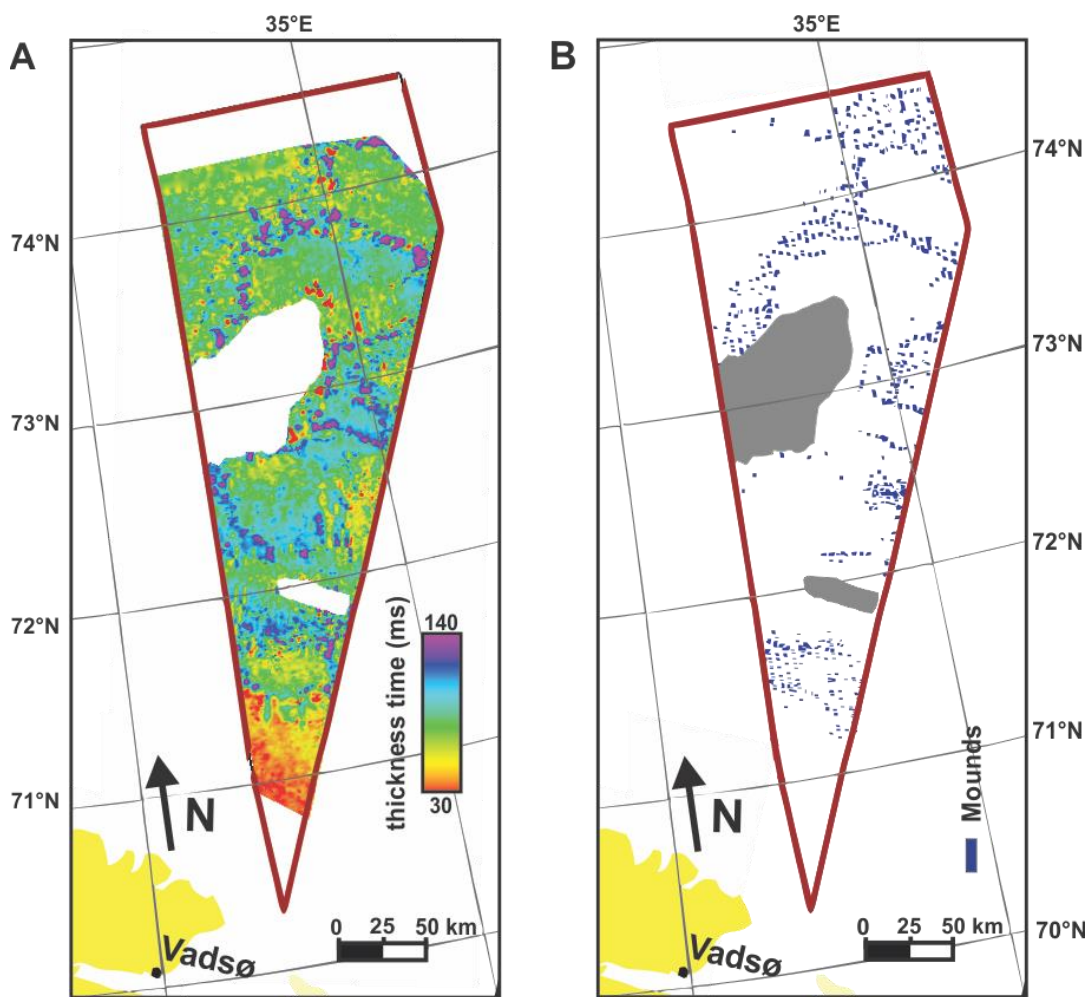


Figure 4.12 A) Time-thickness map of the Bjarmeland Group. B) Map showing the manually interpreted extent of mounds in the Bjarmeland Group, displayed in blue. The unmapped parts of the Nordkapp and Tiddlybanken basins are here shown in grey.

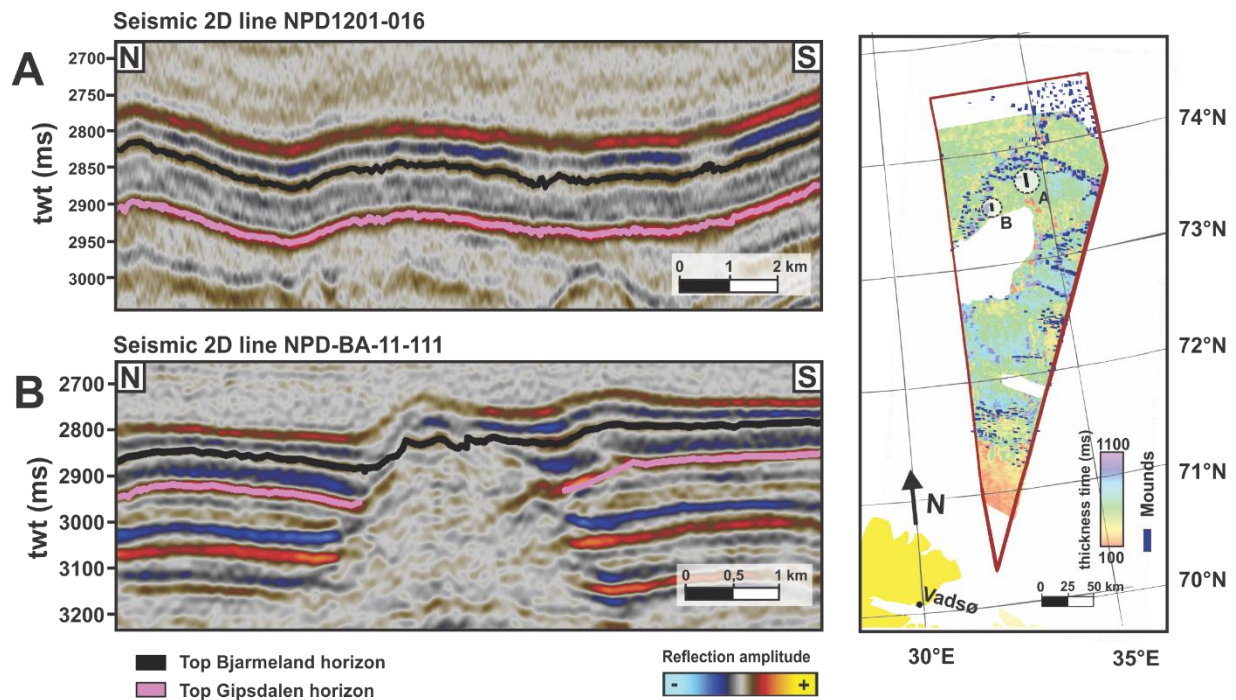


Figure 4.13 Seismic sections from arbitrary 2D lines showing the main outlines of the internal horizons observed in the Bjarmeland Group, located as shown on the time-thickness/mound distribution map. A) The most common seismic pattern of the Bjarmeland Group. B) Mounds with internally chaotic pattern.

The Bjarmeland Group as observed in the BSSE is characterized by low regional variation. As there is not a substantial change in the Bjarmeland Group within the seismic areas, a summary is given with the main differences observed within Seismic Area 1-6 (Figure 4.3).

### Summary of Bjarmeland Group

The main configuration of the Bjarmeland Group (i.e. Figure 4.13A) in Seismic Area 1 has a uniform thickness of 75 ms (twt). The amplitude strength of the group strengthens closer to the surrounding structures (Figure 4.16B), changing from low to medium. There are also internally chaotic and mounded shapes observed in the area. The highest occurrence of mounds on the Bjarmeland Platform appear around the platform's neighboring structural elements; appearing SW-NE oriented on either side of the Nordkapp Basin and northward and in a belt encircling the Haapet Dome (Figure 4.12B). In these instances they coincide with the thickening of the Gipsdalen Group (Figure 4.16, Figure 4.17). Additionally, mounds assumed to appear along the Top Bjarmeland horizon are observed in the NE part of the BSSE to a larger degree than

elsewhere in the study area (Figure 4.12B). West on the platform mounds appear between intermittent appearances of the Intra Gipsdalen Group sub-unit (i.e. Figure 4.16).

Within the Veslekari and Haapet domes in Seismic Area 2 the Bjarmeland Group has a uniform time-thickness and a concordant, generally semi-continuous and low to medium amplitude internal configuration (i.e. Figures 4.12A, 4.13A, 4.17 and 4.18).

Seismic Area 3 has the Bjarmeland Group thinning slightly compared to its surroundings, though the time-thickness is still uniform with 70 ms (tw) where the group can be recognized within the Nordkapp Basin (Figure 4.19). The group appears as a subparallel wavy sheet. Additionally, the Top Gipsdalen horizon is found at its BSSE twt-value maximum, moving from approximately 3000 ms (tw) at the basin edges to 4650 ms (tw) mid-basin., giving a difference of 1650 ms (tw) from edge to mid-basin (Figure 4.6, e.g. Figure 4.19).

Seismic Area 4. Time-thickness variations are observed in the east where an approximately 50 ms (tw) thick interval appears (Figure 4.12A). The eastern side of Seismic Area 4 contains a large collection of mounds (i.e. Figures 4.13B and 4.12B). The mounds are confined to three main areas; one such area is located from 72°27'N and 20 km SW, from the eastern edge of the data set and 24 km further west. Mounds are also observed surrounding the thickening of the Gipsdalen Group and NE of the sub-Fedynsky High depression (Figure 4.20C)

There are few mounds observed in Seismic Area 5, though some are encountered at the northeastern edges of the Tiddlybanken Basin (Figures 4.12B and 4.21). Elsewhere the Bjarmeland Group appears uniform (i.e. Figure 4.13A)

The horizons between the Top Tempelfjorden and Top Gipsdalen horizons are highly distorted and interpretation confidence is considered low in the northern part of Seismic Area 6 (Figures 4.4, 4.9 and 4.22). The Top Gipsdalen horizon follows an undulating path over large parts of this area, seemingly coinciding with what is interpreted to be an opposite undulating path of the Top Bjarmeland horizon (Figure 4.22). Mounds are abundant in the area (Figure 4.12B). Depressions of the Top Gipsdalen horizon coincide with mound shapes of the Top Bjarmeland Group, with an internal time-thickness of 150 ms (tw) under the mounds and 50 ms (tw) between them. Closer towards the defined southern part of the area the undulating path

straightens for both the Top Gipsdalen Group and Top Bjarmeland horizons and the time-thickness of the Bjarmeland becomes more uniform, approximately 70 ms (twl) (Figures 4.9 and 4.22). The configuration of the internal Bjarmeland Group horizon is discontinuous and diffuse, with a low amplitude strength and an internal scattering of discontinuous negative coefficient reflections (i.e. Figure 4.13A). Moving to the southern part of Seismic Area 6 (Figure 4.4), the time-thickness of the Bjarmeland Group decreases, the low amplitude strength of the internal horizon becomes even lower and the horizon becomes more semi-continuous (Figure 4.23). Internal variations are minimal in the approximately 50 ms (twl) thick Bjarmeland Group at southern edge of the Finnmark Platform within the BSSE.

### 4.3.3 Tempelfjorden Group

The uppermost unit of the upper Paleozoic is the Tempelfjorden Group, which is limited by the Top Bjarmeland horizon at the base and the Top Tempelfjorden horizon at the top. The group is mainly represented by a uniform time-thickness of approximately 50 ms (tw), though the twt-values range between 20 and 120 ms (tw) (Figure 4.14). Variations in time-thickness is mainly limited to the distribution of mounds found within the Bjarmeland Group (Figure 4.14, Figure 4.12B). Additionally, furthest south in the study area there are some seemingly isolated mounds within the group.

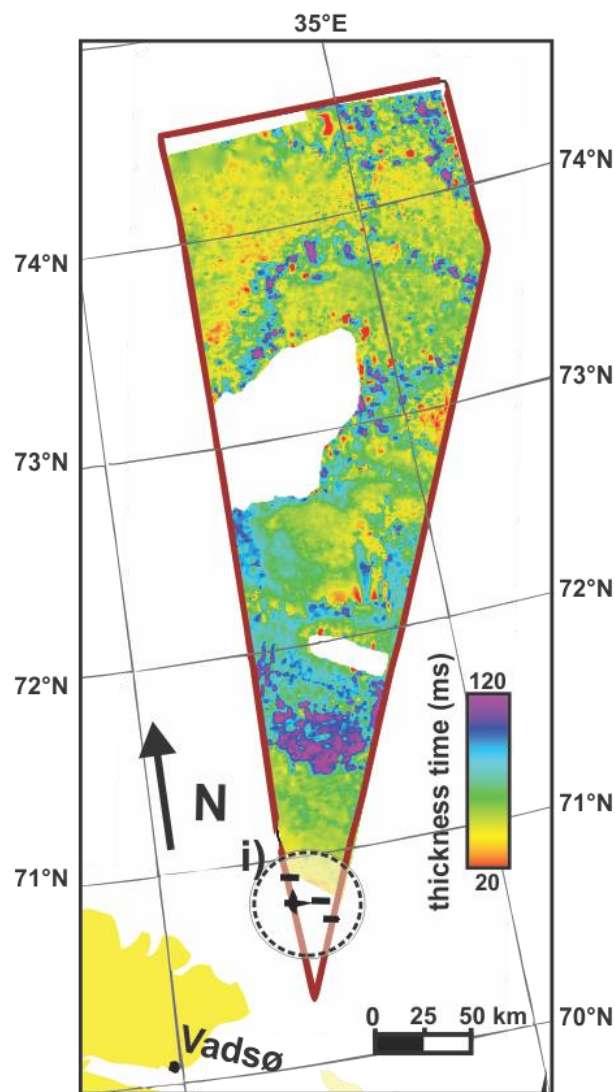


*Figure 4.14* Time-thickness map of the Tempelfjorden Group. The black lines within (i) denote the position of seemingly isolated mounds on the Finnmark Platform.

The Tempelfjorden Group as observed in the BSSE is characterized by low regional variation within both the time-thickness and the internal horizon configuration. In general, the internal configuration of the Tempelfjorden Group is represented by a single horizon characterized by an increase in acoustic impedance. The horizon termination of the group is both upper and lower concordance, and the group appears to be draping the underlying topography. The internal pattern of the group has three main appearances, summarized as: (A) semi-continuous and low amplitude horizons with instances of internal convergence that leaves the appearance of the Tempelfjorden Group unclear (Figure 4.15A); (B) medium to high amplitude, continuous and concordant horizons (Figure 4.15B); (C) low amplitude horizons where negative amplitude signals appear intermittently in its middle (Figure 4.15C).

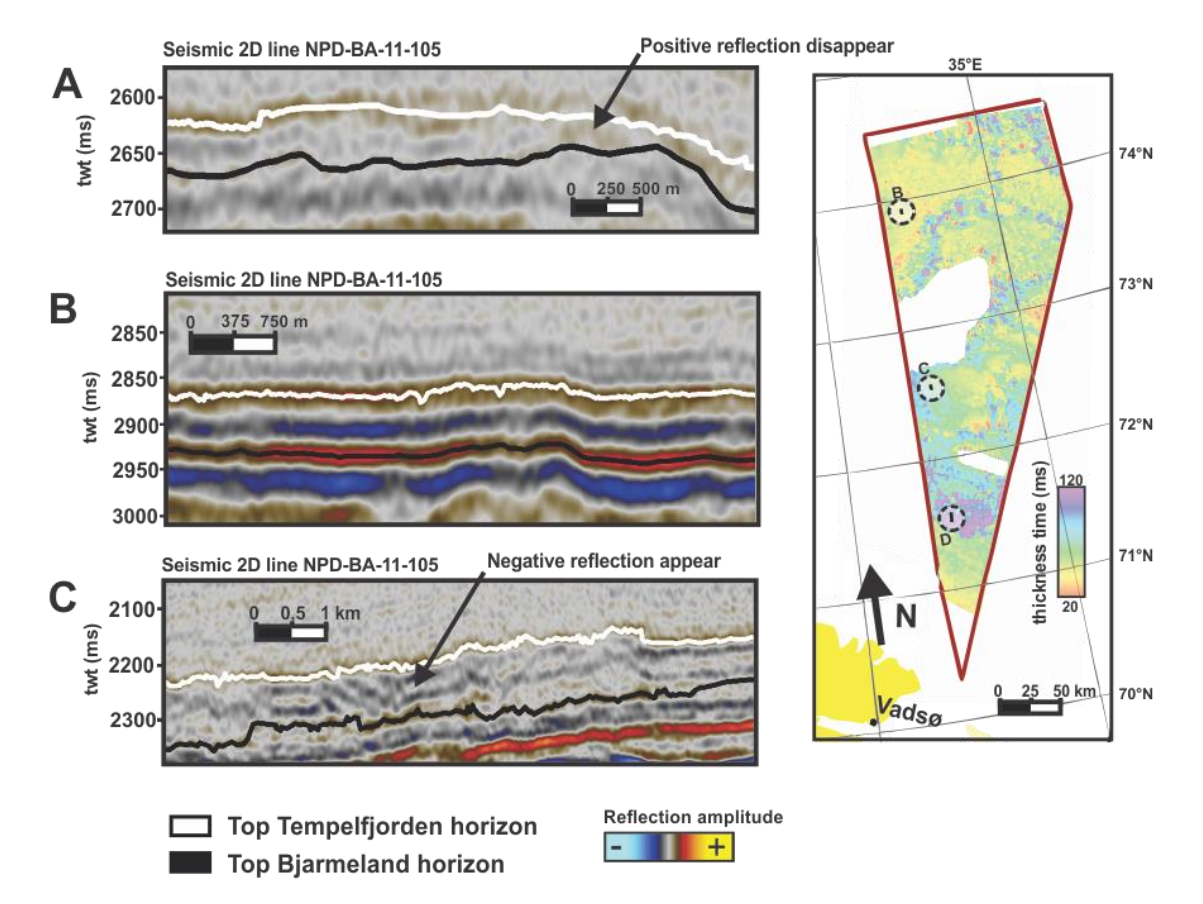


Figure 4.15 Seismic sections from arbitrary 2D lines showing the main outlines of the internal horizons observed in the Tempelfjorden Group, located as shown on the time-thickness map. A) Low amplitude, discontinuous horizons with instances of internal convergence. B) Medium amplitude, continuous horizons. C) Low amplitude, higher time-thickness areas with intermittent negative amplitude signals.

As there is not a substantial change in the Tempelfjorden Group within the seismic areas, a summary is given with the main differences observed within Seismic Area 1-6 (Figure 4.3).

### Summary of Tempelfjorden Group

The Tempelfjorden Group in Seismic Area 1 has a uniform time-thickness of 50 ms (twf), which is the average within the BSSE (Figure 4.14). The amplitude strength of the internal horizons is low on the Bjarmeland Platform and increases to medium closer to the Nordkapp Basin and the Veslekari and Haapet (Figures 4.15A, 4.15B and 4.16). The continuity of the horizons increases as well closer to the surrounding structures (Figure 4.16).

Seismic Area 2 has the Tempelfjorden Group represented by a uniform time-thickness and configuration over and next to the Veslekari and Haapet domes (Figures 4.14, 4.15B, 4.17 and 4.18).

The time-thickness and horizon configuration of the Tempelfjorden Group in Seismic Area 3 appear uniform within and outside of the Nordkapp Basin (Figures 4.14, 4.15B and 4.19). The twf-values of the Top Tempelfjorden horizon are at their BSSE maximum within the basin, changing from approximately 2950 ms (twf) at the basin edge to approximately 4600 ms (twf) mid-basin.

As for Seismic Area 4, the observed Tempelfjorden Group is uniform in time-thickness and horizon configuration over the Fedynsky High and parts of the Finnmark Platform (Figures 4.14, 4.15B and 4.20).

The Tempelfjorden Group has an increase in time-thickness within Seismic Area 5 compared to the general BSSE trend (Figure 4.14). On average, the time-thickness is 70 ms (twf). The internal horizon configuration appears generally uniform (Figure 4.15B), though at times the group observed to be quite diffuse, especially within the Tiddlybanken Basin (Figure 4.21).

The northern part of Seismic Area 6 represents the largest change in the Tempelfjorden Group (Figures 4.4C, 4.9 and 4.22). Worth noticing is that the Top Bjarmeland horizon, which defines the base of the Tempelfjorden Group, is more discontinuous and difficult to consistently

interpret in the northern part than elsewhere in the data set. Additional internal scatterings of negative reflection coefficient signals appear (Figure 4.15C). The time-thickness is uniform within the northern part, 120 ms (twt), which changes to a uniform time-thickness of 50 ms (twt) in the southern part (Figures 4.4C, 4.14 and 4.23). The southern part of Seismic Area 6 thins compared to the northern part, the amplitude strength decreases and the internal scatterings of negative coefficient signals disappear (Figure 4.23). The divide between the Top Tempelfjorden horizon and its overburden is not apparent in close-ups (i.e. Figure 4.23A), however it is clear on a larger scale (i.e. Figure 4.1). Seemingly isolated mounds are found furthest south in the study area (Figures 4.14 and 4.23). These mounds are characterized by an increase in amplitude strength.

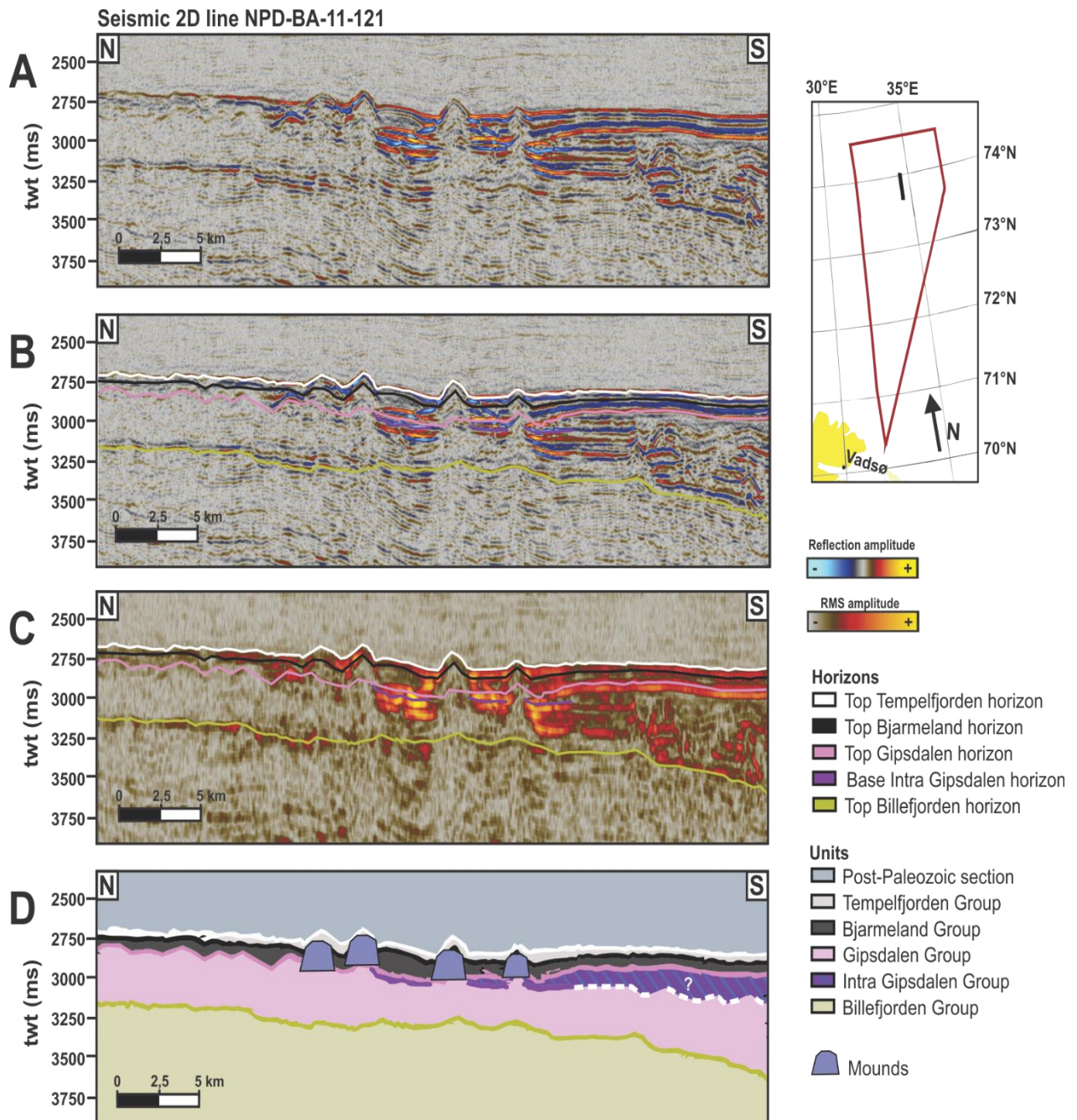


*Figure 4.16* North-south profile of the Bjarmeland Platform, located as shown on the index map. A) Uninterpreted seismic section. B) RMS Amplitude section, displaying change from areas of low acoustic impedance (left) towards higher acoustic impedance zones (right). C) Seismic section with interpreted horizons. D) Geoseismic section.

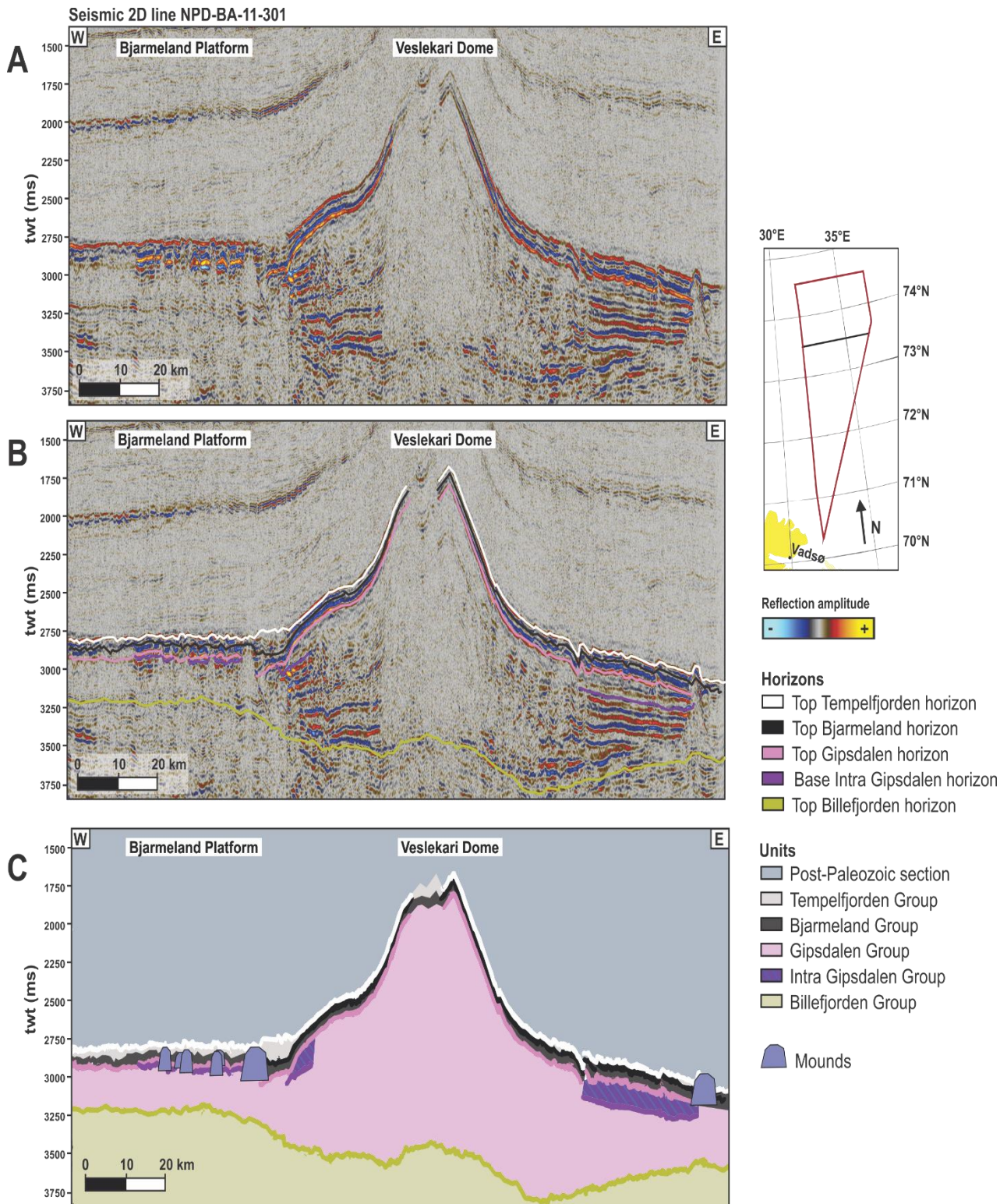


Figure 4.17 West-east profile through the Bjarmeland Platform and the Veslekari Dome, located as shown on the index map. A) Uninterpreted seismic section. B) Seismic section showing the interpreted horizons. C) Geoseismic section.

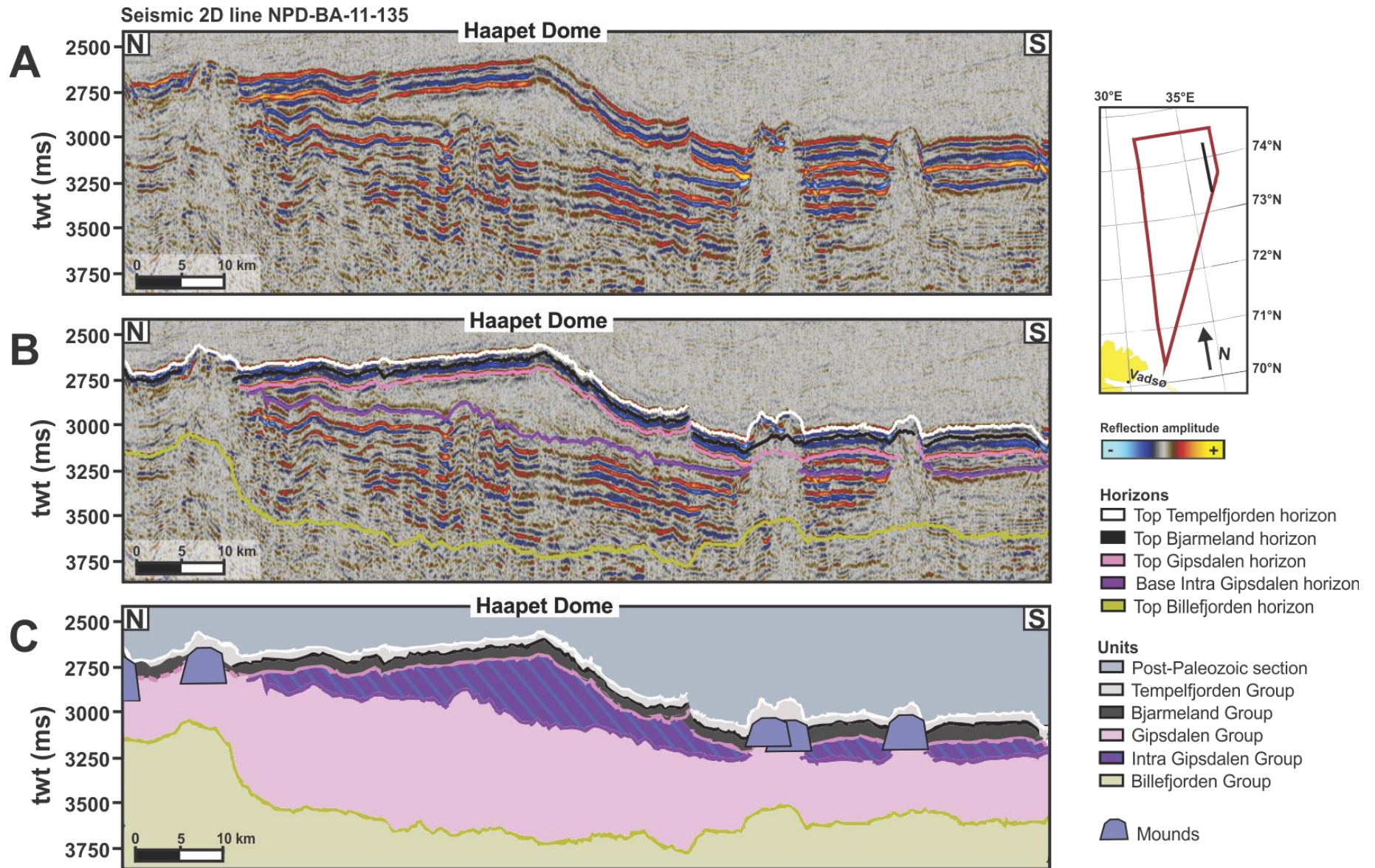


Figure 4.18 North-south profile through the Haapet Dome, located as shown on the index map. A) Uninterpreted seismic section. B) Seismic section showing the interpreted horizons. C) Geoseismic section.

Seismic 2D line NPD-BA-11-115

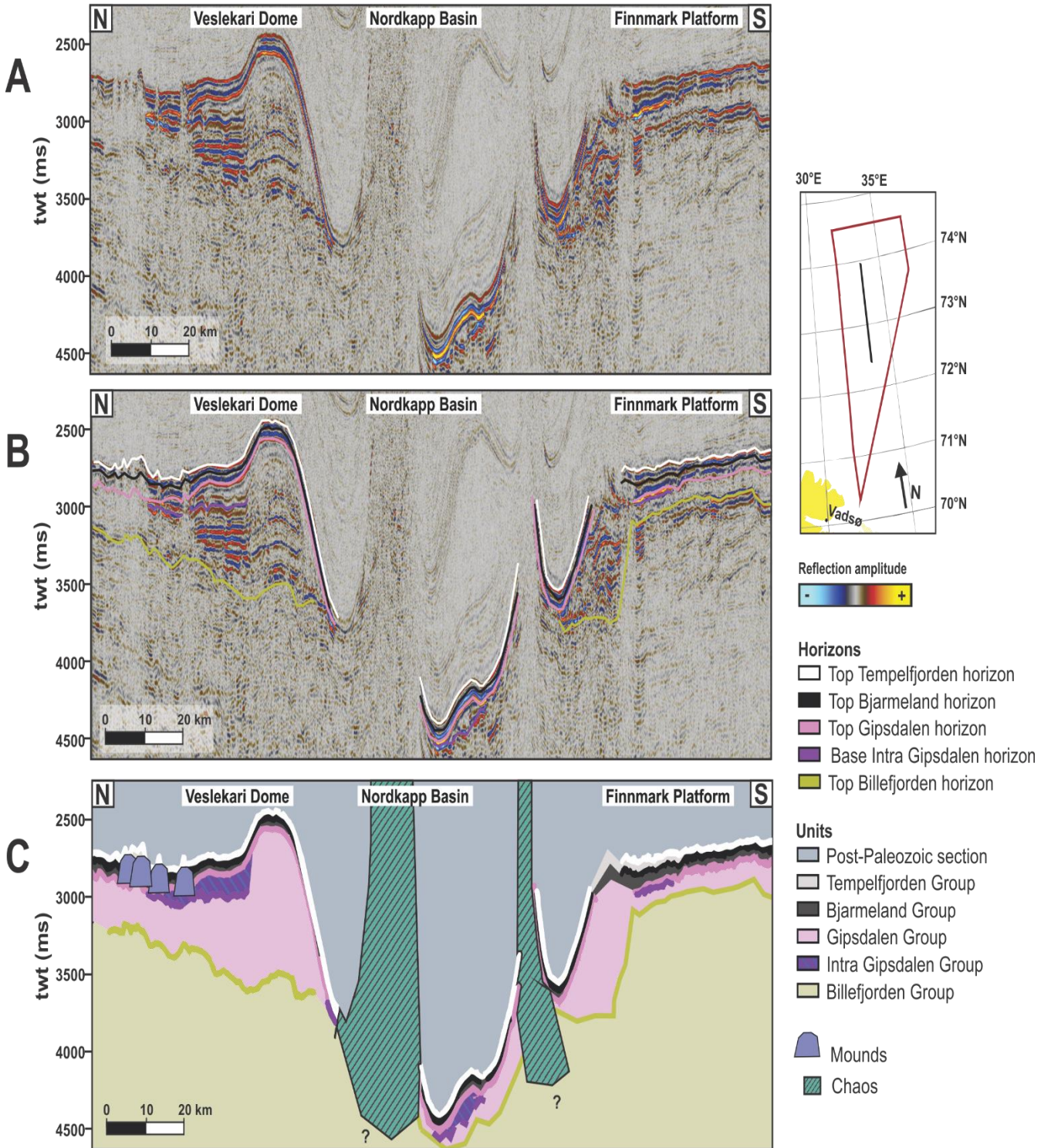


Figure 4.19 North-south profile through the Nordkapp Basin, located as shown on the index map. A) Uninterpreted seismic section. B) Seismic section showing the interpreted horizons. C) Geoseismic section.

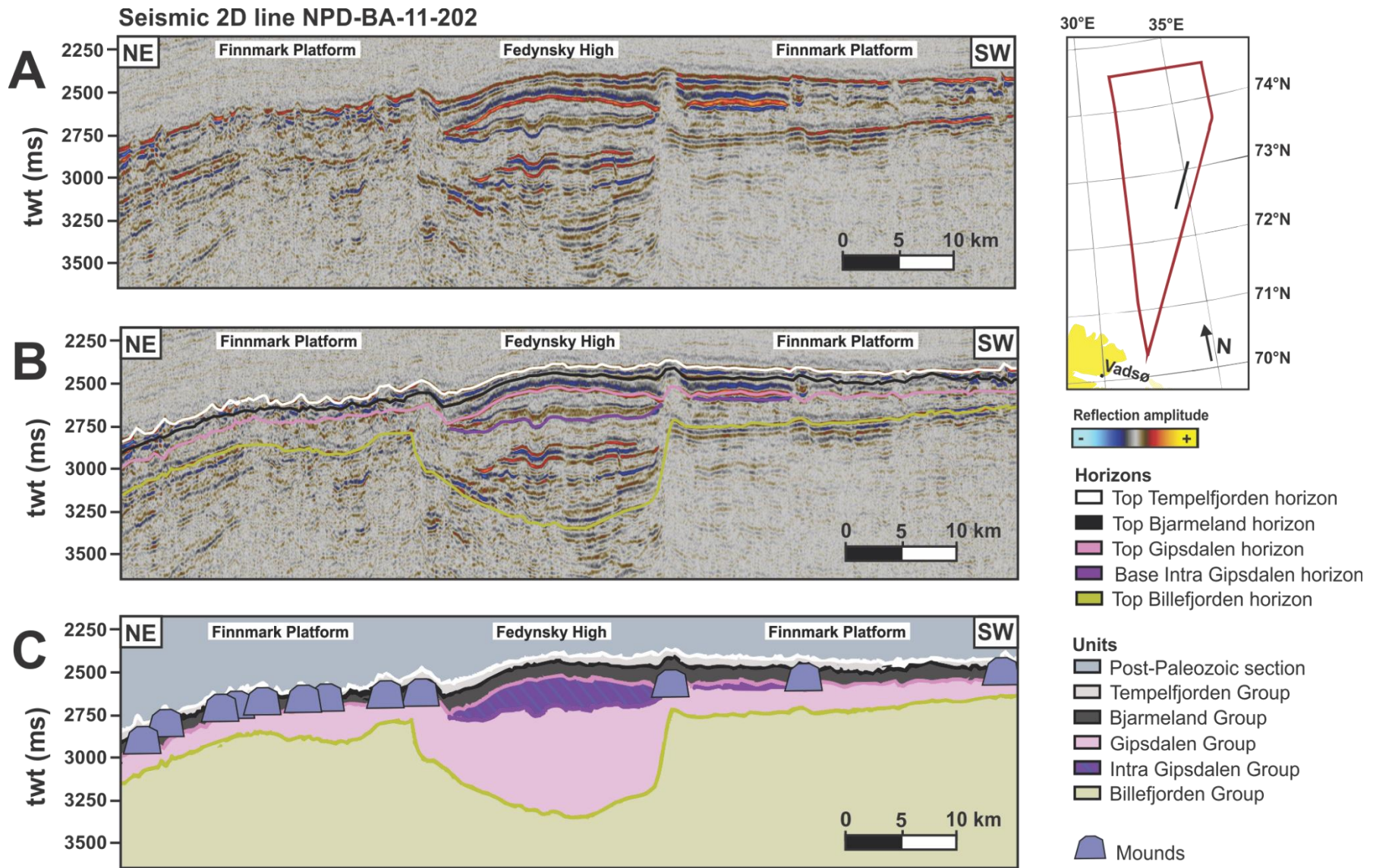


Figure 4.20 NE-SW profile through the Fedynsky High, located as shown on the index map. A) Uninterpreted seismic section. B) Seismic section showing the interpreted horizons. C) Geoseismic section.

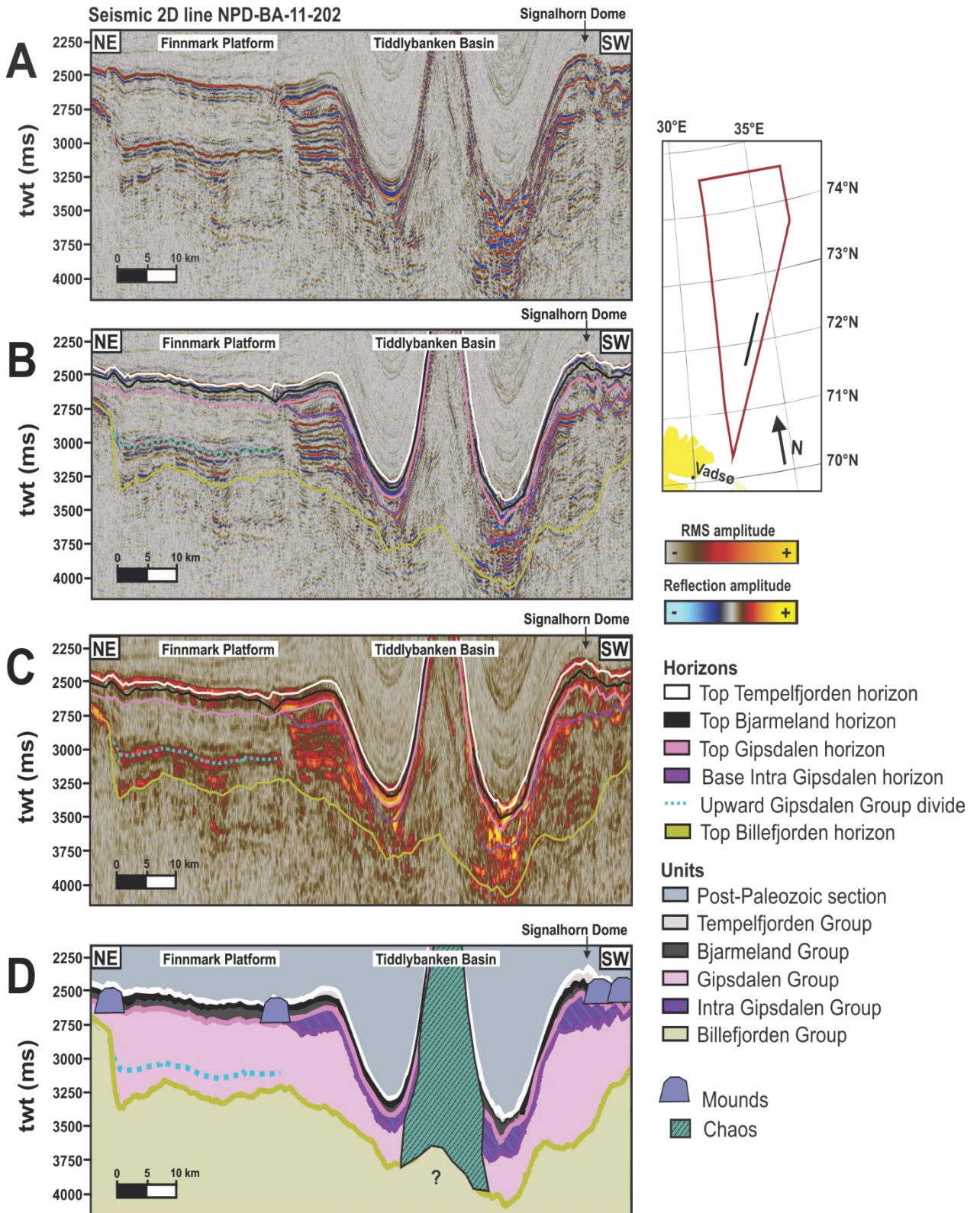


Figure 4.21 NE-SW profile through the Tiddlybanken Basin, located as shown on the index map. A potential velocity pull-up effect on the Billefjorden horizon can be observed under the Tiddlybanken Basin. A local upward divide of the horizons within the Gipsdalen Group is observed NE of the Tiddlybanken Basin. A) Uninterpreted seismic section. B) Seismic section showing the interpreted horizons C) RMS Amplitude section exemplifying the change in internal horizon amplitude strength. D) Geoseismic section.

Seismic 2D line NPD-BA-11-105

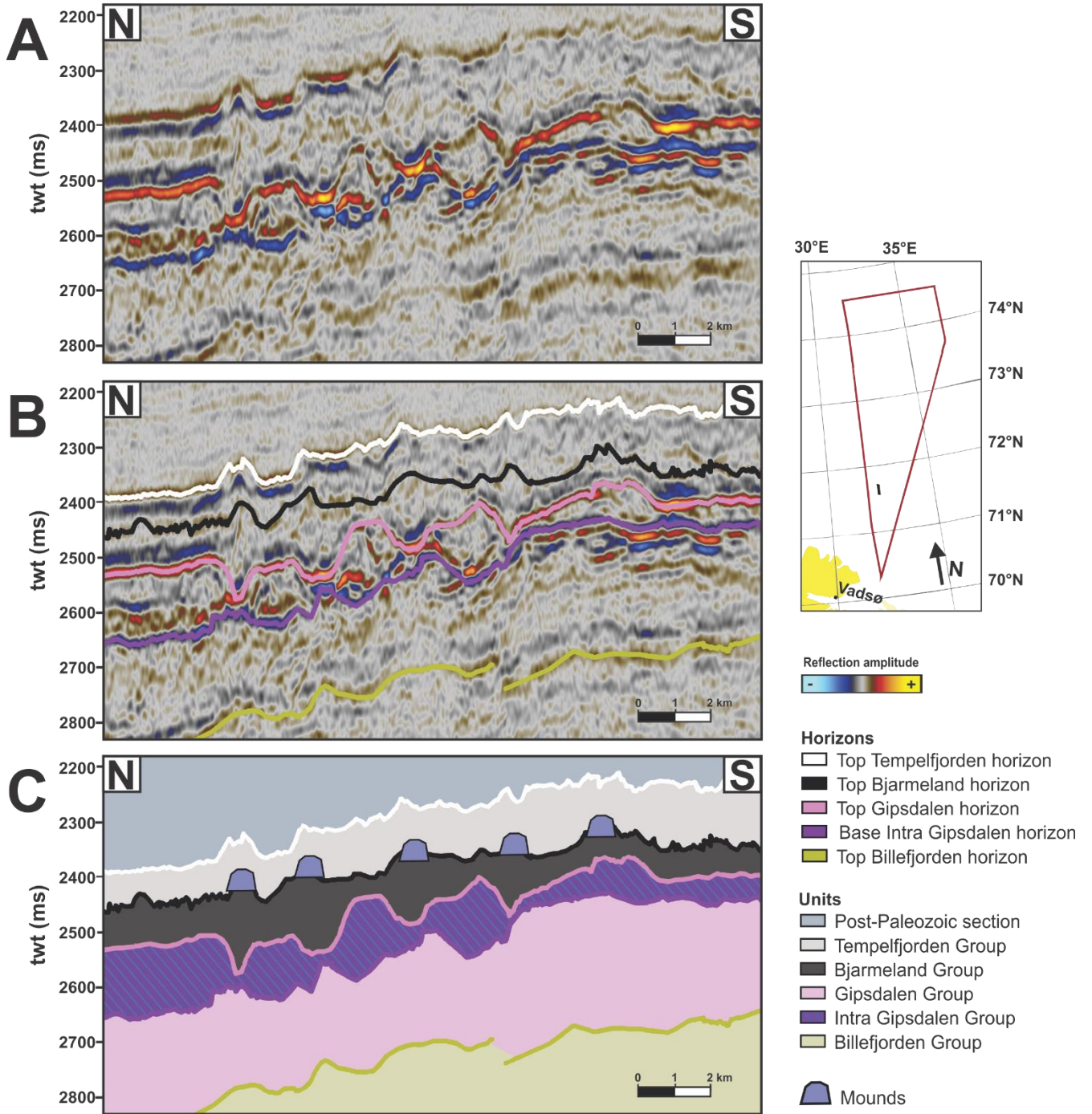


Figure 4.22 N-S profile on the Finnmark Platform, located as shown on the index map. A) Uninterpreted seismic section. B) Seismic section showing the interpreted horizons. C) Geoseismic section.

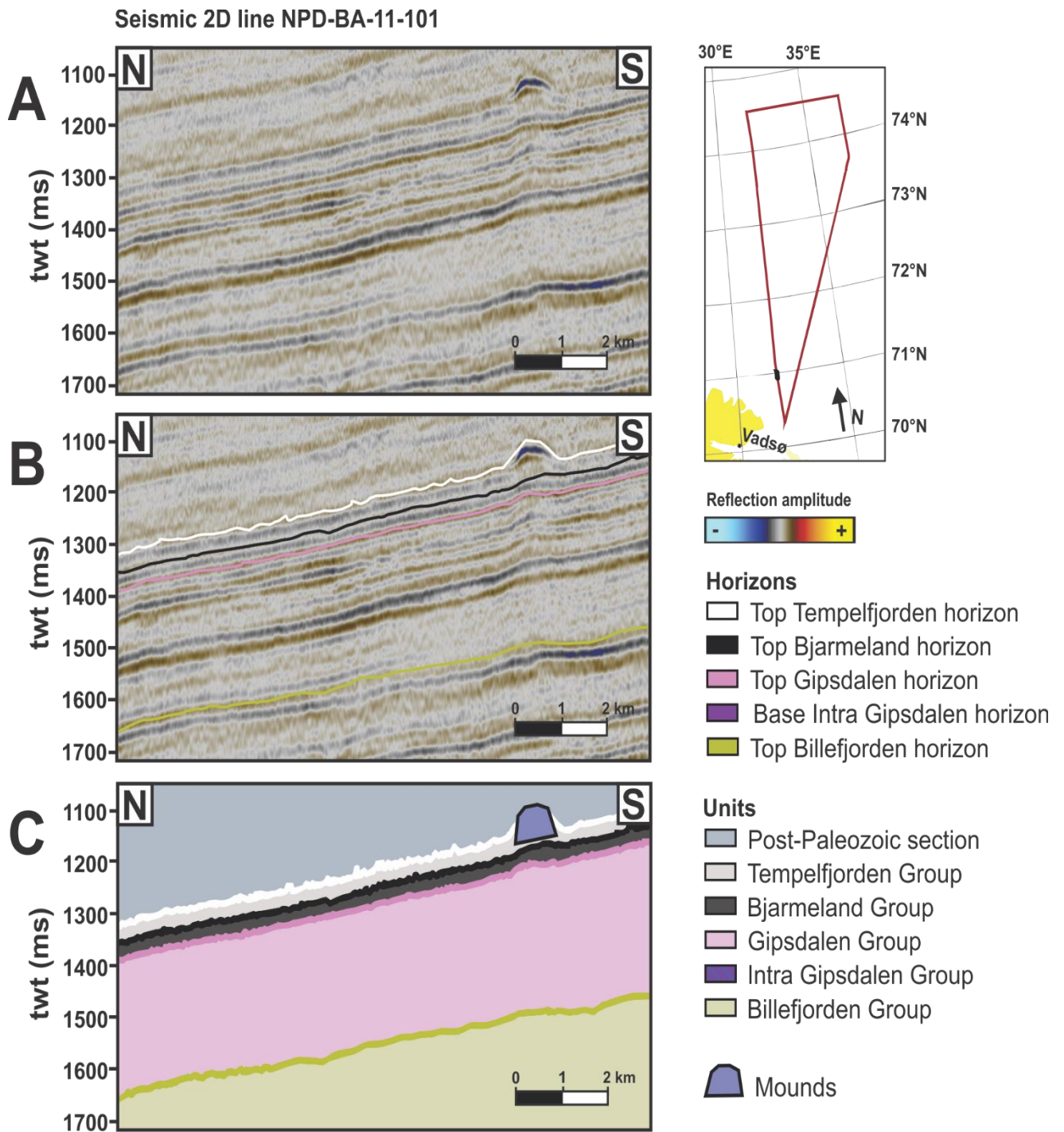


Figure 4.23 N-S profile on the Finnmark Platform, located as shown on index map. A) Uninterpreted seismic section. B) Seismic section showing the interpreted horizons. C) Geoseismic section.



## **5. Discussion**

This chapter considers the observations presented in the previous chapter and discusses the depositional systems in the BSSE during different stages of the upper Paleozoic period. The following interpretation and discussion are made by using the seismic stratigraphy method as defined in Mitchum Jr. et al. (1977) and Veeken and van Moerkerken (2013). Additionally, comparisons are made between the observations in the BSSE and studies from the SW Barents Sea (Gérard and Buhrig, 1990, Nilsen et al., 1993, Bruce and Toomey, 1993, Larssen et al., 2002, Samuelsberg et al., 2003, Colpaert et al., 2007, Rafaelsen et al., 2008, Worsley, 2008, Smelror et al., 2009). Starting with general notes about the area, the chapter continues with a discussion of the depositional environments. The discussion starts with the oldest unit, the Gipsdalen Group and ends with the youngest, the Tempelfjorden Group. The Gipsdalen Group is somewhat more elaborated on, as the seismic expression of the group is more varied than the Bjarmeland and Tempelfjorden Group.

### **5.1 General notes**

The seismic appearance of a sedimentary unit stems from the characteristics of the unit, thus one can assume that depositional environments can be recognized to some degree by grouping horizons with a similar appearance together (Chapter 3.3.2.2). In the BSSE, the changing paleogeographic position and paleo-oceanic circulation patterns during upper Paleozoic have been important for the depositional environments (Chapter 2). Furthermore, seismic stratigraphic observations in the upper Paleozoic interval in the BSSE adds further understanding for the development of the area. Jensen and Sørensen (1992) infer in their publication that no salt movement took place in the Nordkapp Basin during the deposition of the Bjarmeland and Tempelfjorden groups based on the even thickness of the deposits on the surrounding platforms and within the basin. Similar observations of uniformly thick layers of the Bjarmeland and Tempelfjorden groups are made within and around the Nordkapp Basin in the BSSE (Figure 4.19). Likewise, uniformly thick layers of the Bjarmeland and Tempelfjorden groups appear in connection with the other salt structures within the BSSE, i.e. the Tiddlybanken Basin and the Veslekari, Haapet and Signalhorn domes (Figures 4.17, 4.18 and 4.20). This suggests that regional salt movement within the BSSE took place after the deposition of the studied interval, and that the time structure maps of the Top Gipsdalen, Top Bjarmeland and Top Tempelfjorden horizons (Figures 4.6, 4.7 and 4.8) are not indicative of the relief that existed during the time of their group's respective deposition.

## 5.2 Gipsdalen Group

The Gipsdalen Group stratigraphically represents Late Carboniferous to Early Permian (Larsen et al., 2002). There are major differences of the horizon appearance of the Gipsdalen Group within the BSSE. As such, the unit has been divided into a lower and an upper section.

Regarding the tectonic setting of the Gipsdalen Group, no major faulting have been identified in the seismic data. Thickness variations are influenced by the available accommodation space (e.g. Anell et al. (2016)). Changes in relative sea level, either by changes in the global sea level or by tectonic subsidence or uplift, create accommodation space (Church and Coe, 2003). Furthermore, the relative position of accommodation space can be changed by active faulting (Church and Coe, 2003). A recently acquired aeromagnetic survey of the BSSE, as presented by Gernigon et al. (2018), indicate that the regional extensional period in the Late Paleozoic may have ended with a Top Billefjorden hiatus. A reduction in tectonic activity combined with an increase in subsidence has been cited as the start of the deposition of the Gipsdalen Group (Di Lucia et al., 2017). Magnetic data also imply that another, mild and localized, extensional period which was focused along the NE-SW graben axes (i.e. the Nordkapp Basin) started and ended within the time frame of the Gipsdalen Group (Gernigon et al., 2018). The major thickness variations of the Gipsdalen Group follow the topography of the Top Billefjorden horizon, suggesting that the remnant topography was the main influencer for the accommodation space of the Gipsdalen Group. By using the time-structure map of the Top Billefjorden horizon (Figure 5.1A) and the time-thickness map of the Gipsdalen Group (Figure 5.1B), the BSSE morphology assumed to be present at start of the deposition of the Gipsdalen Group is divided into basin and shelf areas (Figure 5.1C).

Given the assumption that Figure 5.1C is at least somewhat representative of the pre-Gipsdalen morphology, the defined basin areas are interpreted to be the site for infill during the deposition of the Gipsdalen Group. An escarpment, i.e. a steep slope created by faulting and/or erosion separating upper and lower flat areas (Sigmond et al., 2013), is assumed to be present between the basin and shelf areas. The interpreted basin areas covered the Nordkapp Basin as well as stretching further NE from below the Veslekari and Haapet domes and continuing to the NE of the study area (Figure 5.1C). Additionally, the Tiddlybanken Basin and the areas around it, including below the Signalhorn Dome, are interpreted to have been basins at the start of deposition of the Gipsdalen Group. Late Devonian rifting in the larger Barents Sea is known to

have created an array of grabens and half-grabens, making a similar configuration probable in the BSSE (Worsley, 2008). The definition of a graben is a section of the earth's crust which has sunk in along one or more faults with steep and close to parallel fault planes (Sigmond et al., 2013). The depression of the Top Billefjorden horizon and increase in time-thickness of the Gipsdalen Group under the present-day Fedynsky High is interpreted to represent a graben (Figure 4.20). It has a W/NW to E/SE orientation and is well expressed on both the time-structure map of the Top Billefjorden horizon (Figure 4.5) and time-thickness map of the Gipsdalen Group (Figure 4.10).

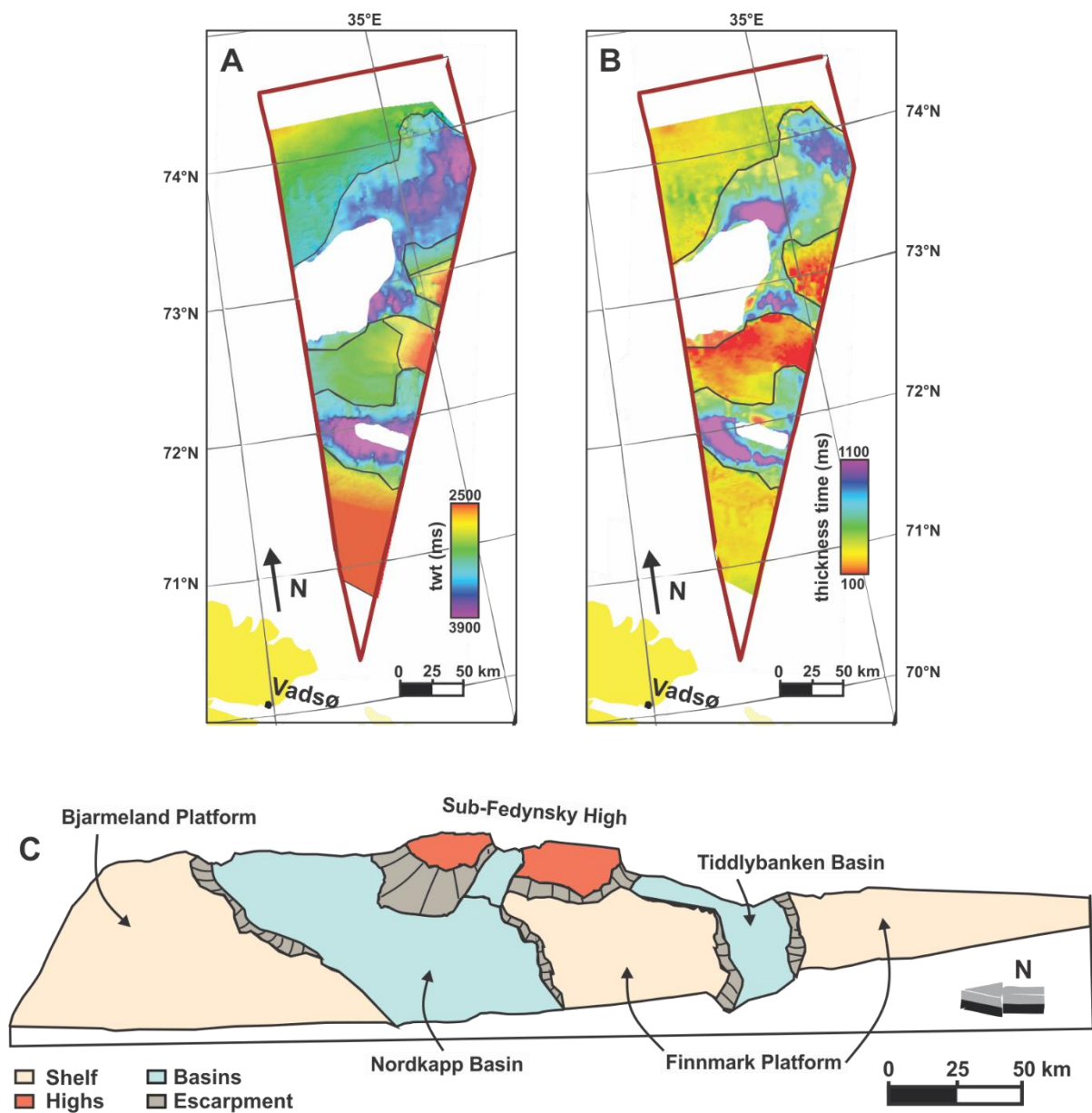


Figure 5.1 A) Time-structure map of Top Billefjorden horizon with major changes in elevations outlined. B) Time-thickness map of the Gipsdalen Group with major changes between low and high time-thickness areas outlined. C) Interpreted morphology present at the start of deposition of the Gipsdalen Group.

For the lower section of the Gipsdalen Group the thicker intervals show an overall similar configuration in the seismic data, making a similar depositional environment is plausible. These areas include the Tiddlybanken Basin, below the present-day Fedynsky High and Signalhorn Dome and also the Nordkapp Basin and further NE in the study area below the Veslekari and Haapet domes. The seismic character is subparallel to slightly diverging and the horizons terminate by onlap towards the older Billefjorden Group (Figures 4.10, 4.11C). Also, the areas are largely represented in the seismic data by stacked horizons with high reflection coefficients (e.g. Figures 4.11C and 4.18). Frequent sea level changes in the Barents Sea during the deposition of the Gipsdalen Group were brought on by major glaciations in the southern hemisphere (Ehrenberg et al., 1998). Bruce and Toomey (1993) suggest that changes in relative sea level have caused the deposition of interbedded evaporites, dolomites and limestones in deeper marine environments in the SW Barents Sea. In seismic data changes in velocity and/or density cause impedance contrasts, seen as changes in the reflection coefficient of horizons (Kearey et al., 2002). Onlap terminations, a sub-parallel to diverging horizon configuration, and the absence of clinoforms are indicative of an aggradational basal fill (Mitchum Jr. et al., 1977, Brown Jr. and Fisher, 1980). By analogy of Bruce and Toomey (1993), the observed high reflection coefficient horizons are assumed to be the result of an interbedded lithology. The thicker areas of the lower Gipsdalen Group in the BSSE are interpreted to have formed as a heterogeneous aggradational infill of negative relief topography created predominantly by pre-depositional rifting (Figure 5.2).

The Nordkapp Basin is known to contain salt deposited as part of the Gipsdalen Group, with the lateral equivalent of the salt deposits assumed to be interbedded sequences of carbonate and anhydrite (Johansen et al., 1992). Salt is also believed to be present in the Tiddlybanken Basin and the Haapet, Veslekari and Signalhorn domes (NPD, 2013b). These structural elements appear in the seismic data as partly disrupted zones (Figures 4.17, 4.18 and 4.21). Partial isolation from the ocean and increase in salinity are required for evaporite sedimentation (Nichols, 2009), and the majority of salt deposits form in arid climates (Bjørlykke, 2015b). The paleogeographic position of the Barents Sea during the deposition of the Gipsdalen Group provided a warm and arid climate, while frequent changes in sea level led to partial isolation of basins (Worsley, 2008). According to Larssen et al. (2005) halite was deposited in SW Barents Sea basins when platforms were subaerially exposed. The presence of salt diapirs in the Nordkapp and Tiddlybanken basins is supported by the observations made in the BSSE, where internally chaotic horizons are neighbored by upward bending horizons and positive relief of

older horizons (Figures 4.19 and 4.21). The upward bending of horizons around columnar structures is indicative of salt presence, as well as internally chaotic horizons (Nichols, 2009, Bjørlykke, 2015b). Apparent anticlines/positive relief of older horizons are additionally associated with salt movements (Selley and Sonnenberg, 2014). Stoupakova et al. (2011) remark how individual salt-bearing formations are found to be present in Late Carboniferous to Permian troughs in the Eastern Barents Sea. A basin stretching from the Nordkapp Basin and further NE has been interpreted as part of the morphology present at the start of Gipsdalen Group (Figure 5.1C). However, both the reflection coefficient and the time-thickness of the Gipsdalen Group are low between the Veslekari and Haapet domes, which could indicate that this area did not receive the same sediments as other interpreted basinal areas (Figures 5.1B). Instead, the Haapet Dome appears to have been isolated from other BSSE basins (Figure 5.2).

The thinner intervals of the lower and upper Gipsdalen Group represents a shift in internal horizon configuration of the unit. These areas, the Finnmark and Bjarmeland platforms, are characterized by decreasing time-thickness, discontinuous horizons and low reflection coefficient horizons compared the thicker intervals of the unit (Figures 4.10 and 4.11A). Smelror et al. (2009) describes how a northward drift of Pangea led to a semi-arid to arid climatic conditions and a prevailing shallow-water carbonate shelf dominating in the Barents Sea. A variety of climatic and tectonic settings can be responsible for carbonate sedimentation, though two criteria have to be met: a lack of clastic input and shallow marine waters (Nichols, 2009). The discontinuous and low amplitude horizons of the Gipsdalen Group in areas of less thickness could suggest a homogenous composition or that any change in lithology is below seismic resolution. The subparallel to chaotic horizons may be the result of diagenesis destroying the original depositional geometries, as happens within carbonate reefs and/or platforms (Chopra and Marfurt, 2007). A continuation of a regional carbonate platform as described in other areas of the Barents Sea is supported by the observed appearance of the Gipsdalen Group on the Finnmark and Bjarmeland platforms, indicating a dominating shallow marine setting cut off from clastic sediment supply (Figures 5.2 and 5.4).

Additionally, on the Finnmark Platform, NE of the Tiddlybanken Basin, there is a thick section of the Gipsdalen Group where a divide between the upper and lower part is apparent (i.e. “Upward Gipsdalen Group divide”, Figure 4.21). This upward divide appears to be older than the Intra Gipsdalen Group sub-unit, which is otherwise the only recognized upward division within the Gipsdalen Group. Unlike thick sections of the Gipsdalen Group elsewhere in the

study area, only the lowermost part is observed to have high amplitude horizons. Additionally, the Intra Gipsdalen Group sub-unit does not occur within the area (Figure 5.3). The rest of the unit in this area appear as described in the above section for thin intervals of the Gipsdalen Group, suggesting an upward change in lithology taking place. The depositional conditions might have changed in the area, becoming less suitable for evaporite deposition while still having a higher accommodation space than surrounding platform areas. As such, the area has been interpreted to be an interbedded salt and carbonate basin during the deposition of the lower Gipsdalen Group (Figure 5.2), which evolved into more dominating carbonate deposits sometime before the deposition of the upper Gipsdalen Group (Figure 5.4).

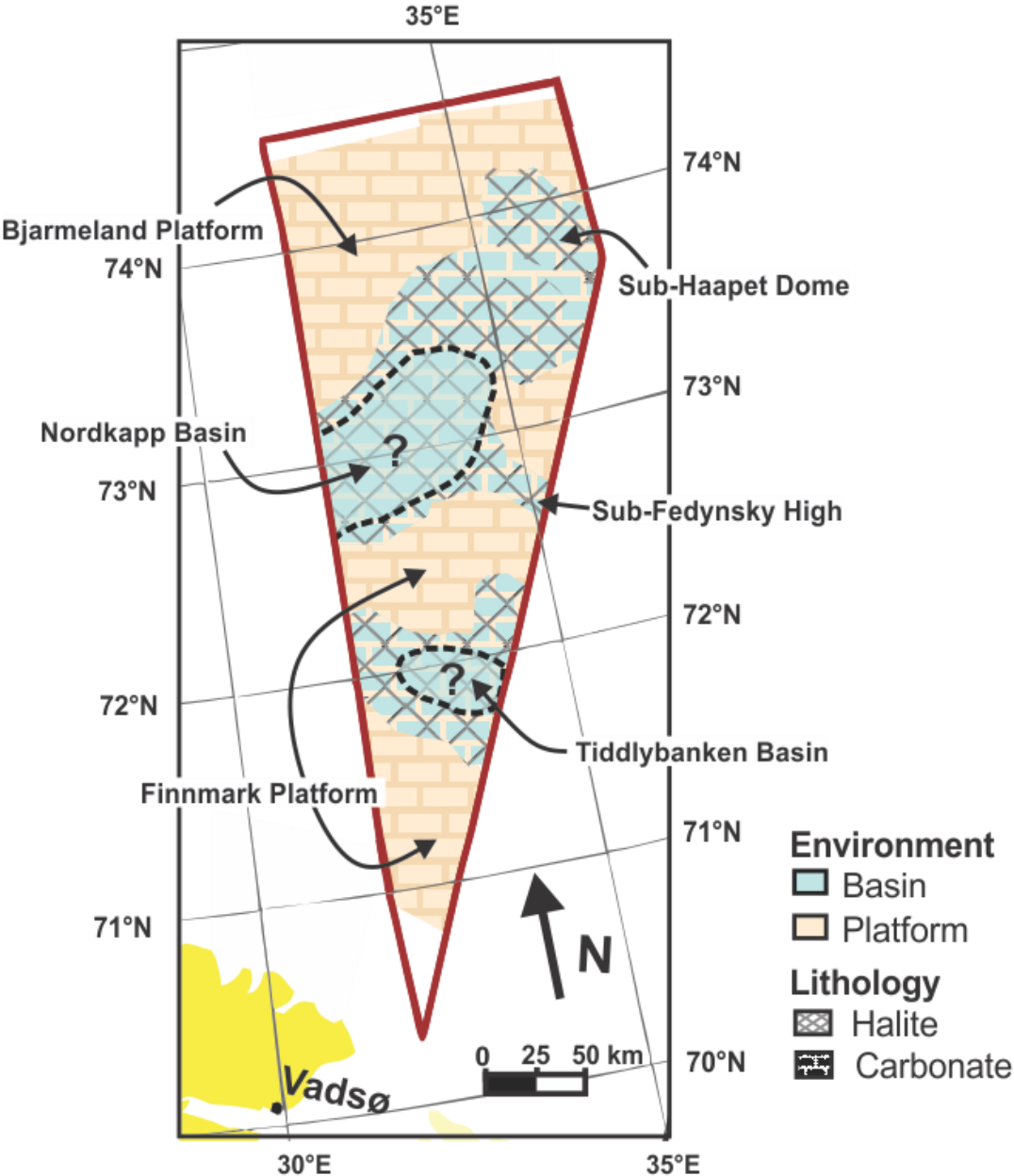


Figure 5.2 Interpreted paleogeographic during deposition of the lower Gipsdalen Group. The basinal areas are thought to consist of an interbedded lithology of carbonates and evaporites. Some areas of the Nordkapp and Tiddlybanken basins have not been mapped, which is why the interpretation of the basins are marked by stippled lines and “?”.

The younger parts of the Gipsdalen Group show a somewhat different evolution than the older interval, and is in this work represented by the deposition of the Intra Gipsdalen Group sub-unit (Figure 4.10B). The upper parts of the interval show a clearly defined lens shape as defined by the high reflection coefficient Base Intra Gipsdalen horizon at the base and Top Gipsdalen horizon at the top. Additionally, thin instances of the Intra Gipsdalen Group sub-unit is mapped locally on the Bjarmeland Platform. The internal configuration of the group, reflection free and featureless, suggests a homogenous composition (i.e. Figure 4.18). Samuelsberg et al. (2003) and Rafaelsen et al. (2008) describe horizons within the Gipsdalen Group comparable in seismic signature to the observed Intra Gipsdalen Group sub-unit. These authors worked on the Finnmark Platform and interpreted the horizons to represent anhydrite beds, which are also correlated to well data and associated seismic signatures. Well 7229/11-1 (Figure 3.1) encountered several levels of anhydrite in the upper Gipsdalen Group (Rafaelsen et al., 2008). Based on observation on the Bjarmeland Platform immediately west of the BSSE, Gérard and Buhrig (1990) describe patchy high amplitude reflections in the upper Gipsdalen Group and interpret them to represent anhydrite-filled depressions in a sabkha environment. Based on its seismic expression and the resemblance to other studies, the Intra Gipsdalen Group sub-unit is interpreted to represent evaporite deposited in the upper Gipsdalen Group.

There is a distinct relationship between the interpreted Top Gipsdalen horizon and the Top Bjarmeland horizon over parts of the Finnmark Platform (Figure 4.3, “Seismic Area 6” and Figure 4.22). Both horizons follow a wavy path. However, where the Top Gipsdalen horizon is mounded the Top Bjarmeland horizon is depressed, and vice versa. Gérard and Buhrig (1990) suggest that similar occurrences of apparent structural inversion are associated with salt solution. Gérard and Buhrig (op. cit) explain that early salt removal is assumed to be the instigator for local sinkholes within deposited evaporites which were filled with younger carbonates. As to why the early salt removal took place, they propose either meteoric water circulation under subaerial exposure, intraformational water along deep-seated faults or halokinesis to be the cause. Later dissolution of the evaporites led to the collapse of the by then flat-lying carbonates, leaving mounds to be formed over the sinkholes as the carbonate deposition had been thicker over them (Gérard and Buhrig, 1990).

Gérard and Buhrig (1990) further interpret that a wide transitional area distinguished by intermittent sabkha deposits existed on the Bjarmeland Platform, north of the Nordkapp Basin and west of the BSSE, during the deposition of the upper Gipsdalen Group. Less restricted

marine environments have higher circulation of seawater, deterring evaporite deposition (Nichols, 2009). According to Ehrenberg et al. (1998) results from well 7128/4-1 (Figure 3.1) indicate that the Finnmark Platform went through periods of mainly subtidal carbonate deposition and subaerial exposure throughout the deposition of the upper Gipsdalen Group. Furthermore, Nilsen et al. (1993) identify and interpret a low-relief upper Gipsdalen Group evaporite basin SW of the BSSE on the Finnmark Platform. While Gipsdalen Group aged build-ups are not observed in the seismic data in the BSSE, well 7229/11-1 (Figure 3.1) drilled through carbonate build-ups of the Gipsdalen Group (Rafaelsen et al., 2008). Nilsen et al. (1993) further suggest that the proposed evaporite basin was limited by the deeper Nordkapp Basin and by marginal Gipsdalen Group build-ups, describing a rimmed shelf to basin morphology influenced by the pre-existing topography with restricted marine, lagoonal and sabkha environments dominating on the shelf (Figure 5.3). Di Lucia et al. (2017) describe the position of the platform to basin margin on the Finnmark Platform to coincide with pinch-outs of the Gipsdalen Group evaporite sequence, assumed here to be equivalent to the Intra Gipsdalen Group sub-unit.

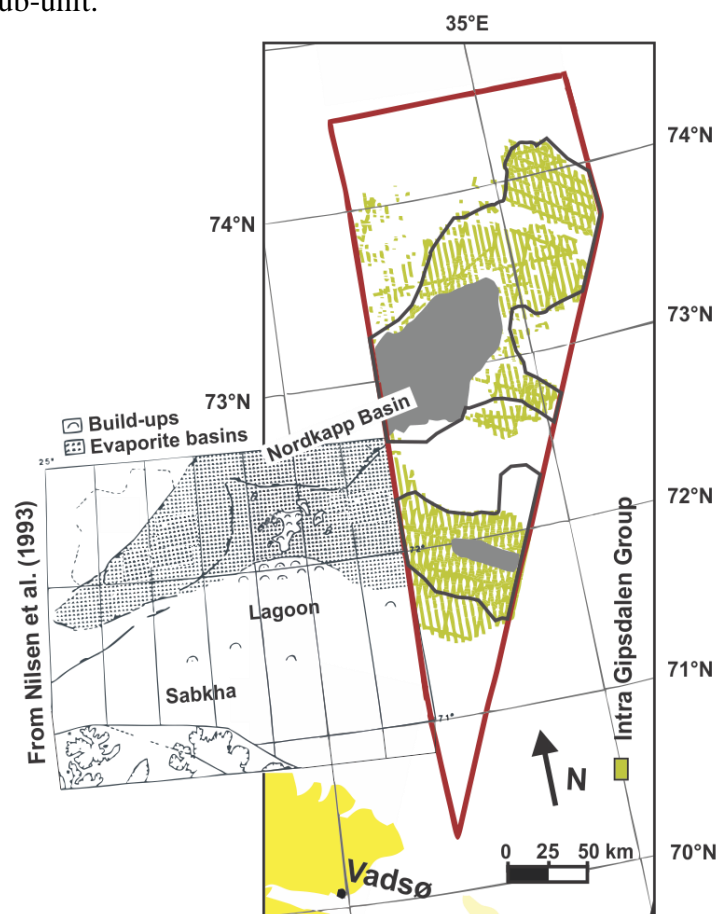


Figure 5.3 Showing where the Intra Gipsdalen Group sub-unit overlap with outlined increased time-thickness areas of the Gipsdalen Group (as presented in Figure 5.1B). Unmapped areas of the Nordkapp and Tiddlybanken basins in the BSSE are shown in grey. Inset interpretation of upper Gipsdalen depositional environment in the SW Barents Sea next to the BSSE modified from Nilsen et al. (1993).

The Intra Gipsdalen Group sub-unit is interpreted to represent evaporites. By using the distribution and pinch-outs of the Intra Gipsdalen Group sub-unit as reference points (Figure 5.3), the dominating environments during the deposition of the upper Gipsdalen Group in the BSSE are interpreted to consist of subtidal carbonate platforms grading into shallow evaporite basins (Figure 5.4). The intermittent appearances of the Intra Gipsdalen Group sub-unit on the Bjarmeland Platform is by analogy of Gérard and Buhrig (1990) interpreted to be indicative of a wider and more restricted transitional area where evaporite deposits formed in depressions.

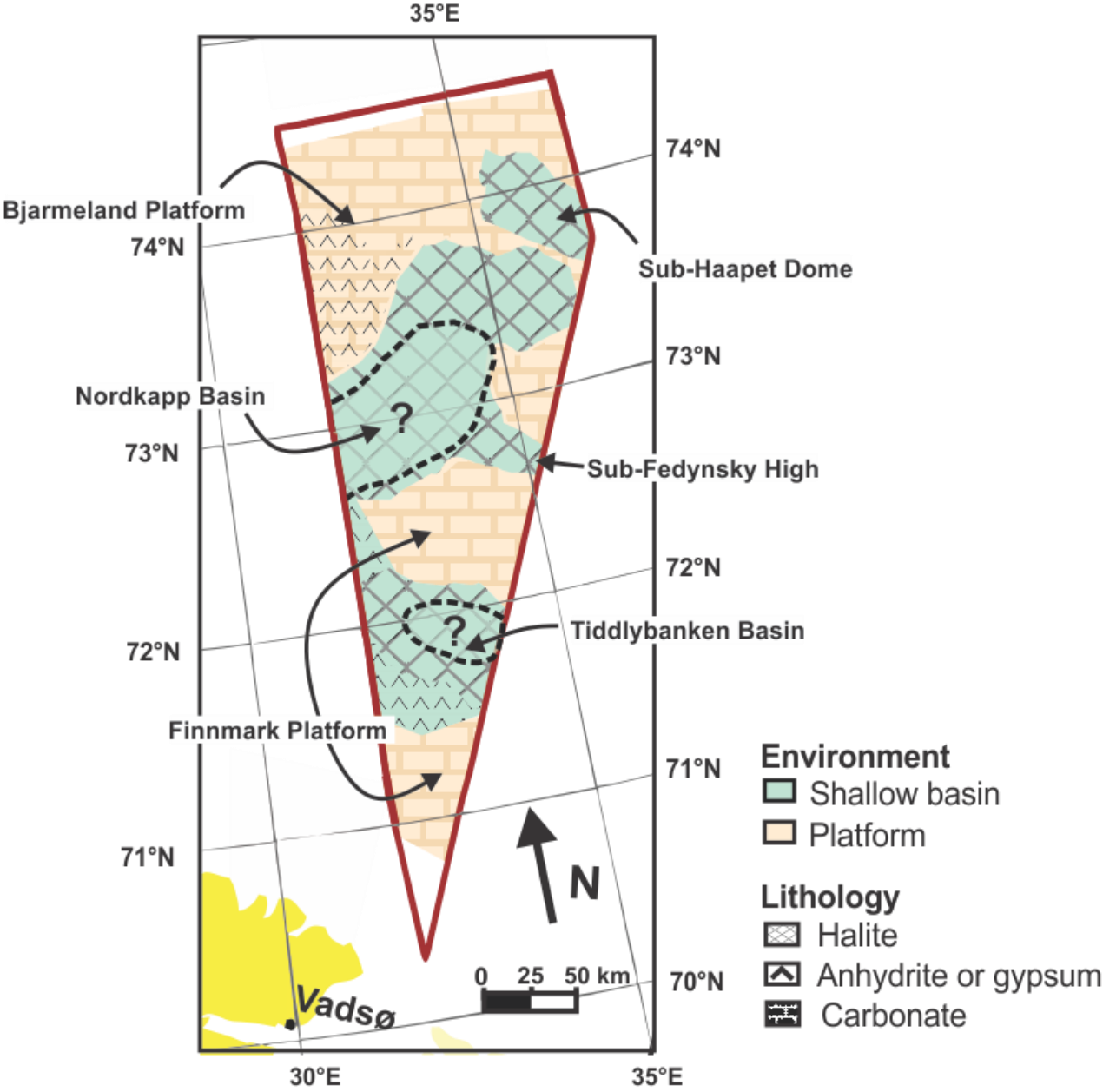


Figure 5.4 Interpreted paleogeography during the deposition of the upper Gipsdalen Group. Some areas of the Nordkapp and Tiddlybanken basins have not been mapped, which is why the interpretation of the basins are marked by stippled lines and “?”.

### 5.3 Bjarmeland Group

The Bjarmeland Group stratigraphically represents Early to Middle Permian. The uniform time-thickness of the Bjarmeland Group in the study area, not including the build-ups, indicates a tectonically quiet setting and few regional changes in accommodation space. The local discontinuous appearance in the seismic can be indicative of subtle changes in energy level that are large enough to give rise to minor acoustic impedance contrasts. Another possible explanation for the discontinuous seismic appearance could be attributed to the resolution of the data sets, as even the most favorable vertical resolution calculation (Table 3.2) finds that sequences below 88 m will not be discernable in the seismic.

Carbonates are sensitive to diagenetic alterations creating lateral velocity variations, which in seismic data show up as changes in reflection coefficient in continuous horizons (Palaz and Marfurt, 1997). Another indication of carbonates is blank zones in the seismic, as diagenesis destroys original depositional geometries (Palaz and Marfurt, 1997). Di Lucia et al. (2017) found in wells 7128/4-1 (Figure 3.1) and 7128/6-1 that carbonates deposited in the Bjarmeland Group are dominated by crinoidal-bryozan grainstones and packstone, indicating cold-water settings. Though these biotic elements are also present in the cored intervals of the Gipsdalen Group and other warm-water settings, they are in those cases secondary to tropical biotic elements (Wahlman and Konovalova, 2002, Di Lucia et al., 2017). The Bjarmeland Group in the greater Barents Sea is found to consist of carbonates deposited during more temperate climatic conditions than the Gipsdalen Group and with less fluctuations in sea level (Worsley, 2008). The seismic appearance of the Bjarmeland Group in the BSSE corresponds with an interpretation of a carbonate platform, as existing in a shallow marine setting.

The appearance of the Bjarmeland Group within mapped areas of the Nordkapp and Tiddlybanken basins displays a similar uniform thickness of approximately 70-75 ms (twt) as found elsewhere in the BSSE. Combined with the overall comparable reflection configuration and reflection coefficient of the horizons in the BSSE, this could imply that the Nordkapp and Tiddlybanken basins shared a common depositional environment with the rest of the BSSE and were not basins at the time. An explanation for the deeper elevation levels of the Bjarmeland Group within the Nordkapp and Tiddlybanken basins as seen today (Figure 4.7) could be that post-Paleozoic subsidence of the basins is responsible for the observed relief.

The internal seismic configuration of the observed mounds within the Bjarmeland Group is characterized as reflection free. This might indicate a homogenous lithological composition, or at least a composition that does not generate reflections in a manner that is detectable by the data applied here (Figure 4.13B). Mounds found in the Bjarmeland Group are largely located above pinch-outs of the older Intra Gipsdalen Group sub-unit (e.g. Figure 4.18), suggesting that they are possibly connected. A comparison between the distribution of mounds found in the Bjarmeland Group and the appearance of the Intra Gipsdalen Group sub-unit shows that both correlate with the pre-Gipsdalen topography. Figure 5.5 displays the correlation, where the black line represent the divide between platform and basin areas of the pre-Gipsdalen topography (i.e. Figure 5.1).

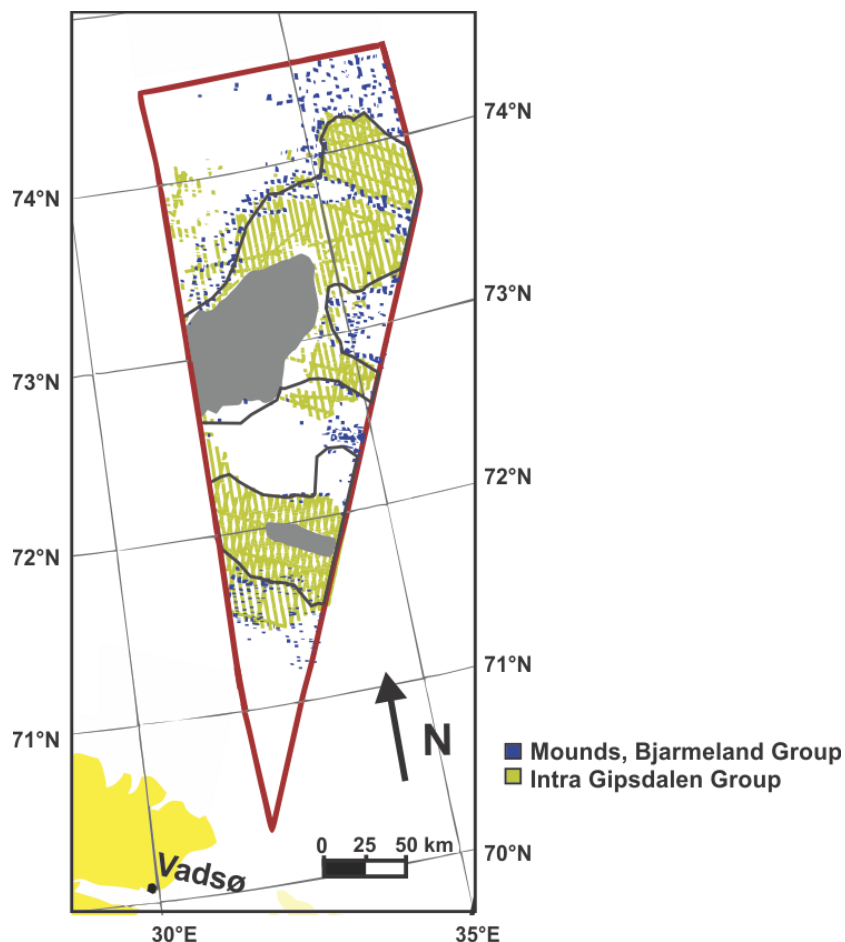


*Figure 5.5* A comparison between mounds found in the Bjarmeland Group and the distribution of high amplitude horizons within the Gipsdalen Group. The black line represent the divide between platform and basins of the pre-Gipsdalen topography, as first presented in Figure 5.1C.

Mounded and draped configurations in seismic data occur within two distinct geologic settings: carbonate shelf/platform areas and clastic deep-water parts of a basin (Brown Jr. and Fisher, 1980). In the BSSE the mounds are mainly found at the edge of slopes or in more flat or low relief sections. Clastic mounds are usually deposited at the base of a slope, a relationship not observed in the BSSE. Clastic mounds may also be the result of infill of low areas where they produce complex mounded to chaotic fill facies (Brown Jr. and Fisher, 1980). While build-ups encountered in the BSSE are interpreted to belong to the Bjarmeland Group, the presence of underlying Gipsdalen Group-level build-ups in the area is possible. Vertically stacked build-ups found within the Gipsdalen and Bjarmeland groups are known from other areas of the Barents Sea, where they are interpreted to be reefs based on their seismic expression and well correlation (Larssen et al., 2002, Samuelsberg et al., 2003, Rafaelsen et al., 2008). Reefs form on topographical highs that can be structural or provided by previous reefs, and as such vertical building of reefs is common (Sheriff and Geldart, 1995). Additionally, occurrences of Bjarmeland Group build-up complexes elsewhere in the Barents Sea are known to coincide with pinch-outs of the Gipsdalen Group evaporites, assumed to be controlled by earlier topography and areas with high subsidence rates (Larssen et al., 2002). It should be noted that the applied seismic 2D data used here puts some restraints on the mapping and extent of the potential build-ups. What appears to be a collection of isolated build-ups (Figure 4.12B) could form interconnected networks (Samuelsberg et al., 2003, Rafaelsen et al., 2008).

The observations of the Bjarmeland Group surrounding the mounds show a uniform appearance in both time-thickness and internal horizon configuration (Figure 4.13B). Assuming the mounds to be carbonate build-ups, the uniform appearance on either side of the build-ups could indicate that a similar environment surrounds them. There are four major reef types: barrier, shelf-margin, pinnacle and patch reefs (Badley, 1985). Among the reef types the patch and pinnacle reefs are usually surrounded on all sides by a fairly equal depositional environment (Sheriff and Geldart, 1995). Patch reefs, thought to be responsible for basin-proximal isolated build-ups, could develop on local paleo-topographical highs (Larssen et al., 2002). The observed seismic build-ups in the BSSE are interpreted to represent isolated patch reefs formed at topographical highs, whose extent may be somewhat controlled by vertical stacking above Gipsdalen Group-level reefs that area not recognized in the seismic data. The build-ups appear to be isolated events, though that could be, as indicated above, due to the spacing of the 2D lines.

Based on the observations of the Bjarmeland Group in the BSSE, and also taking into account well results and seismic investigations from the SW Barents Sea (Larssen et al., 2002, Samuelsberg et al., 2003, Rafaelsen et al., 2008, Di Lucia et al., 2017), the group is interpreted to have been deposited within a regional carbonate platform with build-ups (Figure 5.6). Given the relationship of the observed Bjarmeland Group-level build-ups in the BSSE with the older, underlying topography (Figure 5.3), they are thought to have formed at topographical highs.

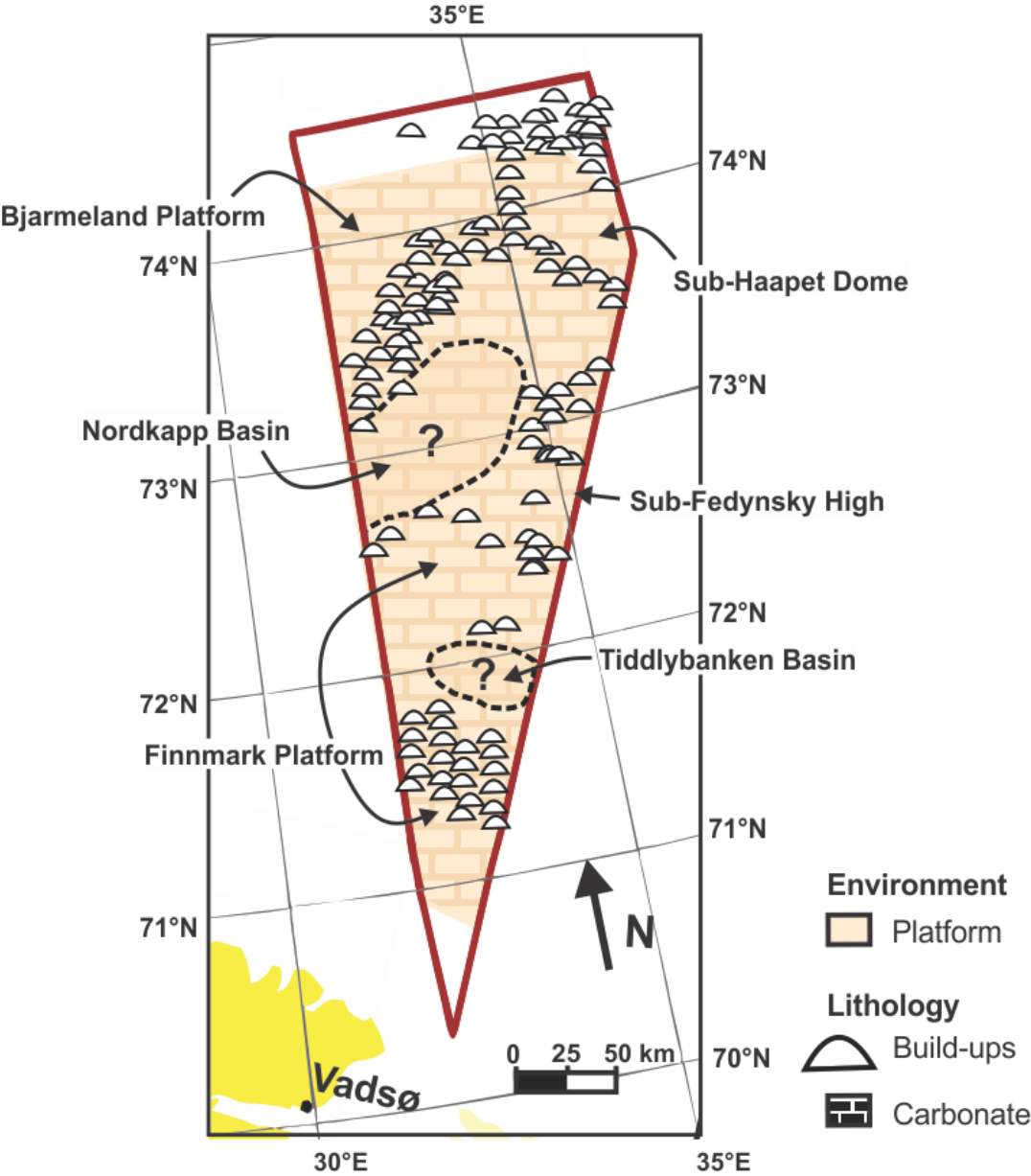


Figure 5.6 Interpreted paleogeography during deposition of the Bjarmeland Group, based on the presence of interpreted mounds and the otherwise uniform time-thickness and horizon appearance of the group. Some areas of the Nordkapp and Tiddlybanken basins have not been mapped, which is why the interpretation of the basins are marked by stippled lines and “?”.

## 5.4 Tempelfjorden Group

The Tempelfjorden Group stratigraphically represents Middle to Late Permian (Larsen et al., 2002). The generally uniform time-thickness of the Tempelfjorden indicates a tectonically quiet setting during deposition, with low regional changes in accommodation space (Figure 4.14). The increase in thickness below the present day Signalhorn Dome could be due to a local increase in accommodation space (Figure 4.3). The Tempelfjorden Group is observed to be draping over the Bjarmeland Group, and the horizon configuration of the group appears generally subparallel (Figure 4.15). Draping over older sediments may indicate deposition from suspension (Vail, 1987). Furthermore, a generally sub-parallel horizon configuration could be indicative of uniform sedimentation conditions found as passive infill (Veeken and van Moerkerken, 2013). Based on the horizon configuration of the Tempelfjorden Group in the BSSE, the group appears to be the result of passive infill deposited from suspension.

In the eastern part of the SW Barents Sea the Tempelfjorden Group is found to consist of uniform lithologies dominated by chert and chert-rich limestone (Larsen et al., 2002). On a larger paleogeographical scale, the greater Barents Sea had moved further north by the time of the deposition of the Tempelfjorden Group and had reached a paleolatitude of approximately 45°N (Stemmerik and Worsley, 2005). Like the crinoidal-bryozoans of the underlying Bjarmeland Group, the siliceous sponges as encountered in the Tempelfjorden Group are not only restricted to cold-water settings. However, their relative abundance compared to other biohermal components indicate deposition in increasingly colder water from the previously deposited units (Wahlman and Konovalova, 2002). The distinctive difference between the Top Tempelfjorden horizon and its overburden (i.e. Figure 4.1) is considered a good regional marker in the greater Barents Sea, as it signifies a shift between a mixed lithology to a pure siliciclastic one (Schjeldsøe Berg and Lie, 2015). The local discontinuous appearance of the group in the seismic data (Figure 4.15B) can be indicative of changes in energy level or of internal convergence; even the most favorable vertical resolution calculation (Table 3.2) finds that sequences below 57 m will not be discernable in the seismic.

The appearance of the Tempelfjorden Group within the Nordkapp and Tiddlybanken basins is comparable to the appearance of the group elsewhere in the BSSE in both time-thickness, internal horizon configuration and amplitude strength of the horizons. As previously discussed for the Bjarmeland Group, the deeper position of the Tempelfjorden Group within the Nordkapp

and Tiddlybanken basins are assumed to mainly be related to post-Paleozoic halokinesis and basin development.

Seismic mounds in the Tempelfjorden Group are known to appear in a belt on the inner Finnmark Platform in the SW Barents Sea (Colpaert et al., 2007). Within the BSSE, mounds found within the Tempelfjorden Group are located to the south on the Finnmark Platform, where they stand out with a high reflection coefficient occurrence in the seismic data (Figures 4.14, 4.23 and 5.7). Unlike the mounds found within the Bjarmeland Group, the BSSE mounds found within the Tempelfjorden Group do not appear to correlate with the previous topography. Instead, the BSSE mounds within the Tempelfjorden Group appear further south than any build-ups or major topographical changes of the older, pre-Tempelfjorden Group, units (Figures 4.14 and 5.5). Well 7128/4-1 on the Finnmark Platform (Figure 3.1) was drilled through a seismic mound on the Tempelfjorden Group level, while well 7128/6-1 was drilled at the flank of another mound at the same level (Ehrenberg et al., 1998). Ehrenberg et al. (1998) suggest that the seismic expression of mounds found in the Tempelfjorden Group are caused by porous spiculites developed and located above older bioclastic mounds. In the case of well 7128/4-1 the spiculite mound was also gas-saturated (Ehrenberg et al., 1998). The older bioclastic mounds were concentrated on the inner Finnmark Platform, where they are assumed to have formed in an environment with favorable topography, water temperature and nutrient supply until rise in sea level and/or environmental stress terminated their development (Ehrenberg et al., 2001). The water depths during the deposition of the spiculite mounds are assumed to have been close to storm wave base, whereas deeper water conditions existed further north (Ehrenberg et al., 1998, Ehrenberg et al., 2001). Comparing the observed mounds in the BSSE in terms of seismic expression and spatial position with the observed mounds elsewhere on the inner Finnmark Platform makes it reasonable to assume that they could represent spiculite mounds. The presence of spiculite mounds south in the BSSE is then considered indicative of an open marine setting in this area during deposition of the Tempelfjorden Group, where the water depth was close to storm wave base.

The Tempelfjorden Group shows low variation on a regional scale as its thickness and seismic appearance are essentially uniform throughout the area, suggesting a stable tectonic and sedimentological setting during the deposition of the group (Figures 4.14 and 4.15). By the appearance of the group in the BSSE and by comparison to seismic surveys and well results in the SW Barents Sea (Ehrenberg et al., 1998, Ehrenberg et al., 2001, Colpaert et al., 2007), the

seismic mounds are interpreted to represent spiculitic mounds while chert and chert-rich limestone dominated elsewhere. The Tempelfjorden Group-level mounds in the BSSE appear to have no correlation to the older and underlying topography. An open marine setting is interpreted to be the dominating depositional environment of the Tempelfjorden Group, with the presence of interpreted spiculite mounds indicating that the water depth was below storm wave base (Figure 5.7).

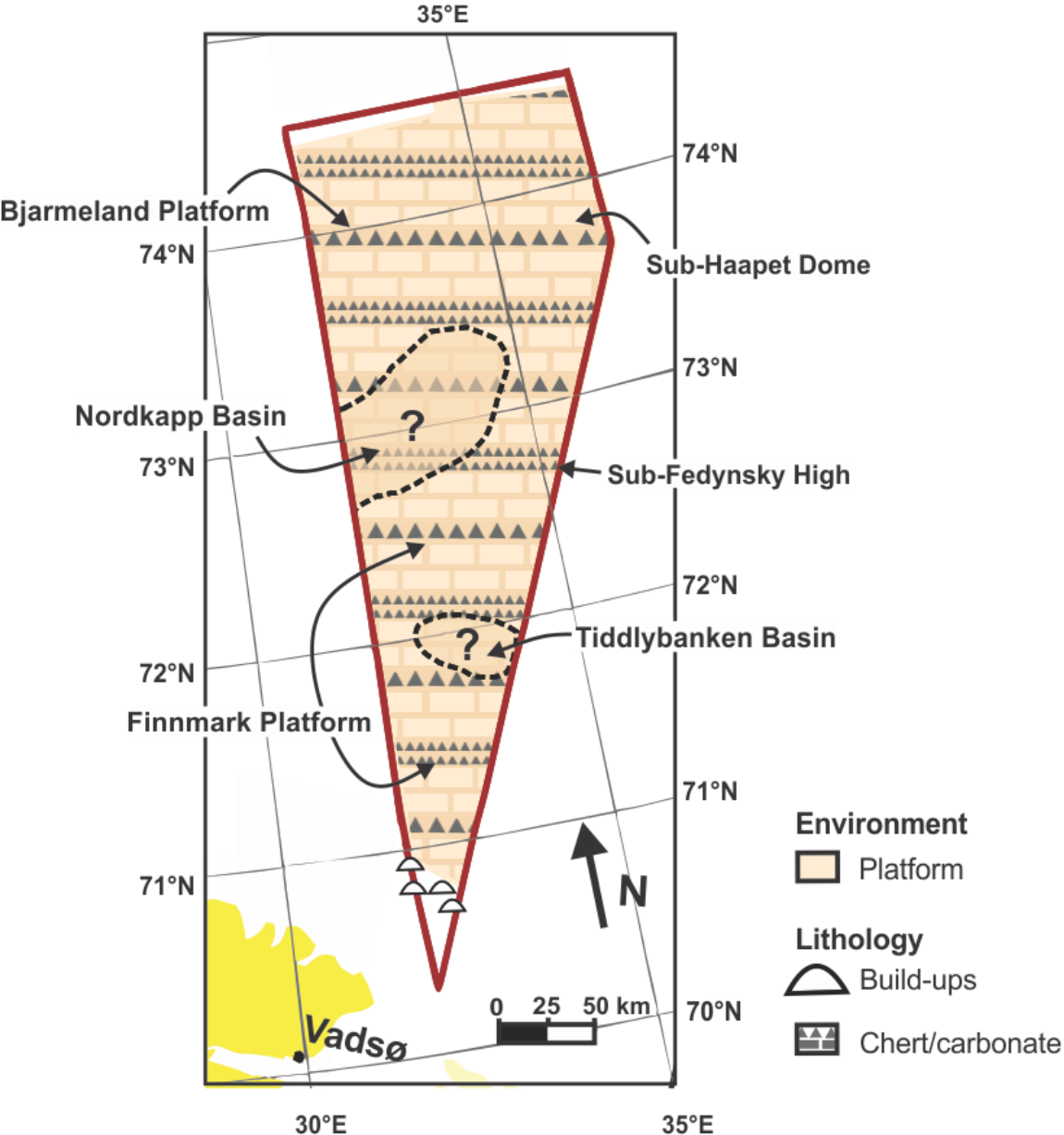


Figure 5.7 Interpreted paleogeography during deposition of the Tempelfjorden Group, based on the presence of interpreted mounds and the otherwise uniform time-thickness and horizon appearance of the group. Some areas of the Nordkapp and Tiddlybanken basins have not been mapped, leaving some uncertainty of the interpretation, which is why the basins are marked by stippled lines and “?”.

## 6. Summary and conclusion

The upper Paleozoic development of the BSSE was dominated by basin fill and platform development with accumulations of evaporites and carbonates. Through the period the northward drift of the greater Barents Sea led to changing paleoclimatic conditions and thus changes in the dominating sediment types. The tectonic regime in the BSSE was dominated by subsidence, and little to no faulting activity took place. The structural relief in the BSSE was more prominent during the deposition of the lower Gipsdalen Group, assumed to be a result of remnant topography from Devonian rifting. Progressive infill of alternating carbonates and evaporites in the basins during the deposition of the Gipsdalen Group resulted in a regional platform existing during the deposition of the Bjarmeland and Tempelfjorden groups. Starting with the lower section of the Gipsdalen Group, the depositional systems dominating in the BSSE at different stages of the upper Paleozoic are summarized below.

- The lower section of the Gipsdalen Group was deposited in shallow marine platform to basin environment, where the lateral changes were related to the existing underlying rift topography. Warm climate conditions combined with frequent changes in relative sea level led to the deposits ranging from an alternating carbonate and evaporite basin infill to a carbonate platform.
- The paleogeographical position of the Barents Sea during the deposition of the upper section of the Gipsdalen Group resulted in an arid and warm climate especially suitable for evaporite deposition, as also encountered in nearby wells. The Nordkapp and Tiddlybanken basins, especially, were dominated by salt deposits. On the flanks of the basins, on the Finnmark and Bjarmeland platforms, salt graded into mixed carbonate and anhydrite deposits.
- The Bjarmeland Group was deposited during an overall shallow marine environment within the BSSE. A regional carbonate platform dominated in the BSSE, with carbonate mounds developing on existing topographical highs.
- The Tempelfjorden Group was deposited from suspension in an open marine environment, and had an overall common depositional system within the BSSE. Wells

7128/4-1 and 7128/6-1 confirmed spiculite mounds on the inner Finnmark Platform, which are mapped to continue into the BSSE. The Tempelfjorden Group-level mounds form topographical highs unrelated to the topography of the older, underlying units.

### ***Future work***

Within this thesis, the regional observations have mainly been compared to existing seismic studies and well data from the SW Barents Sea. For further research of the upper Paleozoic depositional environment in the BSSE there are other types of information to be studied. There are currently (May 2018) no wells within the area, released or otherwise, that penetrate the upper Paleozoic interval (NPD, 2018). In the future, wells within the study area will be able to confirm or disprove the seismic observations and interpretations. Additionally, more knowledge of the geological development east of the BSSE would be useful. Cross-border correlation of seismic data and well results from the Russian sector of the Barents Sea will give a more complete understanding of the upper Paleozoic development in the BSSE. Furthermore, interpretation of 3D seismic data in the BSSE would improve the understanding of the seismic stratigraphy and make it possible to constrict the geometries of the structures (e.g. the build-ups).

## 7. References

- ALLABY, M. (2013). *A dictionary of geology and earth sciences*. Oxford University Press. 660 p.
- ANELL, I., FALEIDE, J. & BRAATHEN, A. (2016). Regional tectono-sedimentary development of the highs and basins of the northwestern Barents Shelf. *Norsk Geologisk Tidsskrift*, 96, p. 27-41.
- BADLEY, M. E. (1985). *Practical seismic interpretation*. Boston: International Human Resources Development Corporation. 266 p.
- BITRUS, P. R., IACOPINI, D. & BOND, C. E. (2016). Defining the 3D geometry of thin shale units in the Sleipner reservoir using seismic attributes. *Marine and Petroleum Geology*, 78, p. 405-425.
- BJØRLYKKE, K. (2015a). Introduction to Petroleum Geology. In: BJØRLYKKE, K. (ed.) *Petroleum Geoscience*. 2 ed.: p. 1-29: Springer.
- BJØRLYKKE, K. (2015b). Mudrocks, Shales, Silica Deposits and Evaporites. In: BJØRLYKKE, K. (ed.) *Petroleum Geoscience*. p. 217-229: Springer.
- BJØRLYKKE, K. (2015c). Seismic Stratigraphy, Sequence Stratigraphy and Basin Analysis. In: BJØRLYKKE, K. (ed.) *Petroleum Geoscience*. 2 ed.: p. 255-271: Springer.
- BROWN, A. R. (2011). *AAPG Memoir 42/SEG Investigations in Geophysics No. 9: Interpretation of Three-Dimensional Seismic Data*. 7 ed. Tulsa: Society of Exploration Geophysicists and AAPG. 615 p.
- BROWN JR., L. & FISHER, W. (1980). Seismic-Stratigraphic Interpretation of Depositional Systems and its Role in Petroleum Exploration (Part 1). *CN 16: Seismic Stratigraphic Interpretation and Petroleum Exploration*, 16, p. 1-65.
- BRUCE, J. & TOOMEY, D. (1993). Late Palaeozoic bioherm occurrences of the Finnmark Shelf, Norwegian Barents Sea: analogues and regional significance. *Norwegian Petroleum Society Special Publications*. p. 377-392: Elsevier.
- BULAT, J. (2005). Some considerations on the interpretation of seabed images based on commercial 3D seismic in the Faroe-Shetland Channel. *Basin Research*, 17 (1), p. 21-42.
- CHOPRA, S. & MARFURT, K. J. (2007). *Seismic attributes for prospect identification and reservoir characterization*. SEG Geophysical Development Series, b. 11: Society of Exploration Geophysicists and European Association of Geoscientists and Engineers. 464 p.
- CHURCH, K. D. & COE, A. L. (2003). Processes controlling relative sea-level change and sediment supply. In: COE, A. L. (ed.) *The Sedimentary Record of Sea-Level Change*. Cambridge: p. 99-117. Cambridge: Cambridge University Press.
- COLPAERT, A., PICKARD, N., MIENERT, J., HENRIKSEN, L. B., RAFAELSEN, B. & ANDREASSEN, K. (2007). 3D seismic analysis of an Upper Palaeozoic carbonate succession of the Eastern Finnmark Platform area, Norwegian Barents Sea. *Sedimentary Geology*, 197 (1), p. 79-98.
- DI LUCIA, M., SAYAGO, J., FRIJIA, G., COTTI, A., SITTA, A. & MUTTI, M. (2017). Facies and seismic analysis of the Late Carboniferous–Early Permian Finnmark carbonate platform (southern Norwegian Barents Sea): An assessment of the carbonate factories and depositional geometries. *Marine and Petroleum Geology*, 79, p. 372-393.
- DODSON, J. (2014). Completing the Picture - Enhancing the understanding of the Barents Sea with full-tensor gravity gradiometry. *GEO ExPro*, 11 (3): 92-96.
- DORÉ, A. (1995). Barents Sea geology, petroleum resources and commercial potential. *Arctic*, p. 207-221.

- EHRENBERG, S., PICKARD, N., HENRIKSEN, L., SVANA, T., GUTTERIDGE, P. & MACDONALD, D. (2001). A depositional and sequence stratigraphic model for cold-water, spiculitic strata based on the Kapp Starostin Formation (Permian) of Spitsbergen and equivalent deposits from the Barents Sea. *AAPG bulletin*, 85 (12), p. 2061-2088.
- EHRENBERG, S. N., NIELSEN, E., SVÅNÅ, T. & STEMMERIK, L. (1998). Depositional evolution of the Finnmark carbonate platform, Barents Sea: results from wells 7128/6-1 and 7128/4-1. *Norsk Geologisk Tidsskrift*, 78, p. 185-224.
- ESRI (2011). Ocean Basemap. ArcGIS Online: Esri.
- FALEIDE, J. I., BJØRLYKKE, K. & GABRIELSEN, R. H. (2010). Geology of the Norwegian Continental Shelf. *Petroleum Geoscience*. p. 467-499.
- FOSSEN, H., DALLMAN, W. & ANDERSEN, T. B. (2013). Fjellkjeden går til grunne. In: RAMBERG, I., BRYHNI, I., NØTTVEDT, A. & RANGNES, K. (eds.) *Landet blir til - Norges geologi*. 2 ed. Trondheim: p. 224-261. Trondheim: Norsk Geologisk Forening.
- GABRIELSEN, R. H., FÆRSETH, R. B., JENSEN, L. N., KALHEIM, J. E. & RIIS, F. (1990). *Structural Elements of the Norwegian Continental Shelf. Part 1: The Barents Sea Region*. NPD-Bulletin, b. 6: Norwegian Petroleum Directorate. 47 p.
- GÉRARD, J. & BUHRIG, C. (1990). Seismic facies of the Permian section of the Barents Shelf: analysis and interpretation. *Marine and Petroleum Geology*, 7 (3), p. 234-252.
- GERNIGON, L., BRÖNNER, M., DUMAIS, M.-A., GRADMANN, S., GRØNLIE, A., NASUTI, A. & ROBERTS, D. (2018). Basement inheritance and salt structures in the SE Barents Sea: Insights from new potential field data. *Journal of Geodynamics*. <https://doi.org/10.1016/j.jog.2018.03.008>.
- GERNIGON, L., BRÖNNER, M., ROBERTS, D., OLESEN, O., NASUTI, A. & YAMASAKI, T. (2014). Crustal and basin evolution of the southwestern Barents Sea: from Caledonian orogeny to continental breakup. *Tectonics*, 33 (4), p. 347-373.
- GUDLAUGSSON, S., FALEIDE, J., JOHANSEN, S. & BREIVIK, A. (1998). Late Palaeozoic structural development of the south-western Barents Sea. *Marine and Petroleum Geology*, 15 (1), p. 73-102.
- HAVFORSKNINGSINSTITUTTET. (2005). *Barentshavet* [Online]. Available: [http://www.imr.no/temasider/havomrader\\_og\\_okosystem/barentshavet/nb-no](http://www.imr.no/temasider/havomrader_og_okosystem/barentshavet/nb-no) [Accessed 20 September 2017].
- HENRIKSEN, E., RYSETH, A., LARSSSEN, G., HEIDE, T., RØNNING, K., SOLLID, K. & STOUPAKOVA, A. (2011). Tectonostratigraphy of the greater Barents Sea: implications for petroleum systems. *Geological Society, London, Memoirs*, 35 (1), p. 163-195.
- JENSEN, L. & SØRENSEN, K. (1992). Tectonic framework and halokinesis of the Nordkapp Basin, Barents Sea. *Structural and tectonic modelling and its application to petroleum geology*. p. 109-120: Elsevier.
- JOHANSEN, S., OSTISTY, B., BIRKELAND, Ø., FEDOROVSKY, Y., MARTIROSIAN, V., CHRISTENSEN, O. B., CHEREDEEV, S., IGNATENKO, E. & MARGULIS, L. (1992). Hydrocarbon potential in the Barents Sea region: play distribution and potential. *Arctic Geology and Petroleum Potential, Norwegian Petroleum Society (NPF), Special Publication*, 2, p. 273-320.
- KEAREY, P., BROOKS, M. & HILL, I. (2002). *An Introduction to Geophysical Exploration*. Wiley-Blackwell. 262 p.
- LARSSSEN, G., ELVEBAKK, G., HENRIKSEN, L., KRISTENSEN, E., NILSSON, I., SAMUELSBERG, T. & STEMMERIK, L. (2005). *Upper Palaeozoic lithostratigraphy of the southern Norwegian Barents Sea. Norges Geologiske Undersøkelse Bulletin 444*. Geological Survey of Norway, b. 444. Trondheim: Geological Survey of Norway.

- LARSSEN, G., ELVEBAKK, G., HENRIKSEN, L. B., KRISTENSEN, S., NILSSON, I., SAMUELSBERG, T., SVÅNÅ, T., STEMMERIK, L. & WORSLEY, D. (2002). *Upper Palaeozoic lithostratigraphy of the Southern Norwegian Barents Sea*. Norwegian Petroleum Directorate Bulletin, b. 9. 145 p.
- LUNDSCHIEN, B. A., HØY, T. & MØRK, A. (2014). Triassic hydrocarbon potential in the Northern Barents Sea; integrating Svalbard and stratigraphic core data. *Norwegian Petroleum Directorate Bulletin*, 11, p. 3-20.
- MATTINGSDAL, R., HØY, T., SIMONSTAD, E. & BREKKE, H. (2015). An updated map of structural elements in the southern Barents Sea. Presented at: 31st Geological Winter Meeting: Norwegian Petroleum Directorate.
- MELD. ST. 36 (2012-2013). (2013). *Nye muligheter for Nord-Norge – åpning av Barentshavet sørøst for petroleumsvirksomhet*. OLJE- OG ENERGIDEPARTEMENTET. 40 p.
- MITCHUM JR., R., VAIL, P. & SANGREE, J. (1977). Seismic stratigraphy and global changes of sea level: Part 6. Stratigraphic interpretation of seismic reflection patterns in depositional sequences: Section 2. Application of seismic reflection configuration to stratigraphic interpretation. p. 117-133.
- MONDOL, N. H. (2015). Seismic exploration. *Petroleum Geoscience*. p. 427-454: Springer.
- NAKREIM, H. A. & WORSLEY, D. (2013). Havet oversvømmer landet. In: RAMBERG, I., BRYHNI, I., NØTTVEDT, A. & RANGNES, K. (eds.) *Landet blir til - Norges geologi*. 2 ed. Trondheim: p. 148-179. Trondheim: Norsk Geologisk Forening.
- NICHOLS, G. (2009). *Sedimentology and stratigraphy*. 2 ed.: John Wiley & Sons. 419 p.
- NIELSEN, L., BOLDREEL, L. O. & SURLYK, F. (2004). Ground-penetrating radar imaging of carbonate mound structures and implications for interpretation of marine seismic data. *AAPG bulletin*, 88 (8), p. 1069-1082.
- NILSEN, K., HENDRIKSEN, E. & LARSSEN, G. (1993). Exploration of the Late Palaeozoic carbonates in the southern Barents Sea—a seismic stratigraphic study. *Norwegian Petroleum Society Special Publications*. p. 393-403: Elsevier.
- NPD. (2013a). *Kartlegging og ressursberegning, Barentshavet sørøst*. Norwegian Petroleum Directorate. 23 p.
- NPD. (2013b). *Petroleum Resources on the Norwegian Continental Shelf 2013 Exploration*. Stavanger: Norwegian Petroleum Directorate. 63 p.
- NPD. (2016). *Undiscovered resources* [Online]. Available: <http://www.npd.no/en/Publications/Resource-Reports/2016/Chapter-3/> [Accessed 20 September 2017].
- NPD. (2018). *FactMaps Norwegian Petroleum Directorate* [Online]. Available: [http://gis.npd.no/factmaps/html\\_21/](http://gis.npd.no/factmaps/html_21/) [Accessed 05 May 2018].
- NØTTVEDT, A. & WORSLEY, D. (2013). Vidstrakte sletter, kull og salt. In: RAMBERG, I., BRYHNI, I., NØTTVEDT, A. & RANGNES, K. (eds.) *Landet blir til - Norges geologi*. 2 ed. Trondheim: p. 262-331. Trondheim: Norsk Geologisk Forening.
- OGG, G. (2013). *Barents Sea Chart* [Online]. Naturhistorisk Museum, UiO. Available: [http://www.nhm2.uio.no/norges/litho/Barents\\_Chart.html](http://www.nhm2.uio.no/norges/litho/Barents_Chart.html) [Accessed 15 October 2017].
- PALAZ, I. & MARFURT, K. J. (1997). Carbonate seismology: An overview. *Carbonate seismology: Society of Exploration Geophysicists Geophysical Developments Series*, 6, p. 1-7.
- QUARLES, S., RIECK, J., SHIRES, E. & FARAH, P. (2016). Barents Sea exploration provides opportunity for new investment. *Oil & Gas Journal*, 114 (2), p. 36-43.
- RAFAELSEN, B., ELVEBAKK, G., ANDREASSEN, K., STEMMERIK, L., COLPAERT, A. & SAMUELSBERG, T. J. (2008). From detached to attached carbonate buildup complexes—3D

- seismic data from the upper Palaeozoic, Finnmark Platform, southwestern Barents Sea. *Sedimentary Geology*, 206 (1-4), p. 17-32.
- SAMUELSBERG, T. J., ELVEBAKK, G. & STEMMERIK, L. (2003). Late Palaeozoic evolution of the Finnmark Platform, southern Norwegian Barents Sea. *Norwegian Journal of Geology/Norsk Geologisk Forening*, 83 (4), p. 351-361.
- SCHJELDSØE BERG, M. & LIE, Ø. (2015). New seismic data enables cross-border correlation. *GEO Energi & ressurser* (5): 34-36.
- SELLEY, R. C. & SONNENBERG, S. A. (2014). *Elements of petroleum geology*. b. 3: Academic Press. 507 p.
- SHERIFF, R. (1985). Aspects of Seismic Resolution: Chapter 1. In: BERG, O. R. & WOOLVERTON, D. G. (eds.) *AAPG Memoir 39: Seismic Stratigraphy II: An Integrated Approach to Hydrocarbon Exploration*. Tulsa: p. 1-10. Tulsa: AAPG.
- SHERIFF, R. E. (2002). *Encyclopedic dictionary of applied geophysics*. 4 ed.: Society of exploration geophysicists. 429 p.
- SHERIFF, R. E. & GELDART, L. P. (1995). *Exploration seismology*. Cambridge university press. 628 p.
- SIGMOND, E., JORDE, K. & BRYHNI, I. (2013). *Norsk geologisk ordbok: Med engelsknorsk ordliste*. Akademika forlag. Trondheim. 496 p.
- SMELROR, M., BASOV, V. A. & NORGES GEOLOGISKE UNDERSØKELSE. (2009). *Atlas : geological history of the Barents Sea*. Trondheim: Geological Survey of Norway. 134 p.
- STEMMERIK, L. & WORSLEY, D. (2005). 30 years on-Arctic Upper Palaeozoic stratigraphy, depositional evolution and hydrocarbon prospectivity. *Norwegian Journal of Geology/Norsk Geologisk Forening*, 85, p. 151-168.
- STOUPAKOVA, A., HENRIKSEN, E., BURLIN, Y. K., LARSEN, G., MILNE, J., KIRYUKHINA, T., GOLYNCHIK, P., BORDUNOV, S., OGARKOVA, M. & SUSLOVA, A. (2011). The geological evolution and hydrocarbon potential of the Barents and Kara shelves. *Geological Society, London, Memoirs*, 35 (1), p. 325-344.
- VAIL, P. R. (1987). Seismic stratigraphy interpretation using sequence stratigraphy: Part 1: Seismic stratigraphy interpretation procedure. p. 1-10.
- VEEKEN, P. C. (2007). *Seismic Stratigraphy, Basin Analysis and Reservoir Characterisation, Volume 37*. Handbook of Geophysical Exploration: Elsevier. 509 p.
- VEEKEN, P. C. & VAN MOERKERKEN, B. (2013). *Seismic stratigraphy and depositional facies models*. EAGE Publications bv. 494 p.
- WAHLMAN, G. P. & KONOVALOVA, M. V. (2002). Upper Carboniferous-Lower Permian Kozhim carbonate bank, subpolar pre-Ural Mountains, northern Russia. In: ZEMPOLICH, W. G. & COOK, H. E. (eds.) *SEPM Special Publication 74: Paleozoic Carbonates of the Commonwealth of Independent States (CIS): Subsurface Reservoirs and Outcrop Analogs*. p. 219-241: SEPM
- WARREN, J. K. (2006). *Evaporites: sediments, resources and hydrocarbons*. Springer Science & Business Media. 1035 p.
- WORSLEY, D. (2008). The post-Caledonian development of Svalbard and the western Barents Sea. *Polar Research*, 27 (3), p. 298-317.